(12) INTERNATIONAL APPLICATION PUBLISHED UNDER THE PATENT COOPERATION TREATY (PCT)

(19) World Intellectual Property Organization
International Bureau

(43) International Publication Date
09 November 2023 (09.11.2023)

WIPO | PCT

(10) International Publication Number
WO 2023/215764 A2

(51) International Patent Classification:
C12N 5/07 (2010.01) *C12Q 1/00* (2006.01)

(21) International Application Number:
PCT/US2023/066517

(22) International Filing Date:
02 May 2023 (02.05.2023)

(25) Filing Language: English

(26) Publication Language: English

(30) Priority Data:
63/337,990 03 May 2022 (03.05.2022) US

(71) Applicants: **THE TRUSTEES OF COLUMBIA UNIVERSITY IN THE CITY OF NEW YORK** [US/US]; 412 Low Memorial Library, 535 W. 116th Street, New York, NY 10027 (US). **STEVENS INSTITUTE OF TECHNOLOGY** [US/US]; 1 Castle Point Terrace, Hoboken, NJ 07030 (US).

(72) Inventors: **VUNJAK-NOVAKOVIC, Gordana**; 2700 Broadway 4G, New York, NY 10025 (US). **O'NEILL, John, D.**; 244 East 51st Street Apt. 3E, New York, NY 10022 (US). **PINEZICH, Meghan, R.**; 315 East 9th Street Apt. 2RW, New York, NY 10003 (US). **GRANEY, Pamela**; 400 West 56th Street, Apt 3F, New York, NY 10019 (US). **TAVAKOL, Daniel, Naveed**; 239 W 20th Street, Apt 18, New York, NY 10011 (US). **KIM, Jinho**; 270 10th Street Apt. 224, Jersey City, NJ 07302 (US). **TAMARGO, Manuel**; 3800 SW 62nd Avenue, Miami, FL 33155 (US).

(74) Agent: **BROWN, Richard, J.**; Reed Smith LLP, 1201 Market Street, Wilmington, DE 19801 (US).

(81) Designated States *(unless otherwise indicated, for every kind of national protection available)*: AE, AG, AL, AM, AO, AT, AU, AZ, BA, BB, BG, BH, BN, BR, BW, BY, BZ, CA, CH, CL, CN, CO, CR, CU, CV, CZ, DE, DJ, DK, DM, DO, DZ, EC, EE, EG, ES, FI, GB, GD, GE, GH, GM, GT, HN, HR, HU, ID, IL, IN, IQ, IR, IS, IT, JM, JO, JP, KE, KG, KH, KN, KP, KR, KW, KZ, LA, LC, LK, LR, LS, LU, LY, MA, MD, MG, MK, MN, MU, MW, MX, MY, MZ, NA, NG, NI, NO, NZ, OM, PA, PE, PG, PH, PL, PT, QA, RO, RS, RU, RW, SA, SC, SD, SE, SG, SK, SL, ST, SV, SY, TH, TJ, TM, TN, TR, TT, TZ, UA, UG, US, UZ, VC, VN, WS, ZA, ZM, ZW.

(84) Designated States *(unless otherwise indicated, for every kind of regional protection available)*: ARIPO (BW, CV, GH, GM, KE, LR, LS, MW, MZ, NA, RW, SC, SD, SL, ST, SZ, TZ, UG, ZM, ZW), Eurasian (AM, AZ, BY, KG, KZ, RU, TJ, TM), European (AL, AT, BE, BG, CH, CY, CZ, DE, DK, EE, ES, FI, FR, GB, GR, HR, HU, IE, IS, IT, LT, LU, LV, MC, ME, MK, MT, NL, NO, PL, PT, RO, RS, SE, SI, SK, SM, TR), OAPI (BF, BJ, CF, CG, CI, CM, GA, GN, GQ, GW, KM, ML, MR, NE, SN, TD, TG).

Published:
— *without international search report and to be republished upon receipt of that report (Rule 48.2(g))*

(54) Title: PATHOLOGICAL REMODELING OF DISTAL LUNG MATRIX IN END-STAGE CYSTIC FIBROSIS PATIENTS

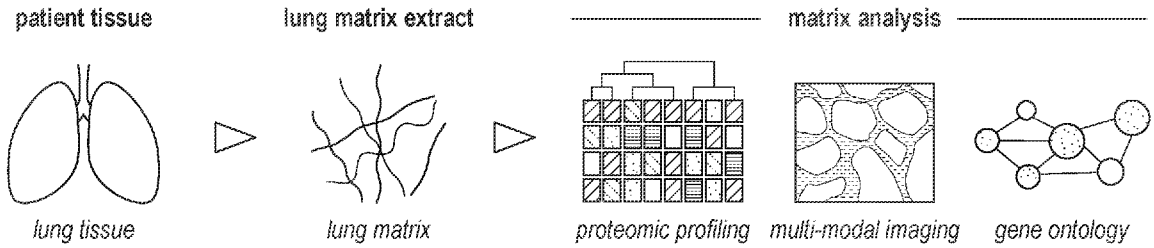

FIG. 1A

(57) Abstract: A biological tissue model for in vitro applications comprising a substrate including a plurality of isolated, soluble matrikines, wherein the substrate is capable of recapitulating one or more of a microstructure, molecular composition, and biomechanical property of a native biological tissue. Preparing the biological tissue model includes isolating a plurality of soluble matrikines from an extracellular matrix; incorporating the plurality of soluble matrikines into a substrate; and recapitulating one or more of a microstructure, molecular composition, and biomechanical property of a native biological tissue with the substrate.

WO 2023/215764 A2

TITLE

PATHOLOGICAL REMODELING OF DISTAL LUNG MATRIX IN END-STAGE CYSTIC FIBROSIS PATIENTS

CROSS REFERENCE TO RELATED APPLICATIONS

[0001] This application claims the benefit of U.S. Provisional application no. 63/337990 filed on May 3, 2022, the contents of which are incorporated by reference herein.

GOVERNMENT SUPPORT CLAUSE

[0002] This invention was made with government support under EB027062 awarded by the National Institutes of Health. The government has certain rights in the invention.

BACKGROUND

[0003] Cystic fibrosis (CF) is a genetic disease caused by a mutation in the cystic fibrosis transmembrane conductance regulator (CFTR) gene. Cystic fibrosis (CF) is characterized by a pathologic cascade of impaired ion transfer, dysregulation of airway surface liquid and mucus, inability to clear infection, chronic inflammation, and ultimately end-stage lung disease necessitating transplantation. As disease severity increases, structural remodeling of the airways (i.e., bronchiectasis) presents as a hallmark feature that is routinely observed on chest radiography and evaluated with established scoring systems. Though these structural alterations to the airways are well-characterized, changes to the distal lung, including structure and composition of the parenchymal extracellular matrix (matrix), are understudied. Despite the recognized importance of the matrix in lung function as well as its involvement in many chronic respiratory diseases, a comprehensive characterization of the CF lung matrix has not been previously reported.

SUMMARY

[0004] A first aspect provides a biological tissue model configured for *in vitro* applications, the biological tissue model comprising: a substrate including a plurality of isolated, soluble matrikines; wherein the substrate is capable of recapitulating one or more of a microstructure, molecular composition, and biomechanical property of a native biological tissue.

[0005] Embodiments of the tissue model include the following, alone or in any combination.

[0006] The plurality of isolated, soluble matrikines may be incorporated into the substrate as a scaffold.

[0007] The plurality of isolated, soluble matrikines may be incorporated into the substrate as a hydrogel.

[0008] The biological tissue model is disease-specific.

[0009] The biological tissue model may be a cystic fibrosis biological tissue model.

[0010] The substrate may be capable of recapitulating one or more of a microstructure, molecular composition, and biomechanical property of a native disease-specific biological tissue.

[0011] The substrate may be capable of recapitulating one or more of a microstructure, molecular composition, and biomechanical property of a native cystic fibrosis biological tissue.

[0012] A second aspect provides a method of preparing a biological tissue model configured for *in vitro* applications, the method comprising: isolating a plurality of soluble matrikines from an extracellular matrix; incorporating the plurality of soluble matrikines into a substrate; and recapitulating one or more of a microstructure, molecular composition, and biomechanical property of a native biological tissue with the substrate.

[0013] Embodiments of the method include the following, alone or in any combination.

[0014] The biological tissue model is that disclosed above, including any of the embodiments alone or in any combination.

[0015] Incorporating the plurality of soluble matrikines into the substrate includes incorporating the plurality of soluble matrikines into the substrate as a scaffold.

[0016] Incorporating the plurality of soluble matrikines into the substrate includes incorporating the plurality of soluble matrikines into the substrate as a hydrogel.

[0017] The method may further comprise processing the isolated, soluble matrikines by crosslinking the isolated, soluble matrikines with each other for incorporation into the substrate.

[0018] The method may further comprise processing the isolated, soluble matrikines by coating a surface of a scaffold for incorporation into the substrate.

[0019] Isolating the plurality of soluble matrikines includes treating a native biological tissue with a CHAPS-based detergent.

[0020] Isolating the plurality of soluble matrikines includes treating a native biological tissue with a Benzonase-based enzyme.

[0021] The method wherein the biological tissue model is disease-specific.

[0022] The method wherein the biological tissue model is a cystic fibrosis biological tissue model.

[0023] The method wherein recapitulating one or more of a microstructure, molecular composition, and biomechanical property includes recapitulating one or more of a microstructure, molecular composition, and biomechanical property of a native disease-specific biological tissue.

[0024] The method wherein recapitulating one or more of a microstructure, molecular composition, and biomechanical property includes recapitulating one or more of a microstructure, molecular composition, and biomechanical property of a native cystic fibrosis biological tissue.

BRIEF DESCRIPTION OF THE FIGURES

[0025] Figure 1A shows aspects of the experimental overview, according to exemplary embodiments of the disclosed subject matter.

[0026] Figure 1B shows aspects of the matrix extracted from human cystic fibrosis lung featuring native disease-specific composition and/or mechanics, according to exemplary embodiments of the disclosed subject matter.

[0027] Figures 2A and 2B show aspects of an *in vitro* cystic fibrosis lung model system, according to exemplary embodiments of the disclosed subject matter.

[0028] Figures 3A and 3B show a comparison of CF and normal lung ECM biomaterials, according to exemplary embodiments of the disclosed subject matter.

[0029] Figures 4A-4D show comparisons of CF and control lung ECM biomaterials composition and ultrastructure, according to exemplary embodiments of the disclosed subject matter.

[0030] Figures 5A and 5B show a comparison of CF and control lung ECM biomaterial key structural constituents, according to exemplary embodiments of the disclosed subject matter.

[0031] Figure 6 shows the composition of CF ECM biomaterials by matrisome category, according to exemplary embodiments of the disclosed subject matter.

[0032] Figure 7 shows quantification of cystic fibrosis and control lung ECM biomaterial cytokine profiles, according to exemplary embodiments of the disclosed subject matter.

[0033] Figures 8A-8C show a global analysis of cystic fibrosis lung matrisome, according to exemplary embodiments of the disclosed subject matter.

[0034] Figures 9A-9D show characterization of the core matrix structure and composition in cystic fibrosis and control lung, according to exemplary embodiments of the disclosed subject matter.

[0035] Figures 10A-10D show an analysis of matrix-associated proteins in cystic fibrosis and control lung, according to exemplary embodiments of the disclosed subject matter.

[0036] Figure 11 shows confirmation of WTC11 and CF iPSC differentiation into macrophages with flow cytometry, according to exemplary embodiments of the disclosed subject matter.

[0037] Figure 12 shows an experimental design for macrophage studies, according to exemplary embodiments of the disclosed subject matter.

[0038] Figure 13 shows aspects of cystic fibrosis and WTC11 macrophage and extracellular matrix co-culture system, according to exemplary embodiments of the disclosed subject matter.

[0039] Figures 14A-C show aspects of WTC11 and cystic fibrosis macrophage cytokine expression in response to CF and control lung extracellular matrix, according to exemplary embodiments of the disclosed subject matter.

[0040] Figures 15A-B show aspects of macrophage cytokine expression in response to CF extracellular matrix, according to exemplary embodiments of the disclosed subject matter.

[0041] Figure 16 shows histological imaging of CF and control lungs, according to exemplary embodiments of the disclosed subject matter.

[0042] Figure 17 shows multi-modal imaging of CF and control lungs, according to exemplary embodiments of the disclosed subject matter.

[0043] Figure 18 shows stereotypical alterations to the airways seen in cystic fibrosis patient tissue versus control lung, according to exemplary embodiments of the disclosed subject matter.

[0044] Figure 19 shows heat maps showing differences in lung matrix proteins in cystic fibrosis and control lung tissue, according to exemplary embodiments of the disclosed subject matter.

[0045] Figure 20 shows aspects of molecular function pathways identified as significantly different through gene ontology (GO) analysis, according to exemplary embodiments of the disclosed subject matter.

[0046] Figure 21 shows aspects of cellular component pathways identified as significantly different through gene ontology (GO) analysis, according to exemplary embodiments of the disclosed subject matter.

[0047] Figure 22 shows aspects of biological processes pathways identified as significantly different through gene ontology (GO) analysis, according to exemplary embodiments of the disclosed subject matter.

[0048] Figure 23 shows aspects of reactome pathways identified as significantly different through gene ontology (GO) analysis, according to exemplary embodiments of the disclosed subject matter.

[0049] Figure 24 shows aspects of preparation of matrix extract from whole patient tissue through detergent and enzyme decellularization, according to exemplary embodiments of the disclosed subject matter.

[0050] Figure 25 shows violin plots showing relative abundance of matrix proteins in cystic fibrosis and control matrix extracts, according to exemplary embodiments of the disclosed subject matter.

[0051] Figure 26 shows aspects of molecular function pathways identified as significantly

different through gene ontology (GO) analysis, according to exemplary embodiments of the disclosed subject matter.

[0052] Figure 27 shows aspects of cellular component pathways identified as significantly different through gene ontology (GO) analysis, according to exemplary embodiments of the disclosed subject matter.

[0053] Figure 28 shows aspects of biological processes pathways identified as significantly different through gene ontology (GO) analysis, according to exemplary embodiments of the disclosed subject matter.

[0054] Figure 29 shows aspects of reactome pathways identified as significantly different through gene ontology (GO) analysis, according to exemplary embodiments of the disclosed subject matter.

[0055] Figures 30A-F shows GO networks identified by filtering for upregulated peptides and downregulated peptides, according to exemplary embodiments of the disclosed subject matter.

[0056] Figures 31A-B show aspects of collagen expression in cystic fibrosis and control lung matrix, according to exemplary embodiments of the disclosed subject matter.

DETAILED DESCRIPTION OF EXEMPLARY EMBODIMENTS

[0057] Reference is made in detail to select embodiments of the disclosed subject matter, examples of which are described herein. The method and corresponding steps of the disclosed subject matter are described in conjunction with the detailed description of the system.

Table of Abbreviations
BAL, bronchoalveolar lavage
EMT, epithelial mesenchymal transition
EVG, elastic van Gieson's
GO, gene ontology
LC-MS/MS, liquid chromatography mass spectrometry
MMP, matrix metalloproteinase
PCA, principal component analysis
SEM, scanning electron microscopy
TEM, transmission electron microscopy
TIMP, tissue inhibitor of metalloproteinase

[0058] Manifestations of cystic fibrosis, although well-characterized in the proximal airways, are understudied in the distal lung. In particular, characterization of the cystic fibrosis lung 'matrisome' (matrix proteome) has not been previously described, and could help identify

biomarkers and inform therapeutic strategies.

[0059] Lung matrix structure and composition facilitate gas exchange by providing mechanical integrity to withstand dynamic changes in pressure during breathing, elasticity to ventilate the distal alveoli, and biochemical cues to guide cell behavior and respond to injury. Key structural and biological matrix constituents in the lung include collagens and laminins, which comprise the basement membrane, and elastin which provides the lungs with elastic recoil enabling ventilation. In healthy patients, coordinated matrix remodeling governs lung tissue repair to restore function of an injured area. In diseased lungs, however, the matrix and its reparative wound-healing functions are compromised in a disease-specific manner. Because matrix structure and composition are intrinsically linked to cell, tissue, and organ-level function, we aimed to identify significantly altered matrix components and dysregulated pathways in CF.

[0060] We performed comprehensive, quantitative characterization of the lung matrix in cystic fibrosis, and determined that the lung matrix is pathologically altered in cystic fibrosis and that these alterations have a downstream effect on cell phenotype. This finding led to the incorporation of patient-derived matrix and matrikines in *in vitro* models of disease.

[0061] Matrikines are peptides liberated by partial proteolysis of extracellular matrix macromolecules, which are able to regulate cell activities. They are messenger peptides capable of regulating cell activities by interacting with their specific receptors and can activate certain genes involved in the process of extracellular matrix renewal and cell proliferation. Among these peptides, some of them may modulate proliferation, migration, protease production, or apoptosis, which suggest that they can play a significant role in the control of disease progression. Without limitation, matrikines nay be derived from elastin, connective tissue glycoproteins, or collagens.

[0062] Described herein are (i) materials (i.e., matrix and/or matrikines) that are isolated from human cystic fibrosis lung tissue. Also described is (ii) a disease model that incorporates these materials, (iii) methods for formulating (i) and (ii), and (iv) methods of use for (i) and (ii). Matrix and matrikines are isolated from patient tissue and feature native tissue biomolecular profiles, including core matrix proteins, growth factors, and cytokines. Although described primarily herein for the study of cystic fibrosis lung disease, the platform can be easily extended to include other diseases and organs. In cystic fibrosis, matrix and matrikine profiles can vary from patient-to-patient. Therefore, these materials enable patient-specific disease models for identification of therapeutic targets, validation of therapeutic efficacy, and studies of disease.

[0063] We performed liquid chromatography-mass spectrometry, gene ontology analysis, and multi-modal imaging, including histology, immunofluorescence, and electron microscopy for a

comprehensive evaluation of distal human lung extracellular matrix (matrix) structure and composition in end-stage cystic fibrosis.

[0064] Quantitative proteomic profiling identified sixty-eight (68) matrix constituents with significantly altered expression in end-stage cystic fibrosis. Over 90% of significantly different matrix peptides detected, including structural and basement membrane proteins, were expressed at lower levels in cystic fibrosis. However, the total abundance of matrix in cystic fibrosis lungs was not significantly different from control lungs, suggesting that cystic fibrosis leads to loss of diversity among lung matrix proteins rather than an absolute loss of matrix. Visualization of distal lung matrix via immunofluorescence and electron microscopy revealed pathological remodeling of distal lung tissue architecture and loss of alveolar basement membrane, consistent with significantly altered pathways identified by gene ontology analysis.

[0065] Dysregulation of matrix organization and aberrant wound healing pathways are associated with loss of matrix protein diversity and obliteration of distal lung tissue structure in end-stage cystic fibrosis. While many therapeutics aim to functionally restore defective cystic fibrosis transmembrane conductance regulator (CFTR), drugs that target dysregulated matrix pathways may serve as adjunct interventions to support lung recovery.

[0066] Previous studies identified elevated levels of proteolytic enzymes and matrix breakdown products in the bronchoalveolar lavage (BAL) fluid, sputum, and serum of CF patients, suggesting that matrix alterations mediated by protease/anti-protease imbalance may be a feature of CF. However, a comprehensive quantitative analysis of the CF lung matrisome, which includes constitutive and associated matrix proteins, remains outstanding. Understanding pathologic alterations to the lung matrix in CF may offer prognostic value and could uncover biomarkers of disease severity to inform therapeutic strategies. While gene therapies under development and currently-available cystic fibrosis transmembrane conductance regulator (CFTR) modulators aim to functionally restore CFTR expression, adjunct interventions targeting matrix remodeling could be developed to slow or reverse tissue damage and lung decline.

[0067] Figure 1A shows a schematic overview of the experimental procedure. Cystic fibrosis and control lung tissues were procured to extract and analyze the distal lung matrix structure and composition through proteomic profiling, multimodal imaging (e.g. histology, immunostaining, electron microscopy) and gene ontology.

[0068] Figure 1B shows aspects of the matrix extracted from human cystic fibrosis lung featuring native disease-specific composition and/or mechanics. Isolated lung ECM is obtained through decellularization and can be used to prepare (i) soluble matrikine cocktails, (ii)

decellularized scaffolds, and (iii) hydrogels for various cell culture substrate applications.

[0069] A hydrogel is a biphasic material, a mixture of porous, permeable solids and at least 10% by weight or volume of interstitial fluid comprising mainly water. In hydrogels the porous permeable solid is a water-insoluble three-dimensional network of natural or synthetic polymers and a fluid, having absorbed a large amount of water or biological fluids. The structure is maintained due to chemical or physical cross-linking of individual polymer chains. Hydrogels also possess a degree of flexibility very similar to natural tissue die to their significant water content, allowing for in vitro study of proteins within a hydrogel.

[0070] Hydrogels may be prepared using a variety of polymeric materials, which can be divided broadly into two categories according to their origin: natural or synthetic polymers. Natural polymers for hydrogel preparation include hyaluronic acid, chitosan, heparin, alginate, gelatin and fibrin. Common synthetic polymers include polyvinyl alcohol, polyethylene glycol, sodium polyacrylate, acrylate polymers and copolymers thereof.

[0071] Figures 2A and 2B show aspects of an *in vitro* cystic fibrosis lung model system showing that the CF model recapitulates cell-cell-matrix crosstalk. Figure 2A shows schematically that isolated lung ECM biomaterials (soluble matrikines, scaffolds, hydrogels) may be prepared for incorporation as a disease-specific substrate with multiple cell types (cell types #1 and #2) such as bronchial epithelium, mesenchymal stromal cells, fibroblasts, macrophages, and other cell types. 2B shows example readouts and outputs from the *in vitro* cystic fibrosis model system.

[0072] Figures 3A and 3B show a comparison of CF and normal lung ECM biomaterials using microscopy by Hematoxylin and eosin (H&E) staining of airways and parenchyma from native lung tissue (Fig. 3A) and decellularized extracellular matrix biomaterials (Fig. 3B). CF lung parenchyma displays proteinaceous fluid filled airways and thrombosis compared to healthy parenchyma with clear airway and alveolar space. CF airway cross section reveals epithelial cell hyperplasia, thickened basement membrane, and abnormal airway mucus compared to healthy control with phenotypically normal basement membrane and pseudostratified airway epithelium. CF ECM biomaterial retains features of native CF lung including parenchymal derangement and basement membrane thickening compared to healthy ECM biomaterial.

[0073] Figures 4A and 4B show a comparison of CF and control lung ECM biomaterials composition and ultrastructure. CF and control lung ECM biomaterials were compared with (Fig. 4A) histology including hematoxylin and eosin (H&E), Masson's trichrome (blue, collagens), elastic van Gieson (EVG) (black, elastin), and (Fig. 4B) electron microscopy including scanning electron microscopy (SEM), and transmission electron microscopy (TEM). Figures 4C

and 4D show additional structural comparisons of cystic fibrosis and control lung tissue. Overall tissue structure and composition of the lung parenchyma were evaluated by histology with hematoxylin and eosin (H&E), Masson's trichrome (blue, collagens), and elastic van Gieson (EVG) (black, elastin) (Fig. 4C). Fig. 4D shows scanning electron microscopy (SEM) and transmission electron microscopy (TEM), where * = Airspace, E = elastic fibers, ATII = alveolar type II pneumocyte and arrows = lamellar bodies.

[0074] Figures 5A and 5B show a comparison of CF and control lung ECM biomaterial key structural constituents. Collagen IV, elastin, fibronectin, and laminin were visualized with immunofluorescent imaging (Fig. 5A) and quantified with LC-MS/MS relative abundance (Fig. 5B).

[0075] Figure 6 shows the composition of CF ECM biomaterials by matrisome category. Collagens, glycoproteins, proteoglycans, ECM-affiliated proteins, ECM-regulator proteins, and secreted factors were quantified using LC-MS/MS.

[0076] Figure 7 shows quantification of cystic fibrosis and control lung ECM biomaterial cytokine profiles. Cytokine levels were measured in CF and control lung ECM. The cytokines included EGF, epidermal growth factor; FGF-2, fibroblast growth factor-2; IL-12P40, interleukin 12B; MDC, C-C motif chemokine ligand 22; IL-13, interleukin-13; G-CSF, colony stimulating factor 3; Flt-3L, fms related receptor tyrosine kinase 3; GM-CSF, granulocyte-macrophage colony stimulating factor; IL-1RA, interleukin-1 receptor agonist; IL-1a, interleukin-1alpha; IL-9, interleukin-9; IFN-a2, interferon alpha-2; GRO alpha, C-X-C motif chemokine ligand 1; MCP-3, chemokine ligand 7; IL-4, interleukin-4; MCP-1, monocyte chemoattractant protein-1; IL-18, and interleukin 18. *$p < 0.05$, **$p < 0.01$.

[0077] The matrisome includes a group of proteins encoded by genes for core ECM proteins (collagens, proteoglycans, and ECM glycoproteins) and ECM-associated proteins (proteins structurally resembling ECM proteins, ECM remodeling enzymes, and secreted factors). In mammals the "core matrisome" comprises ~300 proteins, encoded by an ensemble of over 1000 genes. In addition, there are large numbers of ECM-modifying enzymes, ECM-binding growth factors, and other ECM-associated proteins. These different categories of ECM and ECM-associated proteins cooperate to assemble and remodel extracellular matrices and bind to cells through ECM receptors. Together with receptors for ECM-bound growth factors, they provide multiple inputs into cells to control survival, proliferation, differentiation, shape, polarity, and motility of cells. The matrisome can be elucidated by proteomic techniques used in mapping the genome of organisms.

[0078] Here, we report a comprehensive, quantitative analysis of the distal lung matrix proteome (matrisome) in end-stage CF. We hypothesized that dysregulation of matrix pathways and alterations to distal lung matrix structure and composition accompany the well-described hallmarks of CF, including chronic infection, inflammation, structural changes to the airways, and progressive decline in lung function. Changes to the matrix were visualized at multiple scales by histology and electron microscopy. Towards quantitative analysis of the lung matrix, we (i) extracted matrix from CF and control lung tissues, (ii) quantified the composition of extracted matrix with liquid chromatography-mass spectrometry (LC-MS/MS), and (iii) filtered the resultant LC-MS/MS dataset to identify constituents of the lung matrisome (matrix and matrix-associated proteins). Profiles of collagens, glycoproteins, proteoglycans, secreted factors, matrix-regulating, and matrix-affiliated proteins were quantified, and differentially regulated pathways were identified through gene ontology (GO) analysis.

[0079] Significant loss of expression and structural breakdown of key matrix components, including basement membrane proteins, was observed. Pathways including 'extracellular matrix', 'degradation of the extracellular matrix', and 'structural matrix constituents conferring tensile strength' were significantly downregulated in CF. Correlating with loss of matrix organization and diversity, pathways involved in aberrant wound healing were upregulated in CF. Altogether, our findings suggest that pathological changes to the distal lung matrisome accompany other hallmark indicators of end-stage CF, such as stereotypical remodeling of airway structure, and may serve as therapeutic targets or biomarkers of disease state.

[0080] We investigated alterations to the distal lung matrix in end-stage CF, using tissue obtained from explanted lungs of CF patients undergoing lung transplantation. Patient mutations were determined to be ΔF508/ΔF508 (n=5), ΔF508/G542X (n=1), and ΔF508/unknown (n=2) (Supplementary Table 1). CF lung tissues were obtained from a random sample of patients with end-stage CF, and none of the samples were excluded from the study. As the lung matrix provides structural and biochemical cues to resident cells that together govern development, function, and injury response, we sought to investigate pathologic alterations to matrix structure and composition in end-stage CF, using microscopy and liquid chromatography mass spectrometry (LC-MS/MS) analysis.

[0081] Detailed methods can be found in the Experimental Methods. Briefly, lung tissue was obtained at the time of transplantation from explanted lungs from patients with end-stage CF (n=9) and uninjured regions of donor lungs declined for transplantation to serve as controls (n=3). All CF patient tissue underwent multi-modal imaging (n=9), and a subset of patient tissue samples (n=8)

underwent LC-MS/MS. For one CF patient, the right middle lobe was unavailable and instead, tissue was obtained from the lingula. CF patient mutations were determined by isolating genomic DNA and sequencing regions of the CFTR gene where common mutations are found (Supplementary Table 2). Structure and composition of the lung extracellular matrix was analyzed using histology, immunofluorescence, electron microscopy, liquid chromatography mass spectrometry (LC-MS/MS), and gene ontology (GO) analysis.

[0082] *Ultrastructural abnormalities in CF distal lung matrix.* The lung matrix is a complex, well-organized, 3D structure that supports lung function by providing a large surface area for gas exchange and allowing for lung breathing. For a global comparison of matrix structure and tissue morphology in CF compared to control lung, histological staining was performed on lung specimens from all patients to visualize overall tissue histomorphology (H&E), and the distribution of collagen (Masson's trichrome, blue), and elastin (elastic van Gieson, black) (Figures 16 and 17). Figure 16 shows histological imaging of CF and control lungs with H&E, trichrome, and elastin van Gieson (EVG) for samples from all patients and controls.

[0083] Figure 17 shows multi-modal imaging of CF and control lungs, including high magnification histology (H&E, trichrome, EVG), scanning electron microscopy (SEM), and immunofluorescent staining for elastin. Histological staining of airway sections confirmed stereotypical airway morphology, including elevated levels of glycoproteins and mucins (Alcian blue, blue) in CF (Figure 18). Compared to control lung, CF specimens displayed expected septal thickening, fragmented fibers, and proteinaceous fluid-filled airways and alveoli with varying degrees of severity.

[0084] Lung parenchymal ultrastructure and alveolar architecture were grossly abnormal in CF with airway and alveolar obstruction and collapse, as evidenced by scanning electron microscopy (SEM) imaging, indicative of parenchymal destruction. Visual assessment of the epithelium, endothelium, and alveolar basement membrane by transmission electron microscopy (TEM) revealed basement membrane disruption and alveolar collapse (Figures 4B and 4C).

[0085] Figure 19 shows heat maps showing differences in lung matrix proteins in cystic fibrosis and control lung tissue detected using LC-MS/MS of whole patient tissue. Detected peptides were filtered using The Matrisome Project database to specifically identify differential expression of: (A) collagens, (B) glycoproteins, (C) matrix-affiliates, (D) matrix-regulators, and (E) secreted factors.

[0086] *Quantitative analysis of CF distal lung matrisome.* We performed LC-MS/MS on intact distal lung tissues from CF patients and controls to identify changes to the lung proteome. Gene

ontology (GO) analysis of detected peptides revealed that the extracellular space (p = 4.0E-4) and extracellular organelles (p = 1.68E-5) were significantly altered in CF compared to control lung (Figures 20-23). Identification of significant differences in pathways involving the extracellular environment informed deeper analysis of the CF lung matrix. The matrix was then extracted by decellularization of lung tissues, which led to 95% reduction in DNA content and nearly complete removal of DAPI-stained nuclei (Figure 24), while maintaining intact matrix.

[0087] Figure 20 shows aspects of molecular function pathways identified as significantly different through gene ontology (GO) analysis in whole plant tissue from cystic fibrosis and control lung. (A) shows GO terms and (B) shows relevant pathways.

[0088] Figure 21 shows aspects of cellular component pathways identified as significantly different through gene ontology (GO) analysis in whole plant tissue from cystic fibrosis and control lung. (A) shows GO terms and (B) shows relevant pathways.

[0089] Figure 22 shows aspects of biological processes pathways identified as significantly different through gene ontology (GO) analysis in whole plant tissue from cystic fibrosis and control lung. (A) shows GO terms and (B) shows relevant pathways.

[0090] Figure 23 shows aspects of reactome pathways identified as significantly different through gene ontology (GO) analysis in whole plant tissue from cystic fibrosis and control lung. (A) shows GO terms and (B) shows relevant pathways.

[0091] Figure 24 shows aspects of the preparation of matrix extract from whole patient tissue through detergent and enzyme decellularization that results in nearly complete removal of genetic material shown with (A) absence of DAPI signal on histology, and (B) >95% reduction in DNA content detected with PicoGreen DNA assay.

[0092] The full list of peptides identified using LC-MS/MS of extracted lung matrix was filtered using the open-access 'Matrisome Project,' which categorizes matrix proteins as: core matrisome (i.e., collagens, glycoproteins, proteoglycans), matrix-regulators, matrix-affiliated, and secreted factors. The number of matrisome proteins and their relative intensities across each of these categories were compared for CF and control lungs (Figure 25).

[0093] Figure 25 shows violin plots showing relative abundance of matrix proteins in cystic fibrosis and control matrix extracts, including (A) collagens, (B) proteoglycans, (C) glycoproteins, (D) matrix-affiliates, (E) matrix-regulators and (F) secreted factors. Detected proteins are categorized according to The Matrisone Project database.

[0094] Overall, 243 significantly different proteins were detected in the CF matrix, including 14 collagens, 18 glycoproteins, 4 proteoglycans, 10 matrix-regulators, 6 matrix- affiliated, 9

secreted factors, and 182 others (i.e., significantly altered but not considered to be matrisome constituents) (Figure 8B). All except six of the significantly altered matrix proteins were downregulated (MMP11, IL16, TGFB1, VWA5A, LGALS1 and HRG were significantly upregulated). We observed similar changes in the relative intensities of the proteins in the collagens, glycoproteins, and secreted factors categories (Figure 25), indicating similar coverage in both groups. However, there was a decreased abundance of proteoglycans in CF compared to control lung ($p = 0.016$), suggesting the loss of proteoglycan activity in CF. To validate the matrix extraction method, LC-MS/MS was performed on whole lung tissues, and a decrease in matrix proteins was also detected (Figure 19). Using a principal component analysis (PCA) on the extracted matrix LC-MS/MS dataset, we found that 7 out of 8 CF patients clustered together, while control patient samples did not cluster (Figure 8A). The group size was too small to draw definitive conclusions about any mutation-specific alterations to the lung matrix.

[0095] Figures 8A-8C show aspects of a global analysis of the cystic fibrosis lung matrisome. Fig. 8A shows a Principal component analysis (PCA) of CF and control lung matrix. The shape of marker indicates patient mutations: circle, ΔF508/ΔF508; triangle, ΔF508/G542X; hexagon, ΔF508/unknown. Fig. 8B is a Volcano plot of differentially expressed matrisome components. Fig. 8C shows a gene ontology (GO) analysis of pathways significantly altered in CF. BP, biological processes; CC, cellular components; MF, molecular factors.

[0096] Figures 9A-9D show characterization of the core matrix structure and composition in cystic fibrosis and control lung. Expression of core matrisome components, including collagens (Fig. 9A), glycoproteins (Fig. 9B), and (C) proteoglycans (Fig. 9C), using LC-MS/MS is shown. Fig. 9D shows expression of basement membrane constituents and elastin using immunofluorescence.

[0097] Figures 10A-10D show an analysis of matrix-associated proteins in cystic fibrosis and control lung, including matrix-affiliated (Fig. 10A), matrix-regulators (Fig. 10A), and secreted factors (Fig. 10C) in CF and control lung matrisomes. Fig. 10D shows representative immunostaining of differentially expressed proteins in each category. Arrows indicate positive cytoplasmic galectin staining. Asterisks indicate positive nuclear NFκB.

[0098] Aspects of macrophages related to CF progression and control were studied. Macrophages are specialized white blood cells involved in the detection, phagocytosis and destruction of bacteria and other harmful organisms. In addition, they can also present antigens to T cells and initiate inflammation by releasing molecules (known as cytokines) that activate other cells.

[0099] Figure 11 shows confirmation of WTC11 and CF iPSC differentiation into macrophages with flow cytometry. Flow cytometry confirmed expression of CD11b and CD14 in iPSC-derived CF and WTC11 macrophages.

[0100] Figure 12 shows an experimental design for macrophage studies. CF and WTC11 iPSC-macrophages were co-cultured in basal conditions and with CF and control lung ECM. Primary readouts include cytokine expression, RNA sequencing, and gene ontology.

[0101] Figure 13 shows aspects of cystic fibrosis and WTC11 macrophage and extracellular matrix co-culture system. Bright field images of WTC11 and CF macrophages exposed to CF and control lung ECM *in vitro* are shown.

[0102] Figures 14A-C show aspects of WTC11 and cystic fibrosis macrophage cytokine expression in response to CF and control lung extracellular matrix. Fig. 14A shows WTC11 and CF macrophage cytokine expression at baseline. Fig. 14B shows WTC11 and CF macrophage cytokine expression in response to CF lung extracellular matrix. Fig. 14C shows WTC11 and CF macrophage cytokine expression in response to control lung extracellular matrix. MCP-1, monocyte chemoattractant protein-1; IL-8, interleukin 8; IL-18, interleukin 18. *$p < 0.05$; **$p < 0.01$.

[0103] Figures 15A-B show aspects of macrophage cytokine expression in response to CF extracellular matrix. Fig. 15A shows WTC11 macrophages exposed to CF extracellular matrix cytokine expression fold change over basal WTC11 macrophages. Fig. 15B shows CF macrophages exposed to CF extracellular matrix cytokine expression fold change over basal CF macrophages.

[0104] Figure 18 shows stereotypical alterations to the airways seen in cystic fibrosis patient tissue versus control lung shown with H&E and Alcian blue (Representative images are from CF patient #1, CF patient #9, and control #3).

[0105] GO analysis of the full list of significant peptides identified through LC-MS/MS revealed differences in matrix-related pathways in CF versus control lung matrix. Significantly different GO terms included: extracellular matrix ($p = 3.16E-26$), degradation of the extracellular matrix ($p = 2.73E-7$), collagen trimer ($p = 1.09E-11$), structural matrix constituents conferring tensile strength ($p = 5.78E-11$), collagen chain trimerization ($p = 2.93E-10$), and matrix proteoglycans ($p = 5.86E\ 9$) (Figure 8C). Additional significant GO terms related to cell-matrix interactions and cell signaling were identified, including anion binding ($p = 1.19E-6$), focal adhesion ($p = 1.39E-6$), cell-substrate junction ($p = 1.97E-6$), extracellular vesicle ($p = 1.36E-28$), and extracellular exosome ($p = 3.38E-28$).

[0106] After filtering for peptides with log2FC < -1, GO terms identified included: extracellular matrix structural constituent (p = 6.89E-38), collagen binding (p = 9.02E-7), glycosaminoglycan binding (p = 3.33E-6), extracellular matrix organization (p = 1.00E-18), and extracellular structure organization (p = 1.12E-18). Filtering for peptides with log2FC > 1 identified GO terms including: cadherin binding (p = 6.28E-23), unfolded protein binding (p = 3.57E-9), protein-lipid complex (p = 1.78E-12), response to topologically incorrect protein (p = 2.91E-6), response to unfolded protein (p = 2.44E-4), and negative regulation of wound healing (p = 8.16E-3). The complete lists of identified GO pathways can be found in Figures 26-30 and Supplementary Tables 3 and 4.

[0107] Figure 26 shows aspects of molecular function pathways identified as significantly different through gene ontology (GO) analysis in matrix extract from cystic fibrosis and control lung. (A) shows GO terms and (B) shows relevant pathways.

[0108] Figure 27 shows aspects of cellular component pathways identified as significantly different through gene ontology (GO) analysis in matrix extract from cystic fibrosis and control lung. (A) shows GO terms and (B) shows relevant pathways.

[0109] Figure 28 shows aspects of biological processes pathways identified as significantly different through gene ontology (GO) analysis in matrix extract from cystic fibrosis and control lung. (A) shows GO terms and (B) shows relevant pathways.

[0110] Figure 29 shows aspects of reactome pathways identified as significantly different through gene ontology (GO) analysis in matrix extract from cystic fibrosis and control lung. (A) shows GO terms and (B) shows relevant pathways.

[0111] Figures 30A-F shows GO networks identified by filtering for upregulated peptides ($log_2(FC)>1$) and downregulated peptides ($log_2(FC)< -1$). Figs. 30A-B show downregulated and upregulated molecular function networks, Figs. 30C-D show downregulated and upregulated cellular component networks and Figs. 30E-F show downregulated and upregulated biological process networks.

[0112] *Degradation of core proteins in distal lung matrix.* In total, 36 core matrisome proteins (i.e., collagens, proteoglycans, glycoproteins) of the 143 detected were significantly differentially expressed in CF matrix compared to control lung. The majority of collagens (COL4A1/2/3/6, COL5A3, COL6A2/3/5/6, COL11A1, COL21A1, COL26A1, COL12A1, and COL18A1) were significantly downregulated in CF compared to control tissue (Figure 4A). Other collagens (COL15A1, COL23A1, COL10A1, COL5A1, COL1A2) were upregulated in CF, albeit not significantly (Figures 31A-B). Other key basement membrane constituents, including multiple

isoforms of laminin (LAMA2, 4, and 5) and nidogen1 (NID1) were downregulated in CF (LAMA2, log2FC = -1.6, p = 0.025; LAMA4, log2FC = -1.2, p = 0.012; LAMA5, log2FC = -1.3, p = 0.047; NID1, log2FC = -1.3, p = 0.030), indicative of dysregulation of basement membrane in CF lung disease and consistent with TEM and SEM findings. Elastin (ELN, log2FC = -1.6, p = 0.026) which confers lung elasticity was decreased in CF compared to control lung, a trend indicative of possible emphysema (Figure 4B). Notably, perlecan (HSPG2, proteoglycan found in the basement membrane) downregulation accompanied the loss of collagens and laminins (HSPG2, log2FC = -1.36, p = 0.021). Other collagen-interacting proteoglycans were also downregulated, such as osteoglycin (OGN, log2FC = -1.21, p = 0.014), biglycan (BGN, log2FC = -1.08, p = 0.014), and asporin (ASPN, log2FC = -2.21, p = 0.001) (Figure 4C).

[0113] Figures 31A-B show aspects of collagen expression in cystic fibrosis and control lung matrix. Fig. 31A shows a table of collagen expression. Green highlight indicates significance ($p < .05$). Fig. 31B shows a heat map of differential expression of collagens demonstrating hierarchical clustering of patients and genes.

[0100] In line with the matrisome quantification and GO analysis indicating collagen trimer and basement membrane as significantly altered pathways, immunofluorescent staining for collagen IV – a major component of the lung basement membrane – was sparse, poorly organized, and partially degraded in the alveolar septa in CF lung compared to control lung where well-organized collagen IV staining was ubiquitous in the basement membrane. Elastin, which enables cyclic movement during breathing, and laminin, which provides structural support and promotes cell adhesion to the basement membrane, appeared fragmented in CF lungs compared to controls (Figure 4D).

[0101] *Dysregulation of matrix modifying proteins.* Degradation of basement membrane proteins was accompanied by decreased expression of proteins that promote cell adhesion to the basement membrane (C1QTNF5/7, log2FC = -1.3/-1.4, p = 0.017/0.002; SEMA3B, log2FC = -1.6, p = 0.046). Tetranectin (CLEC3B) was found to be downregulated in CF (log2FC = -1.62, p = 0.001). However, galectin-1 (LGALS1) was overexpressed in CF, at moderate to high levels (log2FC = 1.43, p = 0.009), indicative of infection response and myeloid cell recruitment (Figure 5A). Immunostaining of tetranectin in CF samples showed sparse staining, whereas galectin staining was moderately increased in CF compared to control lung.

[0102] Matrix regulators are proteins responsible for crosslinking, degrading, and remodeling the matrix. Consistent with the breakdown of key matrix constituents, we observed significant downregulation of proteins that inhibit matrix degradation, including trypsin inhibitor (ITIH5,

log2FC = -1.82, p = 0.002), serine protease inhibitor (SERPINA5, log2FC = -1.57, p = 0.013), and tissue inhibitor of metalloproteinase 3 (TIMP3, log2FC = -2.62, p = 0.019). Similarly, lower levels of LOXL2 (log2FC = -1.05, p = 0.019), a collagen and elastin crosslinker, correlates with observed decreases in both collagen and elastin levels in CF lung. Matrix metalloprotease (MMP) expression varied, with upregulation of MMP11 and MMP8 and downregulation of MMP28 (Figure 10D).

[0103] Staining for MMP11 was more pronounced in CF compared to control lung. Histidine rich 241 glycoprotein (HRG) which is expressed by platelets and modulates angiogenesis, fibroblast proliferation, complement activation, coagulation, and fibrinolysis, was significantly upregulated (HRG, log2FC = 1.08, p = 0.014) and showed increased expression and more nuclear localization in CF compared to control lung. Other alterations in proteins expressed by or associated with platelets were also observed, including upregulation of platelet derived growth factor subunit B (PDGF-B, log2FC = -1.7, p = 0.028), fibulin-1 (NS), and type 3 collagen (NS).

[0104] Among the secreted factors that were identified, inflammatory markers – including interleukin 16 (IL-16, log2FC = 3.9, p = 0.031) and transforming growth factor beta (TGF-β, log2FC = 2.3, p = 0.024), were all significantly increased in CF compared to control lung, whereas interleukin 17 (IL-17, log2FC = -2.2, p = 0.009) was downregulated. Several constituents of the WNT pathway were significantly downregulated in CF, and β-catenin and NF-kB demonstrated increased nuclear localization (Figure 5C). Consistent with these findings, WNT ligand biogenesis and trafficking (p = 1.05E-7) was identified as a significantly altered pathway via GO analysis (Supplementary Table 3).

[0105] Lung extracellular matrix serves as the major structural component of the lung and provides large surface area for gas exchange in the form of the alveolar basement membrane. In CF, structural remodeling of the airways and elevated levels of proteolytic enzymes and matrix breakdown products in airway fluid are recognized indicators of worsening disease. These well-described features suggest changes to the lung matrix may also be present in CF. Despite the recognized importance of the matrix in lung development, injury, and disease, a comprehensive characterization of the CF lung matrix has not been previously reported. This study addressesthis gap and provides a comprehensive and quantitative analysis of the distal lung matrix in end-stage CF.

[0106] Analysis of CF lung matrix composition and structure revealed pathological remodeling of tissue architecture, destruction of alveolar basement membranes, and significant loss of key constitutive and associated matrix proteins, including collagens, laminins, and elastin. Obliteration of distal lung parenchymal structure and loss of matrix protein diversity were

identified as features of end-stage CF. Through LC-MS/MS analysis of end-stage CF samples in comparison to control lung tissue, we determined that the majority of significantly altered matrix proteins (> 90%) were expressed at lower levels in CF compared to control lung. Interestingly, the total matrix protein abundance in CF and control lung tissue was not significantly different, suggesting that CF does not change the total amount of matrix but instead leads to loss of diversity among matrix proteins.

[0107] In previous studies, matrix-degrading enzymes including neutrophil elastase, collagenases, serine proteases, and matrix metalloproteinases have been identified in airway secretions, BAL fluid, and sputum of CF patients, with elevated levels correlating with pulmonary exacerbations and respiratory decline. Pathologically low levels of protease inhibitors including TIMPs, alpha1-antitrypsin, and SLPI have also been identified in CF, and matrix breakdown products including collagen and elastin fragments were detected in BAL, serum, and urine of CF patient. Here we report a pathologically altered lung matrisome in end-stage CF, which includes destruction of key structural matrix and matrix-associated proteins. Taken with the prior evidence in the literature, these findings suggest that matrix breakdown may correlate with functional decline of the lung in CF.

[0108] The lung matrix serves as a structural scaffold that provides macro- and micro-scale features to support lung function, including ventilation and oxygenation. For example, elastin confers the lung with appropriate compliance and enables dynamic movement during breathing, and basement membrane proteins provide a well-organized, thin membrane across which gas exchange occurs. Disruption to matrix proteins that enable ventilation and oxygenation has a deleterious effect on lung function. Our findings indicate that matrix constituents involved in lung elasticity (i.e., elastin) and basement membrane integrity (i.e., collagen IV, laminin) are pathologically altered in CF.

[0109] Elastin was degraded in end-stage CF, as evidenced by LC-MS/MS and immunofluorescence. We also observed a loss of lysyl oxidase 2 (LOXL2), which functions as an elastin crosslinker to stabilize the matrix. These findings are consistent with features of emphysema, in which protease and antiprotease imbalance and immune cell recruitment lead to irreversible destruction of the lung parenchyma, loss of tissue elasticity, and impairment of proper ventilation. Evidence of tissue breakdown, similar to that in emphysematous lung, was also observed on histology in CF specimens. Similarly, prior work has suggested emphysema as a unifying feature in end-stage CF based on histopathological and radiographic analysis.

[0110] Basement membrane constituents, including several isoforms of collagen IV and

laminin which were visualized with immunofluorescence and quantified with LC-MS/MS, were degraded in end-stage CF, consistent with dysregulation of the basement membrane and alveolar structure observed on SEM and TEM. Disruption to the basement membrane is a feature of many acute and chronic lung pathologies (e.g., emphysema, COPD, acute respiratory distress syndrome (ARDS)), contributing to functional impairment of the lung by compromising the integrity of the blood-gas barrier. This pattern of destruction may be mediated by an imbalance between proteases and protease inhibitors, and has been shown to correlate with mortality in other respiratory conditions. Loss of basement membrane integrity in CF may contribute to cytokine release that triggers paracrine-mediated inflammation, as well as edema and alveolar fluid retention, leading to impaired gas exchange.

[0111] Gene ontology analysis revealed several pathways involving cell-matrix interactions and cellular function, including cell-substrate junction, focal adhesion, extracellular vesicles, cellular component biogenesis and cellular localization, indicating that matrix degradation has downstream effects on cell populations in the lung. Furthermore, significantly altered matrix-associated proteins were identified via LC-MS/MS, including galectin which mediates cell-matrix interactions and proliferation, and tetranectin which binds to plasminogen and may regulate secretion and exocytosis. IL-16 and TGF-β were both significantly increased in CF lung tissue and response to TGF-β was an identified GO term, indicative of the inflammatory process that contributes to aberrant wound healing and can signal epithelial-mesenchymal transition (EMT), a common pathway implicated in many lung diseases. Proteins involved in EMT including several WNT proteins, were altered in CF compared to control lungs. Dysregulated EMT has deleterious effects on lung cell phenotype and function by: (i) impairing epithelial barrier function and innate defense mechanisms, (ii) enabling migration of activated stromal cells throughout the lung matrix, and (iii) promoting stromal cell hyperplasia while compromising pseudostratified airway epithelium.

[0112] Interestingly, in the filtered LC-MS/MS dataset for downregulated peptides ($log2FC < -1$), GO terms identified included several pathways involved in matrix structure and organization, such as extracellular matrix structural constituent, extracellular matrix organization, and degradation of the extracellular matrix. Additionally, several GO pathways that were identified in the downregulated dataset implicate the basement membrane specifically, including basement membrane, collagen type IV trimer, and laminin complex. In comparison, when the dataset was filtered for upregulated peptides ($log2FC > 1$), the identified GO pathways included cellular responses to topologically incorrect protein and unfolded protein, along with negative regulation

of wound healing. These findings suggest that downregulation of matrix organizational pathways may result in destruction of matrix and aberrant cellular response to matrix fragments (i.e., matrikynes) present in the extracellular environment.

[0113] Described herein are: (i) Matrix extracted from human cystic fibrosis lung featuring native disease-specific composition and/or mechanics; (ii) Matrikines extracted from human cystic fibrosis lung featuring native tissue biomolecular profiles; and (iii) A method for extracting human cystic fibrosis lung matrix and/or matrikines from diseased and normal tissues. The matrix or matrikines can be used to condition or culture cells or to utilize as a therapeutic delivery vehicle. An in vitro cystic fibrosis lung model system that incorporates the CF matrix or matrikines or other disease-specific human tissue components and factors, including cells, matrix, matrikines, mucus, sputum, bronchoalveolar lavage fluid, serum, plasma, extracellular vesicles, micro-organisms, and/or other soluble factors is proposed. This model system can be used to study cystic fibrosis or other lung diseases *ex vivo*. The model system can be used to culture or co-culture cells *in vitro*, including epithelium, endothelium, stromal, or immune lineages, to model disease-specific mechanisms, e.g., cell-cell or cell-matrix interactions, or other crosstalk in vitro. The model system could be used to identify therapeutic targets, develop therapeutics or drugs, test therapeutics or drugs, or evaluate the efficacy of gene or cell therapy to treat cystic fibrosis. The model system could be used to study various CFTR mutations, CFTR signaling, or to evaluate CFTR-targeting therapeutics, including modulators and correctors.

[0114] Several outstanding questions remain toward better understanding of the complex changes in CF matrix. This study only evaluated end-stage CF lung samples obtained at the time of lung transplant. Future studies should assess temporal changes to the matrix in comparison with age-matched controls, and determine specific effects on cell phenotype and function. The number of samples in this study was too small to determine if mutation-specific changes to the matrix occur, and data on clinical history was not available because patient samples were obtained as de-identified surgical waste that was considered non-human subjects research. Future studies with larger patient cohorts could reveal correlations between matrix changes, clinical status, and CFTR mutation(s).

[0115] The study was focused on tissue-level changes, therefore alterations to protease levels in BAL or sputum were not analyzed. Longitudinal proteomic analysis of multiple sample types (i.e., tissue, serum, BAL fluid, urine, etc.) from individual patients may enable mechanistic understanding of disease processes involving matrix degradation. While sampling distal lung tissue via biopsy is challenging, identification of serum or BAL markers that correlate with lung

matrix degradation could inform patient care, as previous studies have shown that administration of nebulized or intravenous medication can mitigate elevated proteolytic enzyme levels in BAL fluid.

[0116] It is unclear if matrix breakdown is intrinsically driven by loss of CFTR expression or if chronic infection is the primary driver of matrix destruction. Comparison of matrix composition in other organs affected by CF (i.e., pancreas, liver) that are not undergoing an infectious process may offer insights into the relative contributions of intrinsic loss of CFTR versus chronic lung infection to matrix breakdown. For example, increased collagen deposition has been reported in liver and pancreas of CF patients, suggesting that matrix degradation in the lung may be primarily driven by chronic infection and corresponding immune response rather than loss of CFTR. Similarly, elevated protease levels correlate with bronchiectasis and tissue damage in primary ciliary dyskinesia, indicating that persistent respiratory infection triggers matrix breakdown pathways even in the presence of functioning CFTR. Nevertheless, the extent to which CFTR loss contributes to parenchymal obliteration in CF should be further evaluated. Comprehensive matrisome analyses of lung tissues from COPD and IPF have been previously reported, and when taken with our findings, suggest that changes to the lung matrix are disease- specific. Though these diseases differ in their underlying pathophysiology, cross-disease matrix comparison may unveil common pathways implicated in lung inflammation, matrix remodeling, and tissue repair, which could serve as therapeutic targets.

[0117] CFTR modulator drugs such as Trikafta have revolutionized the cycle-of-care for CF patients and led to dramatic improvements in functional lung parameters. The ability of these CFTR-targeting medications to indirectly prevent matrix degradation, recover dysregulated matrix pathways, or repair degraded lung matrix should be evaluated. Drivers of matrix destruction identified in this study could act as therapeutic targets or biomarkers to monitor disease progression. Drugs targeting dysregulated matrix pathways may serve as adjunct interventions to CFTR modulators to support repair of damaged tissue and recovery of lung function in CF patients.

EXPERIMENTAL METHODS

Human lung tissue collection

[0118] Lung tissue was obtained at the time of transplantation from the right middle lobe of patients with end-stage cystic fibrosis (CF) (n=9) and from uninjured regions of donor lungs declined for transplant serving as controls (n=3). For one CF patient, the right middle lobe was not available, and tissue was instead collected from the lingula. CF patient tissue underwent processing for multi-modal imaging (n=9, CF Patients #1 – 9) and LC-MS/MS (n=8) (CF Patients #1 – 8).

For the control group, lungs with underlying pathology (e.g., fibrosis) were excluded. Explanted human lung specimen deemed surgical waste were fully de-identified prior to sample processing and analysis. Therefore, no clinical history or patient data was available. Tissue samples were collected from the most distal region of procured lobes and were processed in parallel.

Identification of patient mutations

[0119] DNA was isolated from CF lung tissue samples using Qiagen DNeasy Blood & Tissue Kit according to manufacturer's instructions. Exons 10, 11, 12, 23 and 24 were amplified using PCR and custom primers (**Supplementary Table 2**). Sanger sequencing of amplified regions was performed to identify individual patient mutations (Genewiz).

Histology

[0120] Lung specimens were fixed in cold phosphate-buffered 4% paraformaldehyde for 24 hours, embedded in paraffin, and sectioned at 5 μm thickness. Sections were stained with hematoxylin and eosin (H&E), Masson's trichrome, elastic van Gieson's (EVG), pentachrome, and Alcian blue (pH = 2.5) by the histology service in the Department of Molecular Pathology at Columbia University Medical Center and examined via light microscopy.

Immunohistochemistry

[0121] Lung samples were de-paraffinized, submerged in boiling citrate buffer (pH 6.0) or EDTA buffer (pH 8.0) for antigen retrieval for 20 minutes, and blocked with 10% normal donkey serum in phosphate-buffered saline for 2 hours at room temperature. Primary antibodies were added and incubated for 12 hours at 4°C, or 4 hours at 25°C. Secondary antibody was diluted 1:500 and incubated for 1 hour at 25°C. Sections were mounted in mounting medium (Vectashield Mounting Medium; Vector Laboratories) with DAPI, cover-slipped, and imaged with a Leica DMi8 fluorescence microscope.

Transmission electron microscopy (TEM)

[0122] Lung specimens were fixed with 2.5% glutaraldehyde, 4% paraformaldehyde, and 0.02% picric acid in 0.1 M sodium cacodylate buffer (pH 7.2). Samples were then post-fixed with 1% OsO4 in Soreson's buffer for 1 hour, dehydrated, and embedded in Lx-112 (Ladd Research Industries). Sections (60 nm) were prepared using an ultramicrotome (PowerTome PT XL; RMC), stained with uranyl acetate and lead citrate and examined with a transmission electron microscope (JEM-1200 EXII; JEOL). Images were captured with a digital camera (ORCA-HR; Hamamatsu) and recorded with imaging software (Image Capture Engine v.602.569; AMT). TEM imaging was not available for all control lung samples. Therefore, the representative control lung TEM image was obtained from an additional lung (deceased donor with no underlying disease) that was not

included in the LC-MS/MS analysis.

Scanning electron microscopy (SEM)

[0123] Lung specimens were fixed in 2.5% glutaraldehyde at room temperature for 1 hour then overnight at 4°C, rinsed in 70% ethanol, frozen, and lyophilized. Samples were imaged using a scanning electron microscope (GeminiSEM 300; Zeiss) with accelerating voltage of 5.0 kV.

Extraction of distal lung matrix

[0124] Lung matrix was extracted via detergent and enzyme decellularization. Human lung tissue was rinsed in phosphate-buffered saline. Lungs were sliced into 2-mm sheets and washed with sterile water for 30 minutes to remove residual blood and debris. Tissue slices were then subject to four 2-hour wash cycles with CHAPS detergent (8mM CHAPS, 1M NaCl, and 25mM EDTA) followed by rinses with dH2O and 2X PBS. Following this, tissue sheets were rinsed in benzonase precondition buffer (50mM tris-HCl, 0.1 mg/mL bovine serum albumin (BSA), 1mM MgCl2) and then subject to enzyme decellularization by washing with benzonase (90 U/mL; Sigma-Aldrich) in benzonase precondition buffer. Tissue was then rinsed with PBS, snap frozen in liquid nitrogen, pulverized into a fine powder using mortar and pestle, and dehydrated using a lyophilizer.

Preparation of distal lung matrix for LC-MS

[0125] Lung tissue and extracted lung matrix were resuspended in sodium deoxycholate (SDC) lysis buffer (1% SDC, 10 mM TCEP, 40 mM CAA and 100 mM TrisHCl pH 8.5) and boiled for 20 min at 60°C, 1500 rpm on thermomixer (Eppendorf Thermomixer C) to denature and reduce and alkylate cysteines, followed by sonication in a water bath, cooled down to room temperature. ECM samples then underwent deglycosylation with PNGaseF (500 U/ µl) at 37° C and 1500 rpm in a thermomixer (Eppendorf Thermomixer C) as in previous protocols. Protein digestion was performed by adding LysC and trypsin in a 1:50 ratio (µg of enzyme to µg of protein) at 37°C and 1500 rpm for 2 hours and overnight in a thermomixer (Eppendorf Thermomixer C), respectively. Peptides were then acidified with 1% trifluoroacetic acid (TFA) and subjected to StageTip clean-up via styrenedivinylbenzene-reverse phase sulfonate (SDB-RPS). Peptides were washed with 1% TFA 99% ethyl acetate followed by 0.2% TFA 5% acetonitrile (ACN) at 1000 x g, and eluted with 1% Ammonia, 50% ACN and dried at 60°C in a SpeedVac centrifuge.

Liquid chromatography mass spectrometry for matrisome quantification

[0126] Peptides were resuspended in 3% acetonitrile/0.1% formic acid and injected on Thermo Scientific™ Orbitrap Fusion™ Tribrid™ mass spectrometer for peptide tandem mass spectrometry (MS/MS) analysis. The UltiMate 3000 Ultra High-Performance Liquid

Chromatography (UHPLC) system (Thermo Scientific) and EASY-Spray PepMap column (Thermo Fisher Scientific, RSLC C18 50 cm x 75 μm ID) coupled with Orbitrap Fusion (Thermo) were used to separate fractioned peptides with a 5-30% acetonitrile gradient in 0.1% formic acid over 120 min at a flow rate of 250 nL/min. After each gradient, the column was washed with 90% buffer B for 5 min and re-equilibrated with 98% buffer A (0.1% formic acid, 100% high performance liquid chromatography (HPLC)-grade water) for 40 min. Survey scans of peptide precursors were performed from 350-1200 *m/z* at 120K full width at half maximum (FWHM) resolution (at 200 *m/z*) with a 1 x 106 ion count target and a maximum injection time of 60 ms with 3 s cycles for the survey and the MS/MS scans. After a survey scan, 26 m/z DIA segments were acquired from 200-2000 *m/z* at 60K FWHM resolution (at 200 *m/z*) with a 1 x 106 ion count target and a maximum injection time of 118 ms. High-energy collisional dissociation (HCD) fragmentation was applied with 27% collision energy and resulting fragments were detected using the rapid scan rate in the Orbitrap.

Data analysis

[0127] Data independent acquisition (DIA) data were analyzed with directDIA 2.0 (Deep learning augmented spectrum-centric DIA analysis) in Spectronaut Pulsar X, a mass spectrometer vendor independent software from Biognosys. Default settings were used for targeted analysis of DIA data in Spectronaut, except the decoy generation was set to "mutated." LC-MS/MS data was filtered for proteins identified by more than one unique peptide, and global normalization was applied using the median intensity of identified peptides. Classification of identified proteins into matrisome subgroups was done using the protein lists presented by Naba et al. in the Matrisome Project to subset the dataset into: (i) core matrisome (collagens, proteoglycans, and glycoproteins),

[0128] (ii) matrix-affiliated proteins, and (iii) matrix-regulator proteins, and (iv) secreted proteins.

Gene ontology term enrichment analysis

[0129] Gene ontology (GO) enrichment analysis was performed using g:Profiler. Overrepresented terms were determined using Fisher's exact with FDR multiple test correction ($Q < 0.05$).

Statistical analysis

[0130] The false discovery rate (FDR) was estimated with the mProphet approach and set to 1% at the peptide precursor level and at 1% at the protein level. Results obtained from Spectronaut were further analyzed using the Spectronaut statistical package. Significance wasdetermined by unpaired t-test with a threshold for significance of $p < 0.05$ (permutation-based FDR correction)

and |log2FC| > 1.

Table 1 | Biomolecular profile of cystic fibrosis extracellular matrix biomaterials

Protein Name	Description
Actin, aortic smooth muscle	Marker of activated myofibroblasts in idiopathic pulmonary fibrosis; expressed by airway and vascular smooth muscle cells
Actin, cytoplasmic 2	Regulates mucus secretion and ENaC channel function
Biglycan	Structural component of ECM; signaling molecule indicative of tissue stress or injury; regulates inflammation and immunity
Clusterin	Extracellular clusterin signals apoptosis; Intracellular clusterin promotes wound healing
Collagen alpha-1(I) chain	Expressed by profibrotic airway macrophages in pulmonary fibrosis; correlated with immune infiltration
Collagen alpha-1(II) chain	Marker of epithelial-mesenchymal transition; Mutatons lead to lung hypoplasia
Collagen alpha-1(III) chain	Upregulated in response to lung injury and fibrosis
Collagen alpha-1(VI) chain	Plays a critical role in lung development; Loss of COL6A1 and
Collagen alpha-2(VI) chain	COL6A2 leads to chest wall contractures, scoliosis, and muscle
Collagen alpha-3(VI) chain	weakness; Loss of COL6A2 leads to chest wall contractures, scoliosis, and muscle weakness
Collagen alpha-2(I) chain	Fibril-forming collagen; Involved in myofibroblast differentiation in lung
Cytoplasmic dynein 2 heavy chain 1	Supports ciliary function and innate immune response
Fibrinogen beta chain	Secreted basolaterally by pulmonary epithelium
Lumican	Regulates collagen organization, epithelial cell migration, and tissue repair
Mimecan	Interacts with TGFB and VEGF; Modultes endothelial and vascular smooth muscle integrity
Phosphatidylinositol 3,4,5-trisphosphate-dependent Rac exchanger 2 protein	Plays a role in insulin signaling; Implicated in many cancers
Prolargin	Anchors basement membrane to underlying connective tissue; binds proteoglycans
Translgutaminase 2	Mediates alveolar macrophage activation and lung inflammation; Regulates innate immunity
Vitronectin	Glycoprotein released during inflammation; regulates cell growth and mesenchymal epithelial transition
Zinc finger protein 251	Regulates transcription, proliferation, differentiation via ERK signaling pathway

Supplementary Table 1. Summary of patient mutations.

Patient 1	ΔF508/ΔF508
Patient 2	ΔF508/ΔF508
Patient 3	ΔF508/ΔF508
Patient 4	ΔF508/ΔF508
Patient 5	ΔF508/ΔF508
Patient 6	ΔF508/unknown

Patient 7	ΔF508/G542K
Patient 8	ΔF508/unknown

Supplementary Table 2. Summary of primers used to detect patient mutations using PCR.

Exon	Forward primer	Reverse primer
Exon 10	TTTAGATCATGTCCTCTAGAAACCG	CCATGTGCAAGATACAGTGTTGA
Exon 11	GTGAGCACTTGGCAACTGTTAG	TGCAAGCTTCTTAAAGCATAGGT
Exon 12	AATGGACCTATGGATGATCTACAC	ACACCAAGATACGGGCACAG
Exon 23	AAGGAAGTCTGCATCAGGGGT	CCTGGCGATTGCTAACTTGGA
Exon 24	AAAATGTTCACAAGGGACTCCAA	AGTTAGGGGTAGGTCCAGTC

Supplementary Table 3. GO analysis filtered for peptides with log2(FC) < -1

	GO Term	Adjusted P Value	Relevant Genes Identified
Molecular Factors	extracellular matrix structural constituent	6.8936E-38	TINAGL1, LAMC1, BGN, DPT, MXRA5, COL5A3, COL8A1, LAMA4, LAMB2, OGN, COL6A2, LAMA5, NID1, HSPG2, NPNT, SRPX, COL6A3, TGFBI, THSD4, POSTN, COL7A1, MFGE8, LAMA2, ELN, ABI3BP, COL4A4, COL12A1, COL4A3, COL6A6, COL18A1, COL4A1, COL4A2, COL21A1, ASPN, FMOD, SRPX2, COL4A6, COL11A1, COL4A5, COL6A5, HAPLN1, ACAN, MATN1, MUC5AC, MATN3
	extracellular matrix structural constituent conferring tensile strength	2.9150E-17	COL5A3, COL8A1, COL6A2, COL6A3, COL7A1, COL4A4, COL12A1, COL4A3, COL6A6, COL18A1, COL4A1, COL4A2, COL21A1, COL4A6, COL11A1, COL4A5, COL6A5
	sulfur compound binding	9.0036E-08	CHST12, FGF2, GSTP1, SOD3, COL5A3, LIPH, SULT1A1, CCDC80, HPSE2, ECM2, FBLN7, POSTN, GAL3ST4, SERPINA5, CTSG, CLEC3B, GSTM3, ABI3BP, ENPP1, CFH, APOB, COL11A1, ELANE
	collagen binding	9.0150E-07	ITGA3, COL5A3, COL6A2, PDGFA, NID1, ECM2, TGFBI, ABI3BP, PDGFB, P3H1, ASPN, MMP12
	aldehyde dehydrogenase (NAD+) activity	1.9832E-06	ALDH3B1, ALDH1B1, ALDH1A1, ALDH2, ADH5, ALDH9A1, ALDH1A2
	aldehyde dehydrogenase [NAD(P)+] activity	3.3226E-06	ALDH3B1, ALDH1B1, ALDH1A1, ALDH2, ADH5, ALDH9A1, ALDH1A2
	glycosaminoglycan binding	3.3292E-06	FGF2, SOD3, BGN, COL5A3, LIPH, CCDC80, EPYC, ECM2, FBLN7, POSTN, SERPINA5, CTSG, CLEC3B, ABI3BP, CFH, APOB, COL11A1, ELANE, HAPLN1, ACAN
	heparin binding	1.8197E-05	FGF2, SOD3, COL5A3, LIPH, CCDC80, ECM2, FBLN7, POSTN, SERPINA5, CTSG, CLEC3B, ABI3BP, CFH, APOB, COL11A1, ELANE
	extracellular matrix structural constituent conferring compression resistance	2.7083E-05	BGN, OGN, HSPG2, ASPN, FMOD, HAPLN1, ACAN
	cytokine activity	6.1357E-05	FGF2, WNT4, LEFTY2, WNT7A, BMP5, CXCL12, WNT7B, TNFSF10, BMP3, TNFSF12, WNT11, WNT3A, WNT5A, GDF10, CRLF1, WNT2, WNT2B, IL17D
	frizzled binding	1.0308E-04	WNT4, WNT7A, WNT7B, WNT11, WNT3A, WNT5A, WNT2, WNT2B
	oxidoreductase activity, acting on the aldehyde or oxo group of donors, NAD or NADP as ac	1.0308E-04	ALDH3B1, DLAT, ALDH1B1, ALDH1A1, ALDH2, ADH5, ALDH9A1, ALDH1A2
	oxidoreductase activity, acting on the aldehyde or oxo group of donors	5.8036E-04	ALDH3B1, DLAT, ALDH1B1, ALDH1A1, ALDH2, ADH5, ALDH9A1, ALDH1A2
	extracellular matrix binding	1.4973E-03	TINAGL1, ITGA3, BGN, NID1, TGFBI, DMBT1, ELN, COL11A1
	integrin binding	4.2052E-03	FGF2, ITGA3, LAMB2, CD177, LAMA5, CXCL12, NPNT, ECM2, TGFBI, MFGE8, COL4A3, DST
	3'-phosphoadenosine 5'-phosphosulfate binding	4.9876E-03	CHST12, SULT1A1, GAL3ST4, ENPP1
	endopeptidase inhibitor activity	2.6902E-02	C3, TFPI, RPS6KA1, AMBP, COL6A3, COL7A1, SERPINA5, ITIH5, UBE2Z, COL4A3, SLPI, TIMP3
	peptidase inhibitor activity	3.7137E-02	C3, TFPI, RPS6KA1, AMBP, COL6A3, COL7A1, SERPINA5, ITIH5, UBE2Z, COL4A3, SLPI, TIMP3

Supplementary Table 3. GO analysis filtered for peptides with log2(FC) < -1

GO Term	Adjusted P Value	Relevant Genes Identified
glyceraldehyde-3-phosphate dehydrogenase (NAD+) (non-phosphorylating) activity	4.8492E-02	ALDH1B1, ALDH2, ALDH9A1

Supplementary Table 3. GO analysis filtered for peptides with log2(FC) < -1

	GO Term	Adjusted P Value	Relevant Genes Identified
Biological Processes	extracellular matrix organization	1.0042E-18	ITGA3, LAMC1, LOXL2, DPT, COL5A3, COL8A1, LAMB2, CCDC80, HPSE2, QSOX1, NID1, NPNT, ECM2, TGFBI, THSD4, POSTN, ELN, WNT3A, CTSG, MMP28, ABI3BP, MMP19, COL4A4, COL12A1, COL4A3, COL6A6, COL18A1, COL4A1, COL4A2, COL21A1, FMOD, MMP12, COL4A6, COL11A1, ELANE, COL4A5, COL6A5, ACAN
	extracellular structure organization	1.1219E-18	ITGA3, LAMC1, LOXL2, DPT, COL5A3, COL8A1, LAMB2, CCDC80, HPSE2, QSOX1, NID1, NPNT, ECM2, TGFBI, THSD4, POSTN, ELN, WNT3A, CTSG, MMP28, ABI3BP, MMP19, COL4A4, COL12A1, COL4A3, COL6A6, COL18A1, COL4A1, COL4A2, COL21A1, FMOD, MMP12, COL4A6, COL11A1, ELANE, COL4A5, COL6A5, ACAN
	external encapsulating structure organization	1.3984E-18	ITGA3, LAMC1, LOXL2, DPT, COL5A3, COL8A1, LAMB2, CCDC80, HPSE2, QSOX1, NID1, NPNT, ECM2, TGFBI, THSD4, POSTN, ELN, WNT3A, CTSG, MMP28, ABI3BP, MMP19, COL4A4, COL12A1, COL4A3, COL6A6, COL18A1, COL4A1, COL4A2, COL21A1, FMOD, MMP12, COL4A6, COL11A1, ELANE, COL4A5, COL6A5, ACAN
	renal system development	1.6211E-08	FGF2, ITGA3, MPST, PLXND1, WNT4, LAMB2, PECAM1, LAMA5, PDGFA, NID1, ACE, WNT7B, BMPER, NPNT, WNT11, TEK, WNT5A, PDGFB, COL4A4, COL4A3, CRLF1, COL4A1, WNT2B, CNTRL, MME, ALDH1A2
	kidney development	5.1899E-08	FGF2, ITGA3, MPST, PLXND1, WNT4, LAMB2, PECAM1, LAMA5, PDGFA, NID1, ACE, WNT7B, BMPER, NPNT, WNT11, TEK, WNT5A, PDGFB, COL4A4, COL4A3, CRLF1, WNT2B, CNTRL, MME, ALDH1A2
	collagen fibril organization	1.9608E-07	LOXL2, DPT, COL5A3, COL12A1, COL4A3, COL4A1, COL4A2, COL21A1, FMOD, COL4A6, COL11A1, COL4A5, ACAN
	positive regulation of cell-substrate adhesion	3.1488E-07	ITGA3, RRAS, WNT4, COL8A1, CIB1, CCDC80, NID1, NPNT, ECM2, MYADM, TEK, ABI3BP, PDGFB, LIMS2, EPB41L5, COL26A1
	cartilage development	7.2416E-06	FGF2, ACVRL1, LOXL2, BGN, WNT7A, BMP5, WNT7B, EPYC, BMP3, TGFBI, WNT11, WNT5A, WNT2B, COL11A1, ACAN, MATN1, MATN3, CNMD
	cellular aldehyde metabolic process	1.1511E-05	ALDH3B1, WNT4, BMP5, ALDH1A1, PDXK, ALDH2, AKR1C1, ADH5, ALDH9A1, ESD, ALDH1A2
	regulation of cell-substrate adhesion	2.1389E-05	ITGA3, ACVRL1, RRAS, WNT4, COL8A1, CIB1, CCDC80, NID1, NPNT, ECM2, MYADM, TEK, ABI3BP, PDGFB, LIMS2, EPB41L5, MMP12, COL26A1
	nephron development	3.2046E-05	FGF2, ITGA3, WNT4, LAMB2, PECAM1, LAMA5, NID1, WNT7B, NPNT, WNT11, TEK, PDGFB, COL4A4, COL4A3, WNT2B
	connective tissue development	1.0055E-04	FGF2, ACVRL1, LOXL2, BGN, WNT7A, BMP5, WNT7B, EPYC, BMP3, TGFBI, WNT11, WNT5A, PDGFB, WNT2B, COL11A1, ACAN, MATN1, MATN3, CNMD
	endothelial cell proliferation	3.0255E-04	FGF2, ACVRL1, LOXL2, RPTOR, CXCL12, BMPER, TNFSF12, TEK, WNT5A, PDGFB, COL4A3, WNT2, ALDH1A2, CNMD
	regulation of vasculature development	3.5991E-04	C3, FGF2, ACVRL1, GLUL, RRAS, PLXND1, WNT4, RNH1, BMPER, HSPG2, CLDN5, TNFSF12, TEK, WNT5A, COL4A3, COL4A2, PIK3R6, GTF2I, CNMD

Supplementary Table 3. GO analysis filtered for peptides with log2(FC) < -1

	GO Term	Adjusted P Value	Relevant Genes Identified
Biological Processes	sulfur compound metabolic process	3.7722E-04	CHST12, ABHD14B, DLAT, EEF1G, MPST, GSTP1, BGN, PAPSS2, SULT1A1, SQOR, B3GALT6, CLIC5, SMS, CHST14, GAL3ST4, PDK4, GSTM3, SOD1, ENPP1, GSTM5, HSPA9
	response to transforming growth factor beta	1.0315E-03	ITGA3, ACVRL1, WNT4, MXRA5, LEFTY2, WNT7A, PDGFA, NPNT, CLDN5, CLEC3B, WNT5A, EPB41L5, GDF10, WNT2, COL4A2, ASPN, FMOD
	positive regulation of epithelial cell proliferation	1.2624E-03	FGF2, LAMC1, ACVRL1, GLUL, RPTOR, WNT7A, BMP5, CXCL12, TNFSF12, WNT3A, TEK, WNT5A, PDGFB, WNT2, MMP12
	regulation of epithelial cell proliferation	1.2830E-03	FGF2, LAMC1, ACVRL1, GLUL, RPTOR, WNT7A, BMP5, CXCL12, TNFSF12, EPPK1, WNT3A, TEK, WNT5A, PDGFB, LIMS2, COL4A3, WNT2, ALDH1A2, MMP12, CNMD
	regulation of angiogenesis	1.3767E-03	C3, FGF2, ACVRL1, GLUL, RRAS, PLXND1, RNH1, BMPER, HSPG2, CLDN5, TNFSF12, TEK, WNT5A, COL4A3, COL4A2, PIK3R6, GTF2I, CNMD
	collagen-activated tyrosine kinase receptor signaling pathway	1.6881E-03	COL4A3, COL4A1, COL4A2, COL4A6, COL4A5
	regulation of embryonic development	1.7573E-03	WNT4, LAMA4, RAB14, LAMA5, LAMA2, WNT3A, TRIP12, WNT2, WNT2B
	primary alcohol metabolic process	1.7800E-03	ALDH3B1, WNT4, GPD1, SULT1A1, BMP5, ALDH1B1, ALDH1A1, ALDH2, AKR1C1, ADH5, ALDH1A2
	developmental induction	2.6159E-03	FGF2, WNT4, WNT11, WNT3A, WNT5A, WNT2, WNT2B
	epithelial cell migration	2.6606E-03	FGF2, ITGA3, ACVRL1, GLUL, LOXL2, RRAS, PLXND1, WNT7A, CIB1, BMPER, TNFSF12, EPPK1, TEK, WNT5A, PDGFB, EPB41L5, HDAC7, SRPX2
	epithelium migration	3.0805E-03	FGF2, ITGA3, ACVRL1, GLUL, LOXL2, RRAS, PLXND1, WNT7A, CIB1, BMPER, TNFSF12, EPPK1, TEK, WNT5A, PDGFB, EPB41L5, HDAC7, SRPX2
	positive regulation of animal organ morphogenesis	3.2034E-03	FGF2, WNT4, WNT11, WNT3A, WNT5A, WNT2, WNT2B
	regulation of endothelial cell proliferation	3.4674E-03	FGF2, ACVRL1, RPTOR, CXCL12, TNFSF12, TEK, WNT5A, PDGFB, COL4A3, WNT2, ALDH1A2, CNMD
	cellular response to transforming growth factor beta stimulus	3.6216E-03	ITGA3, ACVRL1, WNT4, LEFTY2, WNT7A, PDGFA, NPNT, CLDN5, CLEC3B, WNT5A, EPB41L5, GDF10, WNT2, COL4A2, ASPN, FMOD
	tissue migration	4.1054E-03	FGF2, ITGA3, ACVRL1, GLUL, LOXL2, RRAS, PLXND1, WNT7A, CIB1, BMPER, TNFSF12, EPPK1, TEK, WNT5A, PDGFB, EPB41L5, HDAC7, SRPX2
	endothelial cell migration	4.3597E-03	FGF2, ACVRL1, GLUL, LOXL2, RRAS, PLXND1, WNT7A, CIB1, BMPER, TNFSF12, TEK, WNT5A, PDGFB, HDAC7, SRPX2
	organ induction	5.0163E-03	FGF2, WNT11, WNT3A, WNT5A, WNT2, WNT2B
	regulation of epithelial cell migration	8.5580E-03	FGF2, ITGA3, ACVRL1, GLUL, RRAS, WNT7A, CIB1, BMPER, EPPK1, TEK, WNT5A, PDGFB, EPB41L5, HDAC7, SRPX2
	formation of primary germ layer	8.8418E-03	ITGA3, PRKACA, COL8A1, COL7A1, WNT11, WNT3A, WNT5A, COL12A1, EPB41L5, COL4A2, COL11A1
	regulation of cell junction assembly	9.7762E-03	VPS35, ACVRL1, WNT4, ADGRL2, PRKACA, WNT7A, ACE, CLDN5, MYO1C, WNT3A, TEK, WNT5A, EPB41L5, SRPX2
	collagen-activated signaling pathway	1.2354E-02	COL4A3, COL4A1, COL4A2, COL4A6, COL4A5

Supplementary Table 3. GO analysis filtered for peptides with log2(FC) < -1

	GO Term	Adjusted P Value	Relevant Genes Identified
	response to toxic substance	1.2418E-02	MPST, GSTP1, SOD3, PRDX6, MAOB, ALDH1A1, ALB, ADH5, DUOX1, ABCB1, GSTM3, SOD1, CDH1, ESD, SLC6A4
	lung development	1.4458E-02	FGF2, ITGA3, LAMA5, PDGFA, ACE, WNT7B, WNT11, WNT5A, WNT2, WNT2B, MME, ALDH1A2, MMP12
	epithelial cell development	1.4557E-02	WNT7A, LAMB2, AFDN, PECAM1, BMP5, WNT7B, CLDN5, MYADM, GSTM3, WNT5A, PDGFB, EPB41L5, COL18A1, CNMD
	regulation of animal organ formation	1.5729E-02	FGF2, WNT11, WNT3A, WNT5A, WNT2, WNT2B
	respiratory tube development	1.8390E-02	FGF2, ITGA3, LAMA5, PDGFA, ACE, WNT7B, WNT11, WNT5A, WNT2, WNT2B, MME, ALDH1A2, MMP12
	gastrulation	2.0689E-02	ITGA3, PRKACA, COL8A1, MYADM, COL7A1, WNT11, WNT3A, WNT5A, COL12A1, EPB41L5, WNK1, COL4A2, COL11A1
	cellular detoxification	2.4474E-02	GSTP1, SOD3, PRDX6, ALDH1A1, ALB, ADH5, DUOX1, GSTM3, SOD1, ESD
	detoxification	2.5450E-02	GSTP1, SOD3, PRDX6, ALDH1A1, ALB, ADH5, DUOX1, ABCB1, GSTM3, SOD1, ESD
	ethanol metabolic process	2.9763E-02	ALDH3B1, SULT1A1, ALDH1B1, ALDH2, ADH5
	regulation of endothelial cell migration	3.6638E-02	FGF2, ACVRL1, GLUL, RRAS, WNT7A, CIB1, BMPER, TEK, WNT5A, PDGFB, HDAC7, SRPX2
	positive regulation of endothelial cell proliferation	4.1006E-02	FGF2, ACVRL1, RPTOR, CXCL12, TNFSF12, TEK, WNT5A, PDGFB, WNT2
	kidney epithelium development	4.3882E-02	FGF2, WNT4, LAMB2, PECAM1, LAMA5, WNT7B, BMPER, NPNT, WNT11, CRLF1, WNT2B
	glomerular basement membrane development	4.4969E-02	LAMB2, NID1, COL4A4, COL4A3
	cellular response to toxic substance	4.5476E-02	GSTP1, SOD3, PRDX6, ALDH1A1, ALB, ADH5, DUOX1, GSTM3, SOD1, ESD
Cellular Components	endoplasmic reticulum lumen	3.0218E-20	C3, LAMC1, CHRDL1, WNT4, TSPAN15, COL5A3, WNT7A, COL8A1, LAMB2, COL6A2, QSOX1, PDGFA, WNT7B, ALB, COL6A3, COL7A1, ARSI, MFGE8, WNT3A, PRSS23, WNT5A, PDGFB, ESD, COL4A4, COL12A1, P3H1, COL4A3, COL18A1, COL4A1, COL4A2, COL21A1, APOB, COL4A6, COL11A1, COL26A1, COL4A5, VCPIP1, MATN3
	basement membrane	1.0005E-19	LAMC1, LOXL2, LAMC3, COL8A1, LAMA4, LAMB2, CCDC80, LAMA5, NID1, HSPG2, NPNT, TGFBI, COL7A1, LAMA2, COL4A4, COL4A3, COL18A1, COL4A1, COL4A2, COL4A6, TIMP3, COL4A5, ACAN, DST
	collagen trimer	1.6350E-17	COL5A3, COL8A1, EMID1, C1QTNF5, COL6A2, C1QTNF7, COL6A3, COL7A1, COL4A4, COL12A1, FCN3, COL4A3, COL6A6, COL18A1, COL4A1, COL4A2, COL21A1, COL4A6, COL11A1, COL26A1, COL4A5, COL6A5
	complex of collagen trimers	7.8781E-11	COL5A3, COL8A1, COL7A1, COL4A4, COL4A3, COL4A1, COL4A2, COL4A6, COL11A1, COL4A5
	collagen network	5.5648E-10	COL8A1, COL4A4, COL4A3, COL4A1, COL4A2, COL4A6, COL4A5
	network-forming collagen trimer	5.5648E-10	COL8A1, COL4A4, COL4A3, COL4A1, COL4A2, COL4A6, COL4A5
	basement membrane collagen trimer	2.4702E-09	COL8A1, COL4A4, COL4A3, COL4A1, COL4A2, COL4A6, COL4A5

Supplementary Table 3. GO analysis filtered for peptides with log2(FC) < -1

GO Term	Adjusted P Value	Relevant Genes Identified
Golgi lumen	1.8915E-08	SOD3, BGN, WNT4, WNT7A, OGN, PDGFA, CSPG4, WNT7B, HSPG2, WNT3A, WNT5A, PDGFB, FMOD, ACAN, MUC5AC
collagen type IV trimer	3.1312E-08	COL4A4, COL4A3, COL4A1, COL4A2, COL4A6, COL4A5
vesicle lumen	1.8321E-05	C3, GSTP1, LEFTY2, NIT2, PRDX6, CYFIP1, PSMD3, QSOX1, PDGFA, PDXK, XRCC6, ALB, LGALS3BP, LYZ, CTSG, CLEC3B, PDGFB, APOB, SLPI, ELANE, TIMP3
secretory granule lumen	6.4986E-05	C3, GSTP1, LEFTY2, NIT2, PRDX6, CYFIP1, PSMD3, QSOX1, PDGFA, PDXK, XRCC6, ALB, LGALS3BP, LYZ, CTSG, CLEC3B, PDGFB, SLPI, ELANE, TIMP3
cytoplasmic vesicle lumen	7.5458E-05	C3, GSTP1, LEFTY2, NIT2, PRDX6, CYFIP1, PSMD3, QSOX1, PDGFA, PDXK, XRCC6, ALB, LGALS3BP, LYZ, CTSG, CLEC3B, PDGFB, SLPI, ELANE, TIMP3
laminin-11 complex	1.1839E-03	LAMC1, LAMB2, LAMA5
vacuolar lumen	7.1717E-03	C3, BGN, PRDX6, OGN, CSPG4, HSPG2, LYZ, CTSG, APOB, FMOD, ELANE, ACAN
actin filament bundle	1.0732E-02	CRYAB, ABLIM3, MYH10, MYH14, TEK, PDLIM3, PGM5, SHROOM4
specific granule lumen	1.4765E-02	NIT2, CYFIP1, QSOX1, PDXK, LYZ, SLPI, ELANE
sarcolemma	1.7850E-02	SLMAP, BGN, SGCD, CIB1, COL6A2, COL6A3, LAMA2, SGCB, ATP1A2, PGM5
lamellipodium	3.0321E-02	NCKAP1, ABLIM3, MYH10, PLXND1, RAPH1, CIB1, CD177, SWAP70, CYFIP1, CSPG4, CDH1, INPPL1
contractile actin filament bundle	3.9321E-02	ABLIM3, MYH10, MYH14, TEK, PDLIM3, PGM5, SHROOM4
stress fiber	3.9321E-02	ABLIM3, MYH10, MYH14, TEK, PDLIM3, PGM5, SHROOM4

Supplementary Table 3. GO analysis filtered for peptides with log2(FC) < -1

	GO Term	Adjusted P Value	Relevant Genes Identified
Reactome	Extracellular matrix organization	7.4076E-22	FGF2, ITGA3, LAMC1, LOXL2, BGN, COL5A3, LAMC3, COL8A1, LAMA4, LAMB2, PECAM1, COL6A2, LAMA5, PDGFA, NID1, HSPG2, COL6A3, COL7A1, LAMA2, ELN, CTSG, PDGFB, CDH1, MMP19, COL4A4, COL12A1, P3H1, COL4A3, COL6A6, COL18A1, COL4A1, COL4A2, COL21A1, ASPN, FMOD, MMP12, COL4A6, COL11A1, ELANE, COL26A1, COL4A5, COL6A5, HAPLN1, ACAN, MATN1, MATN3
	ECM proteoglycans	2.3939E-18	LAMC1, BGN, COL5A3, LAMA4, LAMB2, COL6A2, LAMA5, HSPG2, COL6A3, LAMA2, COL4A4, COL4A3, COL6A6, COL4A1, COL4A2, ASPN, FMOD, COL4A6, COL4A5, COL6A5, HAPLN1, ACAN, MATN1, MATN3
	Laminin interactions	8.7459E-18	ITGA3, LAMC1, LAMC3, LAMA4, LAMB2, LAMA5, NID1, HSPG2, COL7A1, LAMA2, COL4A4, COL4A3, COL18A1, COL4A1, COL4A2, COL4A6, COL4A5
	Collagen chain trimerization	1.2887E-15	COL5A3, COL8A1, COL6A2, COL6A3, COL7A1, COL4A4, COL12A1, COL4A3, COL6A6, COL18A1, COL4A1, COL4A2, COL21A1, COL4A6, COL11A1, COL26A1, COL4A5, COL6A5
	Degradation of the extracellular matrix	1.3278E-15	LAMC1, COL5A3, COL8A1, COL6A2, LAMA5, NID1, HSPG2, COL6A3, COL7A1, ELN, CTSG, CDH1, MMP19, COL4A4, COL12A1, COL4A3, COL6A6, COL18A1, COL4A1, COL4A2, MMP12, COL4A6, COL11A1, ELANE, COL26A1, COL4A5, COL6A5, ACAN
	Collagen degradation	8.4926E-15	COL5A3, COL8A1, COL6A2, COL6A3, COL7A1, MMP19, COL4A4, COL12A1, COL4A3, COL6A6, COL18A1, COL4A1, COL4A2, MMP12, COL4A6, COL11A1, ELANE, COL26A1, COL4A5, COL6A5
	Non-integrin membrane-ECM interactions	4.1577E-13	FGF2, LAMC1, COL5A3, LAMC3, LAMA4, LAMB2, LAMA5, PDGFA, HSPG2, LAMA2, PDGFB, COL4A4, COL4A3, COL4A1, COL4A2, COL4A6, COL11A1, COL4A5
	Collagen biosynthesis and modifying enzymes	4.2490E-13	COL5A3, COL8A1, COL6A2, COL6A3, COL7A1, COL4A4, COL12A1, P3H1, COL4A3, COL6A6, COL18A1, COL4A1, COL4A2, COL21A1, COL4A6, COL11A1, COL26A1, COL4A5, COL6A5
	Collagen formation	9.9904E-12	LOXL2, COL5A3, COL8A1, COL6A2, COL6A3, COL7A1, COL4A4, COL12A1, P3H1, COL4A3, COL6A6, COL18A1, COL4A1, COL4A2, COL21A1, COL4A6, COL11A1, COL26A1, COL4A5, COL6A5
	Assembly of collagen fibrils and other multimeric structures	1.4750E-11	LOXL2, COL5A3, COL8A1, COL6A2, COL6A3, COL7A1, COL4A4, COL12A1, COL4A3, COL6A6, COL18A1, COL4A1, COL4A2, COL4A6, COL11A1, COL4A5, COL6A5
	Integrin cell surface interactions	4.9993E-10	ITGA3, COL5A3, COL8A1, PECAM1, COL6A2, HSPG2, COL6A3, COL7A1, CDH1, COL4A4, COL4A3, COL6A6, COL18A1, COL4A1, COL4A2, COL4A6, COL4A5, COL6A5
	WNT ligand biogenesis and trafficking	1.0475E-07	VPS35, WNT4, WNT7A, VPS29, WNT7B, WNT11, WNT3A, WNT5A, WNT2, WNT2B
	MET activates PTK2 signaling	1.0847E-05	ITGA3, LAMC1, COL5A3, LAMC3, LAMA4, LAMB2, LAMA5, LAMA2, COL11A1

Supplementary Table 3. GO analysis filtered for peptides with log2(FC) < -1

GO Term	Adjusted P Value	Relevant Genes Identified
Anchoring fibril formation	1.1616E-05	COL7A1, COL4A4, COL4A3, COL4A1, COL4A2, COL4A6, COL4A5
NCAM1 interactions	2.0603E-05	COL5A3, COL6A2, COL6A3, COL4A4, COL4A3, COL6A6, COL4A1, COL4A2, COL4A5, COL6A5
Signaling by PDGF	2.4623E-05	COL5A3, COL6A2, COL6A3, PDGFB, COL4A4, COL4A3, COL6A6, COL4A1, COL4A2, COL4A5, COL6A5
Crosslinking of collagen fibrils	5.3964E-05	LOXL2, COL4A4, COL4A3, COL4A1, COL4A2, COL4A6, COL4A5
MET promotes cell motility	1.6763E-04	ITGA3, LAMC1, COL5A3, LAMC3, LAMA4, LAMB2, LAMA5, LAMA2, COL11A1
Diseases associated with glycosaminoglycan metabolism	2.1027E-04	BGN, PAPSS2, OGN, CSPG4, B3GALT6, HSPG2, CHST14, FMOD, ACAN
NCAM signaling for neurite out-growth	6.1185E-04	COL5A3, COL6A2, COL6A3, COL4A4, COL4A3, COL6A6, COL4A1, COL4A2, COL4A5, COL6A5
Signaling by MET	9.1889E-04	ITGA3, LAMC1, RAB4B, COL5A3, LAMC3, LAMA4, LAMB2, LAMA5, SH3KBP1, LAMA2, COL11A1
Serotonin clearance from the synaptic cleft	6.5945E-03	ALDH2, MAOA, SLC6A4
Diseases of glycosylation	1.6138E-02	BGN, DPM1, PAPSS2, OGN, CSPG4, B3GALT6, HSPG2, CHST14, THSD4, LFNG, FMOD, ACAN, MUC5AC
Regulation of Insulin-like Growth Factor (IGF) transport and uptake by Insulin-like Growth Fa	2.1521E-02	C3, LAMC1, CHRDL1, IGFALS, LAMB2, QSOX1, ALB, MFGE8, CTSG, PRSS23, APOB, MATN3
Class B/2 (Secretin family receptors)	3.8154E-02	WNT4, WNT7A, WNT7B, CD55, WNT11, VIPR1, WNT3A, WNT5A, WNT2, WNT2B

Supplementary Table 4. GO analysis filtered for peptides with log2(FC) >1

	GO Term	Adjusted P Value	Relevant Genes Identified
Molecular Factors	cadherin binding	6.2814E-23	VAPB, PLIN3, LRRFIP1, GOLGA3, CTTN, LIMA1, MPRIP, SHTN1, TMOD3, SH3GL1, CAST, CDH11, EIF4H, SERBP1, VAPA, ERC1, SLC9A3R2, FNBP1L, LRRC59, KTN1, EPS15, KRT18, STK38, RANBP 1, SND1, EIF5, CHMP2B, MAPRE1, CAPG, EEF1D, VASN, GIGYF2, SH3GLB2, HSPA5, TBC1D2, RPL7A, CDH5, PDLIM1, CKAP5, CAPZA1, ABCF3, NUDC, KLC2, CCS, SPTAN1, HDLBP, DNAJB1, SEPT IN2, ADD1, TNKS1BP1, CNN2, VASP, CALD1, OLFM4, SCRIB, HSP90AB1, ALDOA, GOLGA2, TLN1, SH3GLB1, RPS26, TAGLN2, BAG3, ARVCF, HSPA8, DDX6, ABI1, CDH13, S100A11, CGN, CRKL
	unfolded protein binding	3.5658E-09	CCDC115, CDC37, NAP1L4, NPM1, UGGT1, DNAJB2, HSP90B1, PFDN1, HSPA5, SRSF10, NACA, PFDN6, NUDC, HSPE1, LMAN1, PFDN4, HSPB6, HSPA14, DNAJB1, TAPBP, HYOU1, DNAJB11, HSP 90AB1, ERLEC1, VBP1, PFDN2, HSPA8
	structural constituent of cytoskeleton	1.4020E-07	TUBB3, CCDC6, EPB41, KRT5, KRT6A, VIM, KRT19, HIP1, ANK1, TPM1, EPB42, SPTA1, KRT15, ARPC5, KRT16, SPTAN1, TUBB, ADD1, KRT2, TUBB6, TLN1, SYNM, ADD3, TUBB1
	actin filament binding	2.1730E-06	TPM3, HCLS1, NEXN, BLOC1S6, PPP1R9B, CTTN, LIMA1, MPRIP, SHTN1, BIN1, ARPC5L, HIP1, TPM1, MARCKSL1, TPM4, CAPG, SPTA1, PSTPIP1, TPM2, ARPC5, CAPZA1, MYO5A, SPTAN1, CAPZ A2, MARCKS, ADD1, PSTPIP2, SYNE2, TLN1, FMNL3, ADD3, MYL4, CORO1C, TMOD1 mRNA binding 3.2191E-05 DHFR, SNRNP70, TAF15, C1QBP, SNRPC, PAIP2, SRSF1, RBM4, SERBP1, ELAVL1, PTBP3, SF1, HNRNPC, CSTF2, ILF3, QKI, RPL26, CARHSP1, TPR, HNRNPAB, PABPC1, HNRNPM, TIAL1, FUBP1, THOC2, IGF2BP2, FXR1, FUBP3, PTBP1, HDLBP, FUS, HNRNPL, HNRNPD, RPS14, HNRNPA3, TSN, RPS26, NUDT21, DDX6, EIF4G1, KHSRP, NHP2, LUC7L3
	mRNA binding	3.2191E-05	DHFR, SNRNP70, TAF15, C1QBP, SNRPC, PAIP2, SRSF1, RBM4, SERBP1, ELAVL1, PTBP3, SF1, HNRNPC, CSTF2, ILF3, QKI, RPL26, CARHSP1, TPR, HNRNPAB, PABPC1, HNRNPM, TIAL1, FUBP1, THOC2, IGF2BP2, FXR1, FUBP3, PTBP1, HDLBP, FUS, HNRNPL, HNRNPD, RPS14, HNRNPA3, TSN, RPS26, NUDT21, DDX6, EIF4G1, KHSRP, NHP2, LUC7L3
	ribonucleoprotein complex binding	4.2616E-05	SRP19, SNRPD1, C1QBP, CBX5, SRP54, EIF1, SEC61G, EIF4H, RPLP1, SERBP1, SRP72, SND1, EIF2S1, NPM1, CD2BP2, HSPA5, CKAP5, SRP68, NME1, EIF3K, EFL1, PTCD3, SPCS1, SRPRA, BAG6, CCDC47
	heat shock protein binding	5.1447E-05	AHR, CDC37, NUP62, NR3C1, DNAJB2, EEF1D, APOA1, HSPA5, TPR, STIP1, DNAJC7, ST13, APOA2, HSPA14, DNAJB1, ITGAM, ITGB2, HSP90AB1, BAG2, BAG3, HSPA8, STUB1, BAG6
M ol	chaperone binding	1.5449E-04	FGB, BIN1, CDC37, TBCA, DNAJB2, ERP29, HSPA5, PFDN6, PLG, HSPE1, CP, PFDN4, HSPB6, DNAJB1, HYOU1, SUGT1, BAG2, BAG3, HSPA8, STUB1

Supplementary Table 4. GO analysis filtered for peptides with log2(FC) >1

GO Term	Adjusted P Value	Relevant Genes Identified
translation regulator activity	1.0740E-03	DHFR, EIF1, PAIP2, EIF4H, ELOC, EIF5, EIF2S1, EEF1B2, EEF1D, EIF2B2, EEF1A1, COPS5, PABPC1, ELOB, IGF2BP2, FXR1, EIF3M, EIF3K, RPS14, EFL1, RPL10, EIF4G1, EIF2D
NADH dehydrogenase activity	1.0840E-03	NDUFV3, NDUFS8, NDUFS6, NDUFS1, NDUFA2, NDUFS3, NDUFV1, AIFM1, NDUFS7, NDUFV2, NDUFS4, NDUFA5
polyubiquitin modification-dependent protein binding	1.3678E-03	PSMD4, UBQLN2, EPS15, DNAJB2, RNF31, RAD23B, TNIP2, BRCC3, NPLOC4, VCP, UBXN1, BAG6, UBQLN1
protein folding chaperone	2.1551E-03	FKBP8, DFFA, PFDN1, HSPA5, CD74, HSPA14, DNAJB1, HSP90AB1, PFDN2, HSPA8, CCDC47
NADH dehydrogenase (ubiquinone) activity	3.5778E-03	NDUFV3, NDUFS8, NDUFS6, NDUFS1, NDUFA2, NDUFS3, NDUFV1, NDUFS7, NDUFV2, NDUFS4, NDUFA5
NADH dehydrogenase (quinone) activity	4.5554E-03	NDUFV3, NDUFS8, NDUFS6, NDUFS1, NDUFA2, NDUFS3, NDUFV1, NDUFS7, NDUFV2, NDUFS4, NDUFA5
translation regulator activity, nucleic acid binding	5.2666E-03	DHFR, EIF1, PAIP2, EIF4H, ELOC, EIF5, EIF2S1, EEF1B2, EEF1D, EIF2B2, EEF1A1, COPS5, PABPC1, ELOB, EIF3M, EIF3K, EFL1, EIF4G1, EIF2D
ubiquitin-like protein binding	6.4700E-03	UBE2L6, STAM2, NUP62, SERBP1, HGS, TSG101, STAM, DNAJB2, RNF31, AUP1, NSFL1C, RAD23B, FAF2, RAE1, NPLOC4, PELP1, RBCK1, UBXN1
NAD(P)H dehydrogenase (quinone) activity	7.2266E-03	NDUFV3, NDUFS8, NDUFS6, NDUFS1, NDUFA2, NDUFS3, NDUFV1, NDUFS7, NDUFV2, NDUFS4, NDUFA5
ubiquitin binding	8.1477E-03	UBE2L6, STAM2, NUP62, HGS, TSG101, STAM, DNAJB2, RNF31, AUP1, NSFL1C, RAD23B, FAF2, RAE1, NPLOC4, RBCK1, UBXN1
antioxidant activity	1.0954E-02	SELENOF, HBM, GPX7, HBQ1, GPX3, EPX, SOD2, SELENOS, PXDN, HBB, PRDX4, APOM, TXNRD1, GPX8, HBG1
ubiquitin-like protein ligase binding	1.2291E-02	UBE2J1, TANK, WASHC1, UBE2L6, HGS, SCAMP3, PTK2B, TSG101, STAM, DTX3L, DNAJB2, RNF31, DDRGK1, AUP1, NGFR, HSPA5, ARIH1, UBE2L3, FAF2, ELOB, NPLOC4, TUBB, VCP, ISG15, SPA RT, HSP90AB1, BAG2, HSPA8, RPL23, STUB1, UBXN1, STAT2, BAG6, BECN1
mRNA 3'-UTR binding	1.4059E-02	TAF15, RBM4, SERBP1, ELAVL1, HNRNPC, ILF3, CARHSP1, PABPC1, TIAL1, IGF2BP2, FXR1, FUS, HNRNPD, NUDT21, KHSRP, NHP2
translation factor activity, RNA binding	1.6031E-02	EIF1, EIF4H, ELOC, EIF5, EIF2S1, EEF1B2, EEF1D, EIF2B2, EEF1A1, COPS5, ELOB, EIF3M, EIF3K, EFL1, EIF4G1, EIF2D
peroxidase activity	2.0497E-02	SELENOF, HBM, GPX7, HBQ1, GPX3, EPX, PXDN, HBB, PRDX4, GPX8, HBG1
structural constituent of muscle	2.3212E-02	NEXN, MYL3, KRT19, TPM1, TPM4, MYL1, TPM2, MYL6B, MYL9, SYNM
microtubule plus-end binding	2.7888E-02	CLIP1, MAPRE1, NUMA1, STIM1, CKAP5, CLASP1, MAPRE2
protein-lipid complex binding	2.8110E-02	LDLR, APOL2, APOA1, PLTP, LPL, APOA2, MSR1, CDH13
lipoprotein particle binding	2.8110E-02	LDLR, APOL2, APOA1, PLTP, LPL, APOA2, MSR1, CDH13
oxidoreductase activity, acting on peroxide as acceptor	4.2852E-02	SELENOF, HBM, GPX7, HBQ1, GPX3, EPX, PXDN, HBB, PRDX4, GPX8, HBG1
proteasome-activating activity	4.9539E-02	PSMC2, PSMC1, PSMC3, PSMC4

Supplementary Table 4. GO analysis filtered for peptides with log2(FC) >1

	GO Term	Adjusted P Value	Relevant Genes Identified
Biological Processes	protein folding	1.1462E-10	SELENOF, SGTA, SNRNP70, CDC37, TBCA, FKBP11, FKBP8, UGGT1, DFFA, DNAJB2, ERP29, PDIA6, HSP90B1, PFDN1, HSPA5, DNAJC7, ST13, GNAI1, PFDN6, PRDX4, NUDC, HSPE1, LMAN1, ER P44, PFDN4, CD74, FKBP2, ERO1A, HSPB6, HSPA14, DNAJB1, DNAJB11, HSP90AB1, VBP1, PFDN2, BAG2, BAG3, HSPA8, TBCEL, CCDC47
	blood coagulation	1.1585E-10	PF4, SERPINE1, F5, WAS, HABP2, FGA, F12, FGB, FGG, BLOC1S6, PROS1, PROC, BLOC1S4, SLC4A1, F13B, PLEK, FCER1G, GAS6, HPS6, SERPINF2, BLOC1S3, F13A1, METAP1, SERPINA10, SER PIND1, DTNBP1, KNG1, HBB, RAP2B, PLAUR, SYK, PLG, LMAN1, APOH, F10, SAA1, TLN1, SERPINA1, MYL9, KRT1, HRG
	Golgi vesicle transport	1.1696E-10	GOLGA5, VAPB, TRIP11, COPE, PROS1, MIA2, SCAMP2, SEC16A, SEC23IP, NAPG, PROC, VAPA, ANK1, SCAMP3, EPS15, KRT18, GOPC, MIA3, COMMD1, GCC2, CCDC91, TFG, COG6, COG7, MY O5A, PRKCI, AP3S1, LMAN1, SEC13, COPZ1, VAMP3, TMED1, SAR1B, VCP, TAPBP, COG4, HYOU1, F10, COPA, GOLGA2, COG2, ERGIC2, EXOC1, ARFRP1, GOLPH3, RABEP1, TRAPPC12, TRAPP C8, COPB2
	coagulation	2.5039E-10	PF4, SERPINE1, F5, WAS, HABP2, FGA, F12, FGB, FGG, BLOC1S6, PROS1, PROC, BLOC1S4, SLC4A1, F13B, PLEK, FCER1G, GAS6, HPS6, SERPINF2, BLOC1S3, F13A1, METAP1, SERPINA10, SER PIND1, DTNBP1, KNG1, HBB, RAP2B, PLAUR, SYK, PLG, LMAN1, APOH, F10, SAA1, TLN1, SERPINA1, MYL9, KRT1, HRG
	hemostasis	2.9128E-10	PF4, SERPINE1, F5, WAS, HABP2, FGA, F12, FGB, FGG, BLOC1S6, PROS1, PROC, BLOC1S4, SLC4A1, F13B, PLEK, FCER1G, GAS6, HPS6, SERPINF2, BLOC1S3, F13A1, METAP1, SERPINA10, SER PIND1, DTNBP1, KNG1, HBB, RAP2B, PLAUR, SYK, PLG, LMAN1, APOH, F10, SAA1, TLN1, SERPINA1, MYL9, KRT1, HRG
	cytoplasmic translation	6.1315E-10	RPS25, RPS28, RPLP2, EIF4H, RPLP1, RBM4, RPL17, DRG2, EIF5, RPL13, RPS17, RPL26, RPL7A, RPS6, RPS18, EIF3M, RPS4X, EIF3K, RPS12, RPL27A, RPS14, RPS21, RPS26, RPL18, RPL32, RPL23 , RPL10, EIF4G1, EIF2D, RPL8, RPL21, RPL38
	protein-containing complex disassembly	4.2360E-07	SMARCE1, VTA1, PPP1R9B, EPS8, LIMA1, TMOD3, SH3GL1, ARID1A, PLEK, TSG101, CHMP2B, CAPG, SET, NES, KIF2A, SPTA1, SNAPIN, PEX14, CALCOCO2, MCOLN1, CKAP5, CAPZA1, SPTAN1, GRWD1, KLC1, CAPZA2, ADD1, VCP, CHMP1A, CLASP1, SNAP29, HSPA8, RPL23, ADD3, UBQLN1, TMOD1
	protein polymerization	5.7738E-07	WAS, HCLS1, EVL, FGA, FGB, FGG, CTTN, EPS8, TMOD3, PDE4DIP, CLIP1, BIN1, ZNF207, ARPC5L, SLAIN2, AKAP9, PTK2B, BLOC1S2, MAPRE1, CAPG, KANK1, SPTA1, PSTPIP1, NUMA1, MZT1, CD H5, ARPC5, ALOX15, CKAP5, CAPZA1, SPTAN1, CAPZA2, ADD1, PSTPIP2, VASP, GOLGA2, CLASP1, ADD3, SSH3, TMOD1

Supplementary Table 4. GO analysis filtered for peptides with log2(FC) >1

	GO Term	Adjusted P Value	Relevant Genes Identified
Biological Processes	endoplasmic reticulum to Golgi vesicle-mediated transport	9.1486E-07	VAPB, TRIP11, COPE, PROS1, MIA2, SEC16A, SEC23IP, PROC, VAPA, ANK1, GOPC, MIA3, TFG, LMAN1, SEC13, TMED1, SAR1B, VCP, HYOU1, F10, COPA, GOLGA2, ERGIC2, TRAPPC12, TRAPPC 8, COPB2
	response to topologically incorrect protein	2.9118E-06	VAPB, F12, UBXN4, HSPB8, EIF2S1, UGGT1, DNAJB2, HSPB7, DDRGK1, AUP1, HSPA5, COPS5, SELENOS, RNF126, FAF2, HSPE1, ERP44, ERO1A, HSPA14, DNAJB1, VCP, HSP90AB1, ERLEC1, BA G3, HSPA8, STUB1, BAG6, PIK3R1
	protein exit from endoplasmic reticulum	4.1757E-06	UBE2J1, MIA2, SEC16A, HSP90B1, AUP1, GCC2, SELENOS, UBE2G2, FAF2, SEC13, NPLOC4, SAR1B, VCP, ERLEC1, TM9SF4
	fibrinolysis	7.0479E-06	SERPINE1, FGA, F12, FGB, FGG, PROS1, SERPINF2, PLG, APOH, KRT1, HRG
	spindle organization	7.5572E-06	MAP4, RCC1, TASOR, PDE4DIP, ZNF207, NUP62, RANBP1, DCTN2, CHMP2B, MAPRE1, SMC1A, KIF2A, NUMA1, MZT1, TACC1, TPR, GNAI1, CKAP5, RAE1, NUDC, TUBB, VCP, EML3, CHMP1A, SEP TIN1, GOLGA2, CLASP1, MAPRE2, TACC2, TUBB1
	viral life cycle	1.7636E-05	LDLR, GYPA, VAPB, VTA1, CTSL, LAMTOR5, VPS37A, CTSB, TASOR, HTATSF1, VAPA, VPS37B, ATG16L1, EPS15, TSG101, CHMP2B, GAS6, CLEC4G, ILF3, NRP1, ITGB6, TRIM26, EEA1, LRSAM1, P TX3, PABPC1, LGALS1, CD74, VCP, TRIM38, CD209, ISG15, CHMP1A, HSP90AB1, CTBP2, TRIM22, APOBEC3C, HSPA8, SPCS1, DDX6
	vesicle organization	2.0133E-05	VAPB, VTA1, BLOC1S6, LAMTOR1, VPS37A, SEC16A, TMF1, STAM2, DNM1, VAPA, HGS, VPS37B, BLOC1S4, FNBP1L, EPS15, TSG101, BLOC1S2, CHMP2B, STAM, MIA3, BLOC1S3, SNAPIN, STX12 , EEA1, TFG, DTNBP1, BLOC1S5, PRKCI, HOOK3, SEC13, VAMP3, STX16, SAR1B, CHMP1A, SNAP29, STX4, GOLPH3, CORO1C, CREB1
	mitotic spindle organization	2.2346E-05	MAP4, RCC1, TASOR, ZNF207, NUP62, DCTN2, CHMP2B, SMC1A, KIF2A, NUMA1, MZT1, TACC1, TPR, GNAI1, CKAP5, RAE1, NUDC, VCP, EML3, CHMP1A, GOLGA2, CLASP1, TACC2
	response to endoplasmic reticulum stress	3.2166E-05	FCGR2B, RCN3, SGTA, VAPB, UBE2J1, UBXN4, SEC16A, UBQLN2, EIF2S1, UGGT1, DNAJB2, ERP29, HSP90B1, DDRGK1, AUP1, HSPA5, COPS5, SELENOS, ALOX15, UBE2G2, FAF2, ERP44, ERO 1A, NPLOC4, VCP, HYOU1, AIFM1, ERLEC1, STUB1, UBXN1, EIF4G1, BAG6, UBQLN1, CCDC47, PIK3R1
	negative regulation of supramolecular fiber organization	3.3695E-05	LDLR, WAS, EPS8, LIMA1, TMOD3, MAPRE1, CAPG, KANK1, SPTA1, PFDN1, CDH5, EMILIN1, PFDN6, CAPZA1, PPFIA1, PFDN4, SPTAN1, CAPZA2, ADD1, CLASP1, VBP1, PFDN2, HSPA8, ADD3, SSH 3, TMOD1, PIK3R1
	regulation of protein polymerization	6.6566E-05	HCLS1, EVL, CTTN, EPS8, TMOD3, PDE4DIP, CLIP1, BIN1, ARPC5L, SLAIN2, AKAP9, PTK2B, MAPRE1, CAPG, KANK1, SPTA1, NUMA1, CDH5, ARPC5, ALOX15, CKAP5, CAPZA1, SPTAN1, CAPZA2, A DD1, VASP, CLASP1, ADD3, SSH3, TMOD1

Supplementary Table 4. GO analysis filtered for peptides with log2(FC) >1

	GO Term	Adjusted P Value	Relevant Genes Identified
Biological Processes	ERAD pathway	7.7139E-05	RCN3, SGTA, UBE2J1, UBXN4, UBQLN2, UGGT1, DNAJB2, HSP90B1, AUP1, HSPA5, SELENOS, UBE2G2, FAF2, NPLOC4, VCP, ERLEC1, STUB1, UBXN1, BAG6, UBQLN1, CCDC47
	actin polymerization or depolymerization	1.1057E-04	WAS, HCLS1, EVL, PPP1R9B, CTTN, EPS8, LIMA1, ENAH, TMOD3, BIN1, ARPC5L, PTK2B, PLEK, CAPG, KANK1, SPTA1, PSTPIP1, ARPC5, ALOX15, CAPZA1, SPTAN1, CAPZA2, ADD1, PSTPIP2, VAS P, ADD3, ABI1, SSH3, TMOD1
	synaptic vesicle cytoskeletal transport	1.3866E-04	BLOC1S6, BLOC1S4, BLOC1S2, BLOC1S3, SNAPIN, DTNBP1, BLOC1S5, AP3M1, AP3S1
	synaptic vesicle transport along microtubule	1.3866E-04	BLOC1S6, BLOC1S4, BLOC1S2, BLOC1S3, SNAPIN, DTNBP1, BLOC1S5, AP3M1, AP3S1
	anterograde synaptic vesicle transport	1.3866E-04	BLOC1S6, BLOC1S4, BLOC1S2, BLOC1S3, SNAPIN, DTNBP1, BLOC1S5, AP3M1, AP3S1
	ubiquitin-dependent ERAD pathway	2.0088E-04	SGTA, UBE2J1, UBXN4, UBQLN2, DNAJB2, HSP90B1, AUP1, HSPA5, SELENOS, UBE2G2, FAF2, NPLOC4, VCP, ERLEC1, STUB1, BAG6, UBQLN1, CCDC47
	response to unfolded protein	2.4439E-04	VAPB, UBXN4, HSPB8, EIF2S1, DNAJB2, HSPB7, DDRGK1, HSPA5, COPS5, SELENOS, FAF2, HSPE1, ERP44, ERO1A, HSPA14, DNAJB1, VCP, HSP90AB1, ERLEC1, BAG3, HSPA8, STUB1, PIK3R1
	regulation of actin filament organization	2.7218E-04	WAS, HCLS1, EVL, CTTN, EPS8, LIMA1, TMOD3, BIN1, ARPC5L, PTK2B, TPM1, PLEK, CAPG, KANK1, ARFIP1, SPTA1, SERPINF2, NRP1, APOA1, ARPC5, ALOX15, CAPZA1, LIMCH1, PPFIA1, SPTAN1 , CAPZA2, ADD1, SYNPO, VASP, CLASP1, ADD3, SSH3, TMOD1, PIK3R1
	microtubule cytoskeleton organization involved in mitosis	2.8893E-04	MAP4, RCC1, TASOR, ZNF207, NUP62, DCTN2, CHMP2B, SMC1A, KIF2A, NUMA1, MZT1, NSFL1C, TACC1, TPR, GNAI1, CKAP5, RAE1, NUDC, VCP, EML3, CHMP1A, GOLGA2, CLASP1, TACC2
	nucleic acid transport	3.2756E-04	CETN3, NUP214, NUP43, NUP50, NUP62, SRSF1, NUP54, NPM1, CETN2, NUP58, QKI, AKAP8L, TPR, CKAP5, THOC2, RAE1, IGF2BP2, SUPT6H, SEC13, HNRNPA3, NUP88, XPOT, RTRAF, TST, KHS RP
	RNA transport	3.2756E-04	CETN3, NUP214, NUP43, NUP50, NUP62, SRSF1, NUP54, NPM1, CETN2, NUP58, QKI, AKAP8L, TPR, CKAP5, THOC2, RAE1, IGF2BP2, SUPT6H, SEC13, HNRNPA3, NUP88, XPOT, RTRAF, TST, KHS RP
	negative regulation of blood coagulation	4.4452E-04	SERPINE1, FGA, F12, FGB, FGG, PROS1, PROC, SERPINF2, KNG1, PLG, APOH, KRT1, HRG
	establishment of RNA localization	4.7045E-04	CETN3, NUP214, NUP43, NUP50, NUP62, SRSF1, NUP54, NPM1, CETN2, NUP58, QKI, AKAP8L, TPR, CKAP5, THOC2, RAE1, IGF2BP2, SUPT6H, SEC13, HNRNPA3, NUP88, XPOT, RTRAF, TST, KHS RP
	macroautophagy	4.8086E-04	ATG13, VTA1, VPS37A, SPTLC2, CDC37, STAM2, HMOX1, HGS, VPS37B, UBQLN2, ATG16L1, HSPB8, TSG101, CHMP2B, STAM, RNF31, SNAPIN,

Supplementary Table 4. GO analysis filtered for peptides with log2(FC) >1

	GO Term	Adjusted P Value	Relevant Genes Identified
			DDRGK1, AUP1, STX12, NSFL1C, LRSAM1, CALC OCO2, SNX6, MCOLN1, EXOC7, SNX18, VCP, SH3GLB1, SNAP29, EXOC1, BAG3, RAB3GAP1, TRAPPC8, UBQLN1, BECN1
	chaperone-mediated protein folding	5.2177E-04	SGTA, FKBP11, DFFA, DNAJB2, HSPA5, DNAJC7, ST13, HSPE1, CD74, FKBP2, ERO1A, HSPB6, HSPA14, DNAJB1, HSPA8
	negative regulation of hemostasis	5.7922E-04	SERPINE1, FGA, F12, FGB, FGG, PROS1, PROC, SERPINF2, KNG1, PLG, APOH, KRT1, HRG
	regulation of intracellular transport	5.9051E-04	ATG13, ZPR1, HCLS1, UBE2J1, NUP214, PPP1R12A, DAB2, NMT1, RBM4, PPP1CC, FIS1, TGFB1, NUP54, ARFIP1, RNF31, GAS6, NUP58, NUMA1, SNAPIN, GCC2, AKAP8L, UBE2L3, TPR, UBE2G2, L MAN1, SUPT6H, ANP32B, TCAF2, SAR1B, ITGAM, ITGB2, HSP90AB1, ERLEC1, SH3GLB1, TM9SF4, BAG3, UBL5, PCM1, PIK3R1
	regulation of actin polymerization or depolymerization	8.7891E-04	WAS, HCLS1, EVL, CTTN, EPS8, LIMA1, TMOD3, BIN1, ARPC5L, PTK2B, PLEK, CAPG, KANK1, SPTA1, ARPC5, ALOX15, CAPZA1, SPTAN1, CAPZA2, ADD1, VASP, ADD3, SSH3, TMOD1
	regulation of actin filament length	9.8885E-04	WAS, HCLS1, EVL, CTTN, EPS8, LIMA1, TMOD3, BIN1, ARPC5L, PTK2B, PLEK, CAPG, KANK1, SPTA1, ARPC5, ALOX15, CAPZA1, SPTAN1, CAPZA2, ADD1, VASP, ADD3, SSH3, TMOD1
	'de novo' posttranslational protein folding	1.0099E-03	SELENOF, UGGT1, HSPA5, DNAJC7, ST13, HSPE1, CD74, ERO1A, HSPA14, DNAJB1, HSPA8
	negative regulation of coagulation	1.2290E-03	SERPINE1, FGA, F12, FGB, FGG, PROS1, PROC, SERPINF2, KNG1, PLG, APOH, KRT1, HRG
Biological Processes	regulation of RNA splicing	1.2944E-03	ZPR1, RBM12B, SNRNP70, SRSF9, C1QBP, AKAP17A, SAP18, RBM4, PTBP3, SF1, QKI, SRSF10, MBNL1, FXR1, PTBP1, FUS, HNRNPL, HNRNPH3, RPS26, HNRNPF, HSPA8, U2AF2, PIK3R1
	establishment of vesicle localization	1.3173E-03	TRIP11, BLOC1S6, SEC16A, DNM1, HGS, BLOC1S4, FNBP1L, DCTN2, TSG101, BLOC1S2, STAM, BLOC1S3, SNAPIN, TFG, COPS5, DTNBP1, BLOC1S5, AP3M1, MYO5A, AP3S1, SAR1B, RAB27B, S CRIB, CLASP1, SNAP29
	RNA localization	1.3697E-03	CETN3, NUP214, NUP43, NUP50, NUP62, SRSF1, NUP54, NPM1, CETN2, NUP58, QKI, AKAP8L, TPR, HNRNPAB, CKAP5, THOC2, RAE1, IGF2BP2, SUPT6H, SEC13, HNRNPA3, NUP88, XPOT, RTRA F, TST, KHSRP, NHP2
	actin filament polymerization	2.4439E-03	WAS, HCLS1, EVL, CTTN, EPS8, TMOD3, BIN1, ARPC5L, PTK2B, CAPG, KANK1, SPTA1, PSTPIP1, ARPC5, ALOX15, CAPZA1, SPTAN1, CAPZA2, ADD1, PSTPIP2, VASP, ADD3, SSH3, TMOD1
	endosomal transport	3.0350E-03	WAS, DPY30, WASHC2A, VTA1, LAMTOR1, WASHC1, SPAG9, HGS, ERC1, EPS15, BLOC1S2, CHMP2B, STAM, ARFIP1, GCC2, EEA1, DCLK1, SNX6, RNF126, ACAP2, VAMP3, STX16, SNX18, VCP, H EATR5B, CHMP1A, SCRIB, ARFRP1, CORO1C

Supplementary Table 4. GO analysis filtered for peptides with log2(FC) >1

	GO Term	Adjusted P Value	Relevant Genes Identified
Biological Processes	regulation of actin cytoskeleton organization	3.0574E-03	WAS, HCLS1, EVL, CTTN, EPS8, LIMA1, TMOD3, BIN1, NOTCH2, ARPC5L, TGFB1, PTK2B, TPM1, PLEK, CAPG, KANK1, ARFIP1, SPTA1, SERPINF2, NRP1, APOA1, ARPC5, ALOX15, CAPZA1, LIMCH 1, PPFIA1, SPTAN1, CAPZA2, ADD1, SYNPO, VASP, CLASP1, HRG, ADD3, SSH3, TMOD1, ARHGAP17, PIK3R1
	'de novo' protein folding	3.2704E-03	SELENOF, UGGT1, HSPA5, DNAJC7, ST13, HSPE1, CD74, ERO1A, HSPA14, DNAJB1, HSPA8
	plasma lipoprotein particle clearance	3.2704E-03	LDLR, CNPY2, APOC2, SOAT1, HMOX1, APOA1, APOA2, APOM, MSR1, APOC3, KHSRP
	regulation of intracellular protein transport	3.3166E-03	ATG13, ZPR1, HCLS1, UBE2J1, NMT1, FIS1, TGFB1, NUP54, RNF31, GAS6, NUP58, GCC2, UBE2L3, TPR, UBE2G2, LMAN1, ANP32B, TCAF2, SAR1B, ITGAM, ITGB2, HSP90AB1, ERLEC1, SH3GLB1, TM9SF4, BAG3, UBL5, PCM1, PIK3R1
	positive regulation of cytoskeleton organization	3.7351E-03	WAS, HCLS1, EVL, CTTN, PDE4DIP, CLIP1, BIN1, NUP62, SLAIN2, AKAP9, PTK2B, TPM1, PLEK, MAPRE1, NES, SERPINF2, NRP1, NUMA1, APOA1, ALOX15, CKAP5, LIMCH1, SYNPO, VASP, CLASP1, PFDN2
	blood coagulation, fibrin clot formation	4.0622E-03	FGA, F12, FGB, FGG, F13A1, APOH
	zymogen activation	4.7030E-03	SERPINE1, FGA, F12, FGB, FGG, CTSL, LGMN, FADD, SERPINF2, MELTF, PRSS3, APOH, CD5L
	regulation of amyloid fibril formation	4.8995E-03	LDLR, PFDN1, PFDN6, APP, PFDN4, VBP1, PFDN2
	regulation of actin filament polymerization	5.0961E-03	HCLS1, EVL, CTTN, EPS8, TMOD3, BIN1, ARPC5L, PTK2B, CAPG, KANK1, SPTA1, ARPC5, ALOX15, CAPZA1, SPTAN1, CAPZA2, ADD1, VASP, ADD3, SSH3, TMOD1
	cellular response to topologically incorrect protein	5.2091E-03	VAPB, HSPB8, EIF2S1, UGGT1, DDRGK1, AUP1, HSPA5, COPS5, SELENOS, RNF126, ERO1A, HSPA14, VCP, ERLEC1, BAG3, HSPA8, STUB1, BAG6, PIK3R1
	mRNA transport	5.2282E-03	CETN3, NUP214, NUP43, NUP50, NUP62, SRSF1, NUP54, CETN2, NUP58, QKI, AKAP8L, TPR, THOC2, RAE1, IGF2BP2, SUPT6H, SEC13, HNRNPA3, NUP88, KHSRP
	regulation of mRNA metabolic process	5.7968E-03	TENT5C, SNRNP70, TAF15, SRSF9, C1QBP, SAP18, RBM4, VIM, SERBP1, ELAVL1, PAF1, SF1, NPM1, HNRNPC, QKI, SAFB2, CARHSP1, GIGYF2, PSMC1, PSMC3, SRSF10, PABPC1, HNRNPM, MBN L1, PSMC4, SUPT6H, FXR1, PTBP1, FUS, HNRNPL, HNRNPD, NUDT21, HSPA8, KHSRP, U2AF2
	protein depolymerization	6.7410E-03	PPP1R9B, EPS8, LIMA1, TMOD3, SH3GL1, PLEK, CAPG, NES, KIF2A, SPTA1, CKAP5, CAPZA1, SPTAN1, CAPZA2, ADD1, CLASP1, HSPA8, ADD3, TMOD1
	endoplasmic reticulum to cytosol transport	7.0735E-03	UBE2J1, HSP90B1, AUP1, SELENOS, UBE2G2, FAF2, NPLOC4, VCP, ERLEC1
	retrograde protein transport, ER to cytosol 7	7.0735E-03	UBE2J1, HSP90B1, AUP1, SELENOS, UBE2G2, FAF2, NPLOC4, VCP, ERLEC1
	vesicle localization	7.5050E-03	TRIP11, BLOC1S6, SEC16A, DNM1, HGS, BLOC1S4, FNBP1L, DCTN2, TSG101, BLOC1S2, STAM, BLOC1S3, SNAPIN, TFG, COPS5, DTNBP1,

Supplementary Table 4. GO analysis filtered for peptides with log2(FC) >1

	GO Term	Adjusted P Value	Relevant Genes Identified
			BLOC1S5, AP3M1, MYO5A, AP3S1, SAR1B, RAB27B, S CRIB, CLASP1, SNAP29
	regulation of plasma lipoprotein particle levels	8.1643E-03	LDLR, CNPY2, APOC2, SOAT1, HMOX1, AGT, APOA1, PLTP, LPL, APOA2, APOM, MSR1, APOC3, KHSRP
	negative regulation of wound healing	8.1643E-03	SERPINE1, FGA, F12, FGB, FGG, PROS1, PROC, SERPINF2, KNG1, PLG, APOH, CLASP1, KRT1, HRG
	high-density lipoprotein particle clearance	8.5808E-03	LDLR, APOC2, APOA1, APOA2, APOM, APOC3
	nucleocytoplasmic transport	9.3034E-03	ZPR1, HCLS1, NUP214, PPP1R12A, NUP50, NUP62, AGT, RBM4, ELAVL1, PPP1CC, TGFB1, NUP54, NPM1, LMNA, GAS6, NUP58, ANP32A, AKAP8L, TPR, IPO7, SYK, THOC2, RAE1, SUPT6H, SEC13, NOP9, ANP32B, HSP90AB1, APPL2, NUP88, XPOT, BAG3, RPL23, PIK3R1
	nuclear transport	9.3034E-03	ZPR1, HCLS1, NUP214, PPP1R12A, NUP50, NUP62, AGT, RBM4, ELAVL1, PPP1CC, TGFB1, NUP54, NPM1, LMNA, GAS6, NUP58, ANP32A, AKAP8L, TPR, IPO7, SYK, THOC2, RAE1, SUPT6H, SEC13, NOP9, ANP32B, HSP90AB1, APPL2, NUP88, XPOT, BAG3, RPL23, PIK3R1
	cytoskeleton-dependent intracellular transport	9.9530E-03	BLOC1S6, BLOC1S4, FNBP1L, BLOC1S2, ARMCX3, HSBP1, BLOC1S3, SNAPIN, PEX14, RHOT2, DYNC1I2, DTNBP1, BLOC1S5, AP3M1, MYO5A, AP3S1, HOOK3, APP, IFT27, TUBB, SYNE2, RAB27 B, BAG3, HSPA8, PCM1
	actin filament depolymerization	1.0405E-02	PPP1R9B, EPS8, LIMA1, TMOD3, PLEK, CAPG, SPTA1, CAPZA1, SPTAN1, CAPZA2, ADD1, ADD3, TMOD1
	plasminogen activation	1.2891E-02	SERPINE1, FGA, F12, FGB, FGG, SERPINF2, MELTF, APOH
	multivesicular body assembly	1.3462E-02	VTA1, VPS37A, STAM2, HGS, VPS37B, TSG101, CHMP2B, STAM, CHMP1A
	protein activation cascade	1.6479E-02	FGA, F12, FGB, FGG, F13A1, APOH
	negative regulation of amyloid fibril formation	1.6479E-02	LDLR, PFDN1, PFDN6, PFDN4, VBP1, PFDN2
	cellular oxidant detoxification	1.7765E-02	DHFR, HBM, GPX7, HBQ1, GPX3, EPX, SOD2, SELENOS, PXDN, HBB, PRDX4, CCS, APOM, TXNRD1, GPX8, HBG1
	multivesicular body organization	1.8182E-02	VTA1, VPS37A, STAM2, HGS, VPS37B, TSG101, CHMP2B, STAM, CHMP1A
	chaperone cofactor-dependent protein refolding	1.8182E-02	HSPA5, DNAJC7, ST13, HSPE1, CD74, ERO1A, HSPA14, DNAJB1, HSPA8
Biological Processes	protein import	1.9113E-02	ZPR1, HCLS1, NUP214, NUP50, NUP62, AGT, ELAVL1, TGFB1, NUP54, LMNA, NUP58, PEX14, TPR, IPO7, SYK, PEX3, SEC13, HSP90AB1, AIFM1, APPL2, NUP88, BAG3, HSPA8, RPL23, TOMM22, PIK 3R1
	biological process involved in symbiotic interaction	2.0279E-02	LDLR, GYPA, PF4, VAPB, CTSL, CTSB, CARD9, KRT6A, VAPA, APOL1, EPS15, GAS6, CLEC4G, NRP1, ITGB6, TRIM26, PSMC3, PTX3, BPIFA1, THOC2, PLG, LGALS1, EXOC7, CD74, TRIM38, CD209, HDAC1, HSP90AB1, TRIM22, HSPA8, HRG
	spindle assembly	2.0791E-02	RCC1, TASOR, ZNF207, CHMP2B, MAPRE1, SMC1A, KIF2A, NUMA1, MZT1, TPR, TUBB, EML3, CHMP1A, SEPTIN1, GOLGA2, CLASP1, MAPRE2, TUBB1
	regulation of nucleocytoplasmic transport	2.0998E-02	ZPR1, HCLS1, NUP214, PPP1R12A, RBM4, PPP1CC, TGFB1, NUP54, GAS6, NUP58, AKAP8L, TPR, SUPT6H, ANP32B, HSP90AB1, BAG3, PIK3R1

Supplementary Table 4. GO analysis filtered for peptides with log2(FC) >1

GO Term	Adjusted P Value	Relevant Genes Identified
Golgi organization	2.1261E-02	GOLGA5, TRIP11, SEC16A, PDE4DIP, GOLGB1, SEC23IP, AKAP9, GCC2, NSFL1C, COG7, LMAN1, NPLOC4, TMED1, STX16, COG4, GOLGA2, COG2, CLASP1, GOLPH3, TRAPPC12, TRAPPC8
regulation of blood coagulation	2.1525E-02	SERPINE1, FGA, F12, FGB, FGG, PROS1, PROC, SERPINF2, KNG1, PLG, APOH, KRT1, HRG
axo-dendritic transport	2.2348E-02	BLOC1S6, BLOC1S4, BLOC1S2, ARMCX3, HSBP1, BLOC1S3, SNAPIN, DTNBP1, BLOC1S5, AP3M1, AP3S1, APP, RAB27B, HSPA8
negative regulation of proteolysis	2.2486E-02	SERPINE1, SGTA, DPEP1, AHSG, LAMTOR5, IGBP1, PROS1, LPA, CAST, BIN1, FETUB, ITIH6, ITIH2, AGT, GLG1, PSMF1, DNAJB2, ALAD, GAS6, SERPINF2, DDRGK1, SERPINA10, ECM1, SERPIND 1, KNG1, PLAUR, ITIH4, APP, POR, HSP90AB1, SERPINA1, RPL23, HRG, UBXN1, BAG6
positive regulation of supramolecular fiber organization	2.2629E-02	WAS, EVL, CTTN, PDE4DIP, CLIP1, BIN1, SLAIN2, AKAP9, PTK2B, TPM1, PLEK, MAPRE1, SERPINF2, NRP1, NUMA1, APOA1, ALOX15, CKAP5, LIMCH1, APP, SYNPO, VASP, CLASP1
negative regulation of actin filament depolymerization	2.2657E-02	EPS8, LIMA1, TMOD3, CAPG, SPTA1, CAPZA1, SPTAN1, CAPZA2, ADD1, ADD3, TMOD1
regulation of actin filament depolymerization	2.3014E-02	EPS8, LIMA1, TMOD3, PLEK, CAPG, SPTA1, CAPZA1, SPTAN1, CAPZA2, ADD1, ADD3, TMOD1
synaptic vesicle transport	2.5006E-02	BLOC1S6, DNM1, BLOC1S4, BLOC1S2, BLOC1S3, SNAPIN, DTNBP1, BLOC1S5, AP3M1, AP3S1
regulation of proteasomal protein catabolic process	2.5888E-02	SGTA, ECSCR, TMF1, DAB2, UBQLN2, PSMF1, DNAJB2, ALAD, DDRGK1, COMMD1, PSMC2, PSMC1, RAD23B, ARIH1, PSMC3, ELOB, PSMC4, VCP, HSP90AB1, BAG2, STUB1, UBXN1, BAG6, UBQL N1
transport along microtubule	2.8807E-02	BLOC1S6, BLOC1S4, BLOC1S2, ARMCX3, HSBP1, BLOC1S3, SNAPIN, PEX14, RHOT2, DYNC1I2, DTNBP1, BLOC1S5, AP3M1, AP3S1, APP, IFT27, SYNE2, RAB27B, BAG3, HSPA8, PCM1
regulation of hemostasis	3.0274E-02	SERPINE1, FGA, F12, FGB, FGG, PROS1, PROC, SERPINF2, KNG1, PLG, APOH, KRT1, HRG
regulation of substrate adhesion-dependent cell spreading	3.3411E-02	FGA, FGB, FGG, C1QBP, DAB2, KANK1, NRP1, APOA1, MELTF, OLFM4, CORO1C, CRKL
negative regulation of RNA splicing	3.6224E-02	SRSF9, C1QBP, SAP18, PTBP3, SRSF10, PTBP1, RPS26, U2AF2
protein maturation	4.0872E-02	SERPINE1, CPXM1, FGA, F12, FGB, FGG, CTSL, CAST, SEC11C, GLRX3, GLG1, LGMN, NCSTN, FADD, SERPINF2, SNAPIN, GALNT2, MELTF, PRDX4, CCS, PRSS3, ERO1A, APOH, CTSS, DNAJB11 , SPCS2, GLRX5, PMPCB, BAG2, SPCS1, STUB1, CD5L
mitochondrial electron transport, NADH to ubiquinone	4.1983E-02	NDUFV3, NDUFS8, NDUFS6, NDUFS1, NDUFA2, NDUFS3, NDUFV1, NDUFS7, NDUFV2, NDUFS4, NDUFA5
actin filament bundle organization	4.2601E-02	WAS, EVL, EPS8, LIMA1, SHTN1, PTK2B, TPM1, PLEK, SERPINF2, HSP90B1, NRP1, APOA1, PDLIM1, LIMCH1, PPFIA1, MARCKS, ADD1, SYNPO, CALD1, CLASP1, PIK3R1

Supplementary Table 4. GO analysis filtered for peptides with log2(FC) >1

	GO Term	Adjusted P Value	Relevant Genes Identified
	nucleobase-containing compound transport	4.6684E-02	CETN3, NUP214, NUP43, NUP50, NUP62, SRSF1, NUP54, NPM1, CETN2, NUP58, QKI, AKAP8L, TPR, CKAP5, THOC2, RAE1, IGF2BP2, SUPT6H, SEC13, LRRC8C, HNRNPA3, NUP88, XPOT, RTRAF, TST, KHSRP
	positive regulation of intracellular protein transport	4.6867E-02	ATG13, ZPR1, HCLS1, NMT1, FIS1, RNF31, GAS6, UBE2L3, TPR, ANP32B, TCAF2, SAR1B, ITGAM, ITGB2, HSP90AB1, SH3GLB1, TM9SF4, BAG3, UBL5, PCM1, PIK3R1
	endosome organization	4.7683E-02	VTA1, LAMTOR1, VPS37A, STAM2, DNM1, HGS, VPS37B, TSG101, CHMP2B, STAM, EEA1, HOOK3, CHMP1A, CORO1C
	regulation of coagulation	4.9235E-02	SERPINE1, FGA, F12, FGB, FGG, PROS1, PROC, SERPINF2, KNG1, PLG, APOH, KRT1, HRG
	regulation of fibrinolysis	4.9385E-02	SERPINE1, F12, SERPINF2, PLG, APOH, HRG
	secretory granule lumen	1.9326E-16	PF4, SERPINE1, RNASE2, F5, AHSG, FGA, FGB, FAM3C, FGG, PROS1, RETN, SPARC, PRG3, HRNR, ARHGAP45, TXNDC5, ALAD, GAS6, EPX, FTL, SERPINF2, APOA1, F13A1, PSMC2, CTSA, ECM1 , PSMC3, EEF1A1, PSMD2, PTX3, ARPC5, OSTF1, KNG1, FAF2, ISLR, ITIH4, PRDX4, PLG, GHDC, ALDOC, APP, ERP44, SPTAN1, BIN2, TUBB, APOH, VCP, CNN2, OLFM4, HSP90AB1, ALDOA, SERPI NA1, COMMD9, HSPA8, IMPDH2, HRG, S100A11, GUSB
	cytoplasmic vesicle lumen	3.0649E-16	PF4, SERPINE1, RNASE2, F5, AHSG, FGA, FGB, FAM3C, FGG, PROS1, RETN, SPARC, PRG3, HRNR, ARHGAP45, TXNDC5, ALAD, GAS6, EPX, FTL, SERPINF2, APOA1, F13A1, PSMC2, CTSA, ECM1 , PSMC3, EEF1A1, PSM 2, PTX3, ARPC5, OSTF1, KNG1, FAF2, ISLR, ITIH4, PRDX4, PLG, GHDC, ALDOC, APP, ERP44, SPTAN1, BIN2, TUBB, APOH, VCP, CNN2, OLFM4, HSP90AB1, ALDOA, SERPI NA1, COMMD9, HSPA8, IMPDH2, HRG, S100A11, GUSB
	vesicle lumen	4.1538E-16	PF4, SERPINE1, RNASE2, F5, AHSG, FGA, FGB, FAM3C, FGG, PROS1, RETN, SPARC, PRG3, HRNR, ARHGAP45, TXNDC5, ALAD, GAS6, EPX, FTL, SERPINF2, APOA1, F13A1, PSMC2, CTSA, ECM1 , PSMC3, EEF1A1, PSMD2, PTX3, ARPC5, OSTF1, KNG1, FAF2, ISLR, ITIH4, PRDX4, PLG, GHDC, ALDOC, APP, ERP44, SPTAN1, BIN2, TUBB, APOH, VCP, CNN2, OLFM4, HSP90AB1, ALDOA, SERPI NA1, COMMD9, HSPA8, IMPDH2, HRG, S100A11, GUSB
Cellular Components	endoplasmic reticulum lumen	5.0884E-15	SELENOF, CSF1, F5, NUCB1, RCN3, GPX7, P4HA1, MZB1, FMO1, P4HA2, AHSG, FGA, RCN1, RCN2, FGG, TNC, FKBP10, CKAP4, ITIH2, CALU, PROC, TGOLN2, KTN1, APOL1, TXNDC5, UGGT1, MI A3, GAS6, ERP29, PDIA6, HSP90B1, APOA1, HSPA5, SERPINA10, SERPIND1, COL10A1, MELTF, KNG1, SUMF2, PLAUR, FSTL1, LGALS1, COL15A1, APP, CP, ERP44, APOA2, ERO1A, HYOU1, F10, D NAJB11, ERLEC1, GOLM1, GPX8, SERPINA1
	cell cortex	1.3323E-12	HCLS1, FGB, RAI14, CLTA, PPP1R9B, CTTN, EPS8, WASHC1, PDE4DIP, EPB41, ERC1, KRT19, GLRX3, FNBP1L, SLC4A1, PTK2B, AKAP12, EPB42,

Supplementary Table 4. GO analysis filtered for peptides with log2(FC) >1

GO Term	Adjusted P Value	Relevant Genes Identified
		TRIP10, TPM4, MAPRE1, C2CD2L, SPTA1, NUMA1 , SLC2A1, EEF1A1, STIM1, MYL12B, GNAI1, EXOC7, TNFAIP2, HMCN1, SPTAN1, BIN2, CLTB, PHLDB1, CAPZA2, MARCKS, SEPTIN2, MPP1, SEPTIN1, CALD1, AGTRAP, CTBP2, CLASP1, MYL9, EXO C1, ADD3, SEPTIN4, CORO1C, TMOD1, SEPTIN6
protein-lipid complex	1.7759E-12	LDLR, APOC2, LPA, BIN1, APOBR, APOL1, APOA1, PLTP, SELENOS, LPL, PEX3, SAA2, APOA2, APOM, HDLBP, APOH, MSR1, APOC3, SAA1
ribosomal subunit	4.3174E-11	MRPL12, MRPL41, MRPL50, RPS25, RPS28, MRPS35, RPLP2, MRPS22, RPLP1, MRPS9, MRPS31, RPL17, RPL13, RPS17, RPL26, RPL7A, MRPL4, RPS6, RPS18, MRPL21, MRPL17, RPS4X, RPS12, R PL27A, ISG15, RPS14, RPS21, RPS26, RPL18, DAP3, RPL32, RPL23, RPL10, EIF2D, RPL8, RPL21, RPL38
plasma lipoprotein particle	1.0316E-10	LDLR, APOC2, LPA, APOBR, APOL1, APOA1, PLTP, SELENOS, LPL, SAA2, APOA2, APOM, HDLBP, APOH, MSR1, APOC3, SAA1
lipoprotein particle	1.0316E-10	LDLR, APOC2, LPA, APOBR, APOL1, APOA1, PLTP, SELENOS, LPL, SAA2, APOA2, APOM, HDLBP, APOH, MSR1, APOC3, SAA1
cytosolic ribosome	5.6261E-10	RPS25, RPS28, RPLP2, RPLP1, RPL17, RPL13, RPS17, RPL26, RPL7A, RPS6, RPS18, RPS4X, RPS12, RPL27A, ISG15, RPS14, RPS21, RPS26, RPL18, RPL32, RPL23, RPL10, EIF2D, RPL8, RPL21, RPL 38
blood microparticle	2.6250E-09	AHSG, FGA, FGB, FGG, PROS1, CPN2, ITIH2, AGT, SLC4A1, APOL1, JCHAIN, AFM, SERPINF2, ITGA2B, APOA1, F13A1, SLC2A1, KNG1, HBB, C1S, ITIH4, PLG, CP, APOA2, KRT1, GC, HSPA8, HRG, C D5L
platelet alpha granule lumen	4.1178E-08	PF4, SERPINE1, F5, AHSG, FGA, FGB, FGG, PROS1, SPARC, GAS6, SERPINF2, F13A1, KNG1, ISLR, PLG, APP, ALDOA, SERPINA1, HRG
ficolin-1-rich granule lumen	2.2155E-07	CTSB, PRG2, ALAD, PSMC2, FTH1, PSMC3, EEF1A1, PSMD2, ARPC5, OSTF1, HBB, PRDX4, ALDOC, BIN2, CTSS, VCP, HSP90AB1, ALDOA, SERPINA1, KRT1, COMMD9, HSPA8, IMPDH2, GUSB, CO MMD3
platelet alpha granule	3.1814E-07	PF4, SERPINE1, F5, AHSG, FGA, FGB, FGG, PROS1, SPARC, GAS6, SERPINF2, ITGA2B, F13A1, THBS2, KNG1, ISLR, PLG, APP, ALDOA, SERPINA1, HRG
contractile fiber	3.3678E-07	TPM3, NEXN, MYL3, TMOD3, PDE4DIP, PPP1R12A, BIN1, KRT8, PDLIM4, KRT19, GLRX3, SLC4A1, ANK1, TPM1, TPM4, SLC2A1, PDLIM1, MYL1, TPM2, MYL12B, MMP2, LMAN1, FXR1, MYL6B, SYNE2 , SYNPO, CALD1, MTMR12, ALDOA, MYL9, SYNM, BAG3, STUB1, MYL4, CORO1C, TMOD1
myofibril	3.9361E-07	TPM3, NEXN, MYL3, TMOD3, PDE4DIP, PPP1R12A, BIN1, KRT8, PDLIM4, KRT19, GLRX3, SLC4A1, ANK1, TPM1, TPM4, SLC2A1, PDLIM1, MYL1, TPM2, MYL12B, MMP2, LMAN1, FXR1, SYNE2, SYNP O, CALD1, MTMR12, ALDOA, MYL9, SYNM, BAG3, STUB1, MYL4, CORO1C, TMOD1
ficolin-1-rich granule	9.5770E-07	LAMTOR1, CTSB, PRG2, FCER1G, ALAD, PSMC2, DOK3, FTH1, PSMC3, EEF1A1, PSMD2, ARPC5, OSTF1, HBB, PRDX4, ALDOC, BIN2, GAA, CTSS,

Supplementary Table 4. GO analysis filtered for peptides with log2(FC) >1

GO Term	Adjusted P Value	Relevant Genes Identified
		VCP, ITGB2, HSP90AB1, ALDOA, SERPINA1, KR T1, COMMD9, HSPA8, IMPDH2, GUSB, COMMD3
spliceosomal complex	9.7864E-07	BUD31, SNRPD1, IK, SF3A2, SNRNP70, AKAP17A, SNRPC, RNF113A, SF3A1, HTATSF1, SRSF1, SNRPE, SF1, HNRNPC, SF3A3, API5, SF3B2, CDC5L, PABPC1, HNRNPM, CLNS1A, BCAS2, SF3B5, S NRPD2, XAB2, HNRNPA3, HNRNPH3, HNRNPF, HSPA8, U2AF2, LUC7L3
very-low-density lipoprotein particle	4.3886E-06	APOC2, APOBR, APOL1, APOA1, SELENOS, LPL, APOA2, APOM, APOH, APOC3
triglyceride-rich plasma lipoprotein particle	4.3886E-06	APOC2, APOBR, APOL1, APOA1, SELENOS, LPL, APOA2, APOM, APOH, APOC3
sarcomere	6.7167E-06	TPM3, NEXN, MYL3, TMOD3, PPP1R12A, BIN1, KRT8, PDLIM4, KRT19, GLRX3, SLC4A1, ANK1, TPM1, TPM4, SLC2A1, PDLIM1, MYL1, TPM2, MYL12B, MMP2, LMAN1, SYNE2, SYNPO, MTMR12, ALD OA, MYL9, BAG3, STUB1, MYL4, CORO1C, TMOD1
BLOC-1 complex	7.4272E-06 B	LOC1S6, BLOC1S4, KXD1, BLOC1S2, BLOC1S3, SNAPIN, STX12, DTNBP1, BLOC1S5
BLOC complex	7.7073E-06	BLOC1S6, BLOC1S4, KXD1, BLOC1S2, HPS6, BLOC1S3, SNAPIN, STX12, DTNBP1, BLOC1S5
polysome	8.5882E-06	RPS28, VIM, EIF2S1, BTF3, RPL7A, RPS6, FXR1, RPS4X, HDLBP, RPS21, VBP1, RPS26, RPL18, RPL32, EIF4G1, RPL8, RPL38
cortical cytoskeleton	1.4444E-05	HCLS1, PPP1R9B, CTTN, PDE4DIP, EPB41, ERC1, KRT19, SLC4A1, EPB42, TPM4, MAPRE1, SPTA1, NUMA1, SLC2A1, EEF1A1, SPTAN1, CAPZA2, MPP1, CALD1, CLASP1, TMOD1
high-density lipoprotein particle	1.4711E-05	APOC2, APOL1, APOA1, PLTP, SAA2, APOA2, APOM, HDLBP, APOH, APOC3, SAA1
U2-type spliceosomal complex	2.0581E-05	BUD31, SNRPD1, IK, SF3A2, SNRNP70, SNRPC, RNF113A, SF3A1, HTATSF1, SNRPE, SF3A3, SF3B2, CDC5L, BCAS2, SF3B5, SNRPD2, XAB2, U2AF2, LUC7L3
small ribosomal subunit	2.5402E-05	RPS25, RPS28, MRPS35, MRPS22, MRPS9, MRPS31, RPS17, RPS6, RPS18, RPS4X, RPS12, ISG15, RPS14, RPS21, RPS26, DAP3, EIF2D
endoplasmic reticulum protein-containing complex	4.2507E-05	P4HA1, MZB1, KRTCAP2, SPTLC2, SEC61G, SEC11C, PDIA6, HSP90B1, AUP1, HSPA5, SELENOS, FAF2, NPLOC4, VCP, TAPBP, HYOU1, DNAJB11, SPCS2, SRPRB, SPCS1, SRPRA, UBXN1
cytosolic large ribosomal subunit	6.6282E-05	RPLP2, RPLP1, RPL17, RPL13, RPL26, RPL7A, RPL27A, RPL18, RPL32, RPL23, RPL10, RPL8, RPL21, RPL38
mitochondrial protein-containing complex	1.2355E-04	MRPL12, MRPL41, NDUFV3, NMES1, MRPL50, MRPS35, MRPS22, PDK1, MRPS9, MRPS31, ATP5F1D, NDUFS8, NDUFS6, CHCHD3, ATP5PF, MRPL4, NDUFS1, TOMM6, NDUFA2, MRPL21, MRPL1 7, BCKDK, NDUFS3, TIMM13, CHCHD6, NDUFV1, NDUFS7, NDUFV2, DAP3, PMPCB, NDUFS4, NDUFA5, AGK, TOMM22

Supplementary Table 4. GO analysis filtered for peptides with log2(FC) >1

	GO Term	Adjusted P Value	Relevant Genes Identified
Cellular Components	catalytic step 2 spliceosome	1.4257E-04	BUD31, SNRPD1, SF3A2, SF3A1, SRSF1, SNRPE, HNRNPC, SF3A3, SF3B2, CDC5L, PABPC1, HNRNPM, BCAS2, SNRPD2, XAB2, HNRNPA3, HNRNPF
	large ribosomal subunit	1.4972E-04	MRPL12, MRPL41, MRPL50, RPLP2, RPLP1, RPL17, RPL13, RPL26, RPL7A, MRPL4, MRPL21, MRPL17, RPL27A, RPL18, RPL32, RPL23, RPL10, RPL8, RPL21, RPL38
	cytosolic small ribosomal subunit	4.8999E-04	RPS25, RPS28, RPS17, RPS6, RPS18, RPS4X, RPS12, ISG15, RPS14, RPS21, RPS26, EIF2D
	chylomicron	5.0906E-04	APOC2, APOBR, APOA1, LPL, APOA2, APOH, APOC3
	chaperone complex	1.3222E-03	CDC37, HSPB8, STIP1, DNAJB11, HSP90AB1, BAG2, BAG3, HSPA8, STUB1
	endoplasmic reticulum chaperone complex	1.6038E-03	MZB1, PDIA6, HSP90B1, HSPA5, HYOU1, DNAJB11
	site of polarized growth	1.7645E-03	ZPR1, HCLS1, PPP1R9B, CTTN, EPS8, TUBB3, SHTN1, PTK2B, DCTN2, FKBP15, THY1, NGFR, ARPC5, DTNBP1, MYO5A, EXOC7, APP, FXR1, KLC1, BASP1, HSP90AB1, COPA, ABI1
	prefoldin complex	1.7691E-03	PFDN1, PFDN6, PFDN4, VBP1, PFDN2
	muscle thin filament tropomyosin	1.9525E-03	TPM3, TPM1, TPM4, TPM2
	condensed chromosome, centromeric region	2.1073E-03	TP53BP1, CBX5, PPP1R12A, PMF1, CLIP1, NUP43, ZNF207, PPP1CC, ANAPC16, DCTN2, SMC1A, SIN3A, CBX3, TPR, CKAP5, SEC13, SEPTIN2, SUGT1, CLASP1, TRAPPC12, SEPTIN6
	endocytic vesicle lumen	2.4094E-03	CTSL, HGS, SPARC, HSP90B1, APOA1, HBB, HYOU1, SAA1
	kinetochore	2.5150E-03	TP53BP1, CBX5, PPP1R12A, PMF1, CLIP1, NUP43, ZNF207, PPP1CC, ANAPC16, DCTN2, SMC1A, SIN3A, TPR, CKAP5, SEC13, SEPTIN2, SUGT1, CLASP1, TRAPPC12, SEPTIN6
	midbody	2.9390E-03	IL16, EML4, NUP62, VPS37B, PPP1CC, RAP2A, ERH, TSG101, CAPG, HSP90B1, PIN1, HSPA5, SLC2A1, TACC1, DTNBP1, GNAI1, NUDC, EXOC7, SEPTIN2, EML3, SPART, SEPTIN1, SH3GLB1, EXOC 1, SEPTIN6
	proteasome regulatory particle, base subcomplex	3.0800E-03	PSMD4, PSMC2, PSMC1, PSMC3, PSMD2, PSMC4
	growth cone	3.2430E-03	ZPR1, PPP1R9B, CTTN, EPS8, TUBB3, SHTN1, PTK2B, DCTN2, FKBP15, THY1, NGFR, ARPC5, DTNBP1, MYO5A, EXOC7, APP, FXR1, KLC1, BASP1, HSP90AB1, COPA, ABI1
	nuclear pore	3.5205E-03	CETN3, NUP214, NUP43, NUP50, NUP62, NUP54, RANBP1, CETN2, NUP58, TPR, IPO7, RAE1, SEC13, NUP88, XPOT
	lamellipodium	4.1767E-03	EVL, PPP1R9B, CTTN, ENAH, TUBB3, SHTN1, CAPRIN1, PDLIM4, PTK2B, FGD3, CAPG, PSTPIP1, SRGAP2, ARPC5, APBB1IP, PABPC1, APP, SYNE2, VASP, SCRIB, CDC42BPB, FGD2, STX4, ABI1, C ORO1C
	polysomal ribosome	4.5327E-03	RPS28, BTF3, RPL7A, RPS21, RPS26, RPL18, RPL32, RPL8, RPL38
	BORC complex	4.5345E-03	KXD1, BORCS8, BLOC1S2, SNAPIN, BORCS6
	spherical high-density lipoprotein particle	4.5345E-03	APOC2, APOA1, APOA2, APOM, APOC3
	microtubule plus-end	4.8878E-03	PDE4DIP, CLIP1, SLAIN2, MAPRE1, NUMA1, CKAP5, CLASP1, MAPRE2

Supplementary Table 4. GO analysis filtered for peptides with log2(FC) >1

	GO Term	Adjusted P Value	Relevant Genes Identified
Cellular Components	pigment granule	5.0574E-03	CTSB, CALU, NCSTN, NAP1L1, SND1, CAPG, ERP29, PDIA6, HSP90B1, HSPA5, SLC2A1, DTNBP1, MYO5A, TPP1, RAB27B, HSP90AB1, HSPA8
	melanosome	5.0574E-03	CTSB, CALU, NCSTN, NAP1L1, SND1, CAPG, ERP29, PDIA6, HSP90B1, HSPA5, SLC2A1, DTNBP1, MYO5A, TPP1, RAB27B, HSP90AB1, HSPA8
	low-density lipoprotein particle	5.4926E-03	LDLR, APOC2, APOBR, SELENOS, APOM, MSR1
	ruffle	5.5858E-03	PPP1R9B, CTTN, EPS8, LIMA1, CLIP1, TPM1, PLEK, ARHGAP45, FGD3, CAPG, KANK1, EEF1A1, ADGRE2, MYO5A, ACAP2, JCAD, NME1, RASGRP2, APPL2, TLN1, FGD2, S100A11, CORO1C
	ESCRT complex	6.7708E-03	VPS37A, STAM2, HGS, VPS37B, TSG101, CHMP2B, STAM, CHMP1A
	cell cortex region	9.3035E-03	CLTA, EPB41, ERC1, NUMA1, MYL12B, GNAI1, CLTB, PHLDB1, CTBP2, CLASP1
	cortical microtubule cytoskeleton	9.3978E-03	PDE4DIP, MAPRE1, NUMA1, CLASP1
	endolysosome lumen	9.3978E-03	CTSL, CTSB, LGMN, CTSS NADH dehydrogenase complex 9.5358E-03 NDUFV3, NDUFS8, NDUFS6, NDUFS1, NDUFA2, NDUFS3, NDUFV1, NDUFS7, NDUFV2, NDUFS4, NDUFA5
	mitochondrial respiratory chain complex I	9.5358E-03	NDUFV3, NDUFS8, NDUFS6, NDUFS1, NDUFA2, NDUFS3, NDUFV1, NDUFS7, NDUFV2, NDUFS4, NDUFA5
	respiratory chain complex I	9.5358E-03	NDUFV3, NDUFS8, NDUFS6, NDUFS1, NDUFA2, NDUFS3, NDUFV1, NDUFS7, NDUFV2, NDUFS4, NDUFA5
	axon cytoplasm	1.0589E-02	BLOC1S6, BLOC1S4, BLOC1S2, ARMCX3, HSBP1, BLOC1S3, SNAPIN, DTNBP1, BLOC1S5, AP3M1, AP3S1, RAB27B
	tertiary granule lumen	1.6609E-02	PRG3, FTH1, PTX3, HBB, ALDOC, PRSS3, SPTAN1, CTSS, CNN2, OLFM4, ALDOA
	ruffle membrane	1.7928E-02 P	PP1R9B, EPS8, TPM1, PLEK, ARHGAP45, KANK1, EEF1A1, ADGRE2, JCAD, NME1, RASGRP2, APPL2, TLN1, FGD2, CORO1C
	endoplasmic reticulum-Golgi intermediate compartment	1.8381E-02	F5, NUCB1, CCDC115, TRIP11, GOLGB1, SEC23IP, UGGT1, PDIA6, HSPA5, ASPSCR1, LMAN1, ERP44, TMED1, TAPBP, GOLGA2, SERPINA1, ERGIC2, TRAPPC12
	trans-Golgi network membrane	2.0264E-02	CLTA, IMPAD1, SCAMP2, SCAMP3, TMEM165, ARFIP1, COG6, COG7, APP, CD74, VAMP3, STX16, COG4, COG2, ARFRP1
	prespliceosome	2.2700E-02	SF3A2, SNRNP70, SNRPC, SF3A1, U2AF2, LUC7L3
	U2-type prespliceosome	2.2700E-02	SF3A2, SNRNP70, SNRPC, SF3A1, U2AF2, LUC7L3
	pICln-Sm protein complex	2.7142E-02	SNRPD1, SNRPE, CLNS1A, SNRPD2
	actin filament bundle	2.9567E-02	TPM3, LIMA1, PDLIM4, TPM1, TPM4, PDLIM1, MYL12B, LIMCH1, MARCKS, CNN2, SYNPO, MYL9, BAG3
	actomyosin	2.9567E-02	TPM3, LIMA1, PDLIM4, TPM1, TPM4, PDLIM1, MYL12B, LIMCH1, CNN2, SYNPO, CDC42BPB, MYL9, BAG3
	mitotic spindle	3.0066E-02	IK, MAP4, CTTN, EPB41, EML4, NUP62, RMDN2, MAPRE1, CAPG, SMC1A, NUMA1, TPR, RMDN3, RAE1, NUDC, EML3, GOLGA2, CLASP1, PYCR3, RTRAF

Supplementary Table 4. GO analysis filtered for peptides with log2(FC) >1

	GO Term	Adjusted P Value	Relevant Genes Identified
	U2-type precatalytic spliceosome	3.7005E-02	SNRPD1, IK, SF3A2, RNF113A, SF3A1, SNRPE, SF3A3, SF3B2, SF3B5, SNRPD2
	condensed chromosome	3.7260E-02	P3H4, TP53BP1, CBX5, RCC1, PPP1R12A, PMF1, CLIP1, NUP43, ZNF207, PPP1CC, RAD21, ANAPC16, DCTN2, SMC1A, SIN3A, CBX3, TPR, CKAP5, SEC13, SEPTIN2, CHMP1A, SUGT1, CLASP1, AD D3, TRAPPC12, SEPTIN6
	ESCRT-0 complex	4.1766E-02	STAM2, HGS, STAM
	stress fiber	4.2587E-02	TPM3, LIMA1, PDLIM4, TPM1, TPM4, PDLIM1, MYL12B, LIMCH1, CNN2, SYNPO, MYL9, BAG3
	contractile actin filament bundle	4.2587E-02	TPM3, LIMA1, PDLIM4, TPM1, TPM4, PDLIM1, MYL12B, LIMCH1, CNN2, SYNPO, MYL9, BAG3
	I band	4.8200E-02	NEXN, MYL3, PPP1R12A, BIN1, KRT8, PDLIM4, KRT19, GLRX3, SLC4A1, SLC2A1, PDLIM1, MYL12B, SYNE2, SYNPO, ALDOA, MYL9, BAG3, STUB1
	Translation	3.1093E-16	SRP19, MRPL12, MRPL41, MRPL50, RPS25, RPS28, MRPS35, SRP54, SEC61G, RPLP2, SEC11C, EIF4H, CARS1, MRPS22, RPLP1, SRP72, MRPS9, SSR3, MRPS31, TARS1, RPL17, EIF5, EIF2S1, RPL 13, EEF1B2, RPS17, EEF1D, RPL26, RPL7A, MRPL4, EIF2B2, EEF1A1, RPS6, EEF1E1, PABPC1, SSR1, RPS18, MRPL21, MRPL17, SRP68, EIF3M, PARS2, RPS4X, AIMP1, EIF3K, RPS12, RPL27A, AAR S2, RPS14, SPCS2, RPS21, SRPRB, RPS26, RPL18, DAP3, TRMT112, PTCD3, SSR2, SPCS1, RPL32, SRPRA, RPL23, RPL10, EIF4G1, MRPS25, RPL8, RPL21, RPL38
	SRP-dependent cotranslational protein targeting to membrane	3.7934E-13	SRP19, RPS25, RPS28, SRP54, SEC61G, RPLP2, SEC11C, RPLP1, SRP72, SSR3, RPL17, RPL13, RPS17, RPL26, RPL7A, RPS6, SSR1, RPS18, SRP68, RPS4X, RPS12, RPL27A, RPS14, SPCS2, RPS21, SRPRB, RPS26, RPL18, SSR2, SPCS1, RPL32, SRPRA, RPL23, RPL10, RPL8, RPL21, RPL38
Reactome	Regulation of Insulin-like Growth Factor (IGF) transport and uptake by Insulin-like Growth Factor Binding	1.8173E-09	CSF1, F5, NUCB1, AHS PGro, FteGinAs, R(ICGNF1B, PFsG)G, TNC, CKAP4, ITIH2, CALU, PROC, TGOLN2, KTN1, APOL1, MIA3, GAS6, PDIA6, HSP90B1, APOA1, SERPINA10, SERPIND1, MELTF, KNG1, FSTL1, PLG, L GALS1, MMP2, APP, CP, APOA2, GOLM1, SERPINA1, IGFBP2
	Influenza Viral RNA Transcription and Replication	3.1882E-09	NUP214, RPS25, RPS28, RPLP2, NUP43, NUP50, RPLP1, NUP62, NUP54, RPL17, RPL13, RPS17, RPL26, RPL7A, RPS6, TPR, POLR2J, RPS18, RAE1, SEC13, POLR2I, RPS4X, RPS12, RPL27A, RPS14, RPS21, NUP88, RPS26, RPL18, RPL32, RPL23, RPL10, RPL8, RPL21, RPL38
	Post-translational protein phosphorylation	3.4114E-09	CSF1, F5, NUCB1, AHSG, FGA, RCN1, FGG, TNC, CKAP4, ITIH2, CALU, PROC, TGOLN2, KTN1, APOL1, MIA3, GAS6, PDIA6, HSP90B1, APOA1, SERPINA10, SERPIND1, MELTF, KNG1, FSTL1, LGALS1, APP, CP, APOA2, GOLM1, SERPINA1
	Influenza Infection	9.8609E-09	CLTA, NUP214, RPS25, RPS28, RPLP2, NUP43, NUP50, RPLP1, NUP62, NUP54, RPL17, RPL13, RPS17, RPL26, RPL7A, RPS6, TPR, POLR2J, RPS18, RAE1, SEC13, POLR2I, RPS4X, RPS12, RPL27A, ISG15, RPS14, RPS21, NUP88, RPS26, RPL18, RPL32, RPL23, RPL10, RPL8, RPL21, RPL38

Supplementary Table 4. GO analysis filtered for peptides with log2(FC) >1

GO Term	Adjusted P Value	Relevant Genes Identified
Eukaryotic Translation Initiation	1.7761E-08	RPS25, RPS28, RPLP2, EIF4H, RPLP1, RPL17, EIF5, EIF2S1, RPL13, RPS17, RPL26, RPL7A, EIF2B2, RPS6, PABPC1, RPS18, EIF3M, RPS4X, EIF3K, RPS12, RPL27A, RPS14, RPS21, RPS26, RPL18, RPL32, RPL23, RPL10, EIF4G1, RPL8, RPL21, RPL38
Cap-dependent Translation Initiation	1.7761E-08	RPS25, RPS28, RPLP2, EIF4H, RPLP1, RPL17, EIF5, EIF2S1, RPL13, RPS17, RPL26, RPL7A, EIF2B2, RPS6, PABPC1, RPS18, EIF3M, RPS4X, EIF3K, RPS12, RPL27A, RPS14, RPS21, RPS26, RPL18, RPL32, RPL23, RPL10, EIF4G1, RPL8, RPL21, RPL38
Processing of Capped Intron-Containing Pre-mRNA	4.4100E-08	BUD31, SNRPD1, SF3A2, FIP1L1, CCAR1, SNRNP70, SRSF9, NUP214, SNRPC, NUP43, NUP50, SF3A1, NUP62, SRSF1, ELAVL1, SNRPE, NUP54, SF1, CD2BP2, HNRNPC, SRRT, CSTF2, SF3A3, SF3B2, CDC5L, TPR, SRSF10, HNRNPM, POLR2J, BCAS2, THOC2, RAE1, SEC13, POLR2I, SF3B5, PTBP1, FUS, SNRPD2, HNRNPL, HNRNPD, XAB2, HNRNPA3, NUP88, HNRNPF, NUDT21, HSPA8, U2AF2
L13a-mediated translational silencing of Ceruloplasmin expression	6.5189E-08	RPS25, RPS28, RPLP2, EIF4H, RPLP1, RPL17, EIF2S1, RPL13, RPS17, RPL26, RPL7A, RPS6, PABPC1, RPS18, EIF3M, RPS4X, EIF3K, RPS12, RPL27A, RPS14, RPS21, RPS26, RPL18, RPL32, RPL23, RPL10, EIF4G1, RPL8, RPL21, RPL38
GTP hydrolysis and joining of the 60S ribosomal subunit	8.2859E-08	RPS25, RPS28, RPLP2, EIF4H, RPLP1, RPL17, EIF5, EIF2S1, RPL13, RPS17, RPL26, RPL7A, RPS6, RPS18, EIF3M, RPS4X, EIF3K, RPS12, RPL27A, RPS14, RPS21, RPS26, RPL18, RPL32, RPL23, RPL10, EIF4G1, RPL8, RPL21, RPL38
Eukaryotic Translation Elongation	9.8435E-08	RPS25, RPS28, RPLP2, RPLP1, RPL17, RPL13, EEF1B2, RPS17, EEF1D, RPL26, RPL7A, EEF1A1, RPS6, RPS18, RPS4X, RPS12, RPL27A, RPS14, RPS21, RPS26, RPL18, RPL32, RPL23, RPL10, RPL8, RPL21, RPL38
Response to elevated platelet cytosolic Ca2+	1.6994E-07	PF4, SERPINE1, F5, AHSG, FGA, FGB, FAM3C, FGG, PROS1, CALU, SPARC, PLEK, GAS6, SERPINF2, ITGA2B, APOA1, F13A1, HSPA5, ECM1, KNG1, ISLR, ITIH4, PLG, APP, APOH, RAB27B, ALDOA, TLN1, SERPINA1, TAGLN2, STX4, HRG

Supplementary Table 4. GO analysis filtered for peptides with log2(FC) >1

	GO Term	Adjusted P Value	Relevant Genes Identified
Reactome	Platelet degranulation	2.6365E-07	PF4, SERPINE1, F5, AHSG, FGA, FGB, FAM3C, FGG, PROS1, CALU, SPARC, PLEK, GAS6, SERPINF2, ITGA2B, APOA1, F13A1, HSPA5, ECM1, KNG1, ISLR, ITIH4, PLG, APP, APOH, RAB27B, ALDOA, TLN1, SERPINA1, TAGLN2, HRG
	Nonsense Mediated Decay (NMD) independent of the E	8.7308E-07	RPS25, RPS28, RPLP2, RPLP1, RPL17, RPL13, RPS17, RPL26, RPL7A, RPS6, PABPC1, RPS18, RPS4X, RPS12, RPL27A, RPS14, RPS21, RPS26, RPL18, RPL32, RPL23, RPL10, EIF4G1, RPL8, RPL21, RPL38
	Selenoamino acid metabolism	9.7247E-07	PAPSS1, RPS25, RPS28, RPLP2, RPLP1, RPL17, RPL13, RPS17, RPL26, RPL7A, RPS6, EEF1E1, RPS18, HNMT, RPS4X, AIMP1, RPS12, RPL27A, TXNRD1, RPS14, RPS21, RPS26, RPL18, RPL32, RPL23, RPL10, RPL8, RPL21, RPL38
	Peptide chain elongation	1.0106E-06	RPS25, RPS28, RPLP2, RPLP1, RPL17, RPL13, RPS17, RPL26, RPL7A, EEF1A1, RPS6, RPS18, RPS4X, RPS12, RPL27A, RPS14, RPS21, RPS26, RPL18, RPL32, RPL23, RPL10, RPL8, RPL21, RPL38
	mRNA Splicing - Major Pathway	1.2100E-06	BUD31, SNRPD1, SF3A2, FIP1L1, CCAR1, SNRNP70, SRSF9, SNRPC, SF3A1, SRSF1, ELAVL1, SNRPE, SF1, CD2BP2, HNRNPC, SRRT, CSTF2, SF3A3, SF3B2, CDC5L, SRSF10, HNRNPM, POLR2J, BCAS2, POLR2I, SF3B5, PTBP1, FUS, SNRPD2, HNRNPL, HNRNPD, XAB2, HNRNPA3, HNRNPF, NUDT21, HSPA8, U2AF2
	Eukaryotic Translation Termination	2.7104E-06	RPS25, RPS28, RPLP2, RPLP1, RPL17, RPL13, RPS17, RPL26, RPL7A, RPS6, RPS18, RPS4X, RPS12, RPL27A, RPS14, RPS21, RPS26, RPL18, TRMT112, RPL32, RPL23, RPL10, RPL8, RPL21, RPL38
	Signaling by ROBO receptors	3.2410E-06	EVL, PSMD4, ENAH, RPS25, RPS28, RPLP2, RPLP1, PSMF1, ELOC, RPL17, RPL13, RPS17, NRP1, PSMC2, RPL26, SRGAP2, PSMC1, RPL7A, PSMC3, PSMD2, RPS6, PABPC1, RPS18, ELOB, PSMC4, RPS4X, RPS12, RPL27A, VASP, RPS14, RPS21, CLASP1, RPS26, RPL18, RPL32, RPL23, RPL10, EIF4G1, RPL8, RPL21, RPL38
	Formation of a pool of free 40S subunits	3.5644E-06	RPS25, RPS28, RPLP2, RPLP1, RPL17, RPL13, RPS17, RPL26, RPL7A, RPS6, RPS18, EIF3M, RPS4X, EIF3K, RPS12, RPL27A, RPS14, RPS21, RPS26, RPL18, RPL32, RPL23, RPL10, RPL8, RPL21, RPL38
	mRNA Splicing	4.2789E-06	BUD31, SNRPD1, SF3A2, FIP1L1, CCAR1, SNRNP70, SRSF9, SNRPC, SF3A1, SRSF1, ELAVL1, SNRPE, SF1, CD2BP2, HNRNPC, SRRT, CSTF2, SF3A3, SF3B2, CDC5L, SRSF10, HNRNPM, POLR2J, BCAS2, POLR2I, SF3B5, PTBP1, FUS, SNRPD2, HNRNPL, HNRNPD, XAB2, HNRNPA3, HNRNPF, NUDT21, HSPA8, U2AF2
	Regulation of expression of SLITs and ROBOs	5.0318E-06	PSMD4, RPS25, RPS28, RPLP2, RPLP1, PSMF1, ELOC, RPL17, RPL13, RPS17, PSMC2, RPL26, PSMC1, RPL7A, PSMC3, PSMD2, RPS6, PABPC1, RPS18, ELOB, PSMC4, RPS4X, RPS12, RPL27A, RPS14, RPS21, RPS26, RPL18, RPL32, RPL23, RPL10, EIF4G1, RPL8, RPL21, RPL38

Supplementary Table 4. GO analysis filtered for peptides with log2(FC) >1

	GO Term	Adjusted P Value	Relevant Genes Identified
Reactome	Viral mRNA Translation	5.1885E-06	RPS25, RPS28, RPLP2, RPLP1, RPL17, RPL13, RPS17, RPL26, RPL7A, RPS6, RPS18, RPS4X, RPS12, RPL27A, RPS14, RPS21, RPS26, RPL18, RPL32, RPL23, RPL10, RPL8, RPL21, RPL38
	Cellular response to heat stress	1.2607E-05	NUP214, NUP43, NUP50, NUP62, HSPB8, NUP54, HSBP1, HSPA5, EEF1A1, TPR, DNAJC7, ST13, RAE1, RPA3, SEC13, HSPA14, DNAJB1, VCP, HSP90AB1, NUP88, BAG2, BAG3, HSPA8
	Selenocysteine synthesis	1.3125E-05	RPS25, RPS28, RPLP2, RPLP1, RPL17, RPL13, RPS17, RPL26, RPL7A, RPS6, RPS18, RPS4X, RPS12, RPL27A, RPS14, RPS21, RPS26, RPL18, RPL32, RPL23, RPL10, RPL8, RPL21, RPL38
	Response of EIF2AK4 (GCN2) to amino acid deficiency	1.6333E-05	RPS25, RPS28, RPLP2, RPLP1, RPL17, EIF2S1, RPL13, RPS17, RPL26, RPL7A, RPS6, RPS18, RPS4X, RPS12, RPL27A, RPS14, RPS21, RPS26, RPL18, RPL32, RPL23, RPL10, RPL8, RPL21, RPL38
	Common Pathway of Fibrin Clot Formation	4.0226E-05	PF4, F5, FGA, FGB, FGG, PROS1, PROC, F13B, F13A1, SERPIND1, F10
	trans-Golgi Network Vesicle Budding	4.2217E-05	CLTA, BLOC1S6, TPD52, GOLGB1, HGS, BLOC1S4, TGOLN2, TXNDC5, ACBD3, FTL, BLOC1S3, SNAPIN, SH3D19, FTH1, DTNBP1, AP3S1, APP, CLTB, HSPA8, STX4
	Nonsense-Mediated Decay (NMD)	6.1187E-05	RPS25, RPS28, RPLP2, RPLP1, RPL17, RPL13, RPS17, RPL26, RPL7A, RPS6, PABPC1, RPS18, RPS4X, RPS12, RPL27A, RPS14, RPS21, RPS26, RPL18, RPL32, RPL23, RPL10, EIF4G1, RPL8, RPL21, RPL38
	Nonsense Mediated Decay (NMD) enhanced by the Exon	6.1187E-05	RPS25, RPS28, RPLP2, RPLP1, RPL17, RPL13, RPS17, RPL26, RPL7A, RPS6, PABPC1, RPS18, RPS4X, RPS12, RPL27A, RPS14, RPS21, RPS26, RPL18, RPL32, RPL23, RPL10, EIF4G1, RPL8, RPL21, RPL38
	ER to Golgi Anterograde Transport	6.1709E-05	F5, COPE, TUBB3, MIA2, SEC16A, GOLGB1, SEC23IP, NAPG, ANK1, DCTN2, MIA3, SPTA1, DYNC1I2, TFG, COG6, COG7, CAPZA1, LMAN1, SEC13, SPTAN1, CAPZA2, COPZ1, SAR1B, COG4, COPA , GOLGA2, TUBB6, COG2, SERPINA1, COPB2, TUBB1
	Formation of Fibrin Clot (Clotting Cascade)	1.1451E-04	PF4, F5, FGA, F12, FGB, FGG, C1QBP, PROS1, PROC, F13B, F13A1, SERPIND1, KNG1, F10
	Transport to the Golgi and subsequent modification	1.4799E-04	MAN1A2, F5, COPE, TUBB3, MIA2, SEC16A, GOLGB1, SEC23IP, NAPG, ANK1, DCTN2, MIA3, FUT8, SPTA1, DYNC1I2, TFG, COG6, COG7, CAPZA1, LMAN1, SEC13, MAN2A1, SPTAN1, CAPZA2, COPZ1, SAR1B, COG4, COPA, GOLGA2, TUBB6, COG2, SERPINA1, COPB2, TUBB1
	Cellular response to starvation	2.7837E-04	LAMTOR5, LAMTOR1, RPS25, RPS28, RPLP2, RPLP1, RPL17, EIF2S1, RPL13, RPS17, RPL26, RPL7A, RPS6, RPS18, ATP6V1F, SEC13, RPS4X, RPS12, RPL27A, RPS14, RPS21, RPS26, RPL18, RPL32, RPL23, RPL10, LAMTOR3, RPL8, RPL21, RPL38
	Regulation of HSF1-mediated heat shock response	3.2513E-04	NUP214, NUP43, NUP50, NUP62, NUP54, HSPA5, TPR, DNAJC7, ST13, RAE1, RPA3, SEC13, HSPA14, DNAJB1, NUP88, BAG2, BAG3, HSPA8
	Intra-Golgi and retrograde Golgi-to-ER traffic	3.7548E-04	MAN1A2, GOLGA5, TRIP11, PLIN3, COPE, TUBB3, TMF1, NAPG, CYTH4, TGOLN2, DCTN2, KIF2A, GALNT2, GCC2, DYNC1I2, COG6, COG7, CAPZA1,

Supplementary Table 4. GO analysis filtered for peptides with log2(FC) >1

GO Term	Adjusted P Value	Relevant Genes Identified
		KLC2, MAN2A1, KLC1, CAPZA2, COPZ1, PAFAH1B3, VAMP3, STX16, COG4, COPA, TUBB6, COG2, SNAP29, ARFRP1, RAB3GAP1, COPB2, TUBB1
Interactions of Rev with host cellular proteins	1.0514E-03	NUP214, RCC1, NUP43, NUP50, NUP62, NUP54, RANBP1, NPM1, TPR, RAE1, SEC13, NUP88
Ribosomal scanning and start codon recognition	1.1942E-03	RPS25, RPS28, EIF4H, EIF5, EIF2S1, RPS17, RPS6, RPS18, EIF3M, RPS4X, EIF3K, RPS12, RPS14, RPS21, RPS26, EIF4G1
Translation initiation complex formation	1.1942E-03	RPS25, RPS28, EIF4H, EIF2S1, RPS17, RPS6, PABPC1, RPS18, EIF3M, RPS4X, EIF3K, RPS12, RPS14, RPS21, RPS26, EIF4G1
Clathrin-mediated endocytosis	1.5007E-03	LDLR, CLTA, CTTN, SH3GL1, BIN1, STAM2, DAB2, DNM1, HGS, UBQLN2, HIP1, TGOLN2, FNBP1L, EPS15, TRIP10, STAM, COPS8, PACSIN3, COPS5, ARPC5, COPS6, CLTB, VAMP3, SNX18, COPS4, HSPA8, UBQLN1
Activation of the mRNA upon binding of the cap-binding complex	1.5224E-03	RPS25, RPS28, EIF4H, EIF2S1, RPS17, RPS6, PABPC1, RPS18, EIF3M, RPS4X, EIF3K, RPS12, RPS14, RPS21, RPS26, EIF4G1
Golgi Associated Vesicle Biogenesis	1.7811E-03	BLOC1S6, TPD52, GOLGB1, BLOC1S4, TGOLN2, TXNDC5, ACBD3, FTL, BLOC1S3, SNAPIN, SH3D19, FTH1, DTNBP1, AP3S1, HSPA8
Nuclear import of Rev protein	2.6632E-03	NUP214, RCC1, NUP43, NUP50, NUP62, NUP54, NPM1, TPR, RAE1, SEC13, NUP88
Signaling by BRAF and RAF1 fusions	3.7979E-03	FGA, FGB, FGG, PAPSS1, MPRIP, FAM114A2, AKAP9, SND1, LMNA, QKI, ITGA2B, APBB1IP, FXR1, AGTRAP, TLN1, AGK
Rev-mediated nuclear export of HIV RNA	3.7992E-03	NUP214, RCC1, NUP43, NUP50, NUP62, NUP54, RANBP1, TPR, RAE1, SEC13, NUP88
COPI-mediated anterograde transport	4.2136E-03	COPE, TUBB3, GOLGB1, NAPG, ANK1, DCTN2, SPTA1, DYNC1I2, COG6, COG7, CAPZA1, SPTAN1, CAPZA2, COPZ1, COG4, COPA, GOLGA2, TUBB6, COG2, COPB2, TUBB1
rRNA processing in the nucleus and cytosol	7.1773E-03	RPS25, RPS28, RPLP2, RPLP1, WDR18, RPL17, HEATR1, XRN2, RPL13, RPS17, RPL26, RPL7A, RPS6, RPS18, DDX21, RPS4X, PELP1, RPS12, RPL27A, RPS14, RPS21, RPS26, RPL18, TRMT112, RPL32, RPL23, RPL10, NHP2, RPL8, RPL21, RPL38
Platelet activation, signaling and aggregation	7.2243E-03	PF4, SERPINE1, F5, AHSG, FGA, FGB, FAM3C, FGG, PROS1, CALU, SPARC, PLEK, FCER1G, GAS6, SERPINF2, ITGA2B, APOA1, F13A1, HSPA5, ECM1, APBB1IP, KNG1, GNAI1, ISLR, ITIH4, SYK, PLG, APP, RASGRP2, APOH, RAB27B, ALDOA, TLN1, SERPINA1, TAGLN2, STX4, HRG, PIK3R1
Asparagine N-linked glycosylation	1.3704E-02	MAN1A2, GFPT2, F5, COPE, TUBB3, MIA2, SEC16A, GOLGB1, SEC23IP, NAPG, ANK1, DCTN2, UGGT1, MIA3, FUT8, SPTA1, CTSA, PSMC1, DYNC1I2, RAD23B, TFG, COG6, COG7, CAPZA1, ALG5, LMAN1, SEC13, MAN2A1, SPTAN1, CAPZA2, COPZ1, SAR1B, VCP, COG4, COPA, GOLGA2, TUBB6, COG2, SERPINA1, UBXN1, COPB2, TUBB1
Major pathway of rRNA processing in the nucleolus and cytosol	1.7423E-02	RPS25, RPS28, RPLP2, RPLP1, WDR18, RPL17, HEATR1, XRN2, RPL13, RPS17, RPL26, RPL7A, RPS6, RPS18, DDX21, RPS4X, PELP1, RPS12, RPL27A, RPS14, RPS21, RPS26, RPL18, RPL32, RPL23, RPL10, RPL8, RPL21, RPL38

Supplementary Table 4. GO analysis filtered for peptides with log2(FC) >1

GO Term	Adjusted P Value	Relevant Genes Identified
rRNA processing	1.9965E-02	PS25, RPS28, RPLP2, RPLP1, WDR18, RPL17, HEATR1, XRN2, RPL13, RPS17, RPL26, RPL7A, RPS6, RPS18, DDX21, RPS4X, PELP1, RPS12, RPL27A, RPS14, RPS21, RPS26, RPL18, TRMT112, RPL32, RPL23, RPL10, NHP2, RPL8, RPL21, RPL38
Intra-Golgi traffic	2.0847E-02	MAN1A2, GOLGA5, TRIP11, NAPG, CYTH4, COG6, COG7, MAN2A1, STX16, COG4, COG2, SNAP29
snRNP Assembly	2.1884E-02	SNRPD1, NUP214, NUP43, NUP50, NUP62, SNRPE, NUP54, TPR, CLNS1A, RAE1, SEC13, SNRPD2, NUP88
Metabolism of non-coding RNA	2.1884E-02	SNRPD1, NUP214, NUP43, NUP50, NUP62, SNRPE, NUP54, TPR, CLNS1A, RAE1, SEC13, SNRPD2, NUP88
Formation of the ternary complex, and subsequently, the	2.7305E-02	RPS25, RPS28, EIF2S1, RPS17, RPS6, RPS18, EIF3M, RPS4X, EIF3K, RPS12, RPS14, RPS21, RPS26
Oncogenic MAPK signaling	2.7686E-02	FGA, FGB, FGG, PAPSS1, MPRIP, FAM114A2, PPP1CC, AKAP9, SND1, LMNA, QKI, ITGA2B, APBB1IP, FXR1, AGTRAP, TLN1, AGK
Host Interactions of HIV factors	3.3854E-02	NUP214, PSMD4, RCC1, NUP43, NUP50, NUP62, NUP54, PSMF1, ELOC, RANBP1, NPM1, PSMC2, SKP1, PSMC1, PSMC3, PSMD2, TPR, ELOB, RAE1, PSMC4, SEC13, NUP88
Viral Messenger RNA Synthesis	4.0217E-02	NUP214, NUP43, NUP50, NUP62, NUP54, TPR, POLR2J, RAE1, SEC13, POLR2I, NUP88

CLAIMS

1. A biological tissue model configured for *in vitro* applications, the biological tissue model comprising:

a substrate including a plurality of isolated, soluble matrikines;

wherein the substrate is capable of recapitulating one or more of a microstructure, molecular composition, and biomechanical property of a native biological tissue.

2. The biological tissue model of claim 1, wherein the plurality of isolated, soluble matrikines are incorporated into the substrate as a scaffold.

3. The biological tissue model of any of claims 1-2, wherein the plurality of isolated, soluble matrikines are incorporated into the substrate as a hydrogel.

4. The biological tissue model of any of claims 1-3, wherein the biological tissue model is disease-specific.

5. The biological tissue model of claim 4, wherein the biological tissue model is a cystic fibrosis biological tissue model.

6. The biological tissue model of any of claims 1-5, wherein the substrate is capable of recapitulating one or more of a microstructure, molecular composition, and biomechanical property of a native disease-specific biological tissue.

7. The biological tissue model of claim 6, wherein the substrate is capable of recapitulating one or more of a microstructure, molecular composition, and biomechanical property of a native cystic fibrosis biological tissue.

8. A method of preparing a biological tissue model configured for *in vitro* applications, the method comprising:

isolating a plurality of soluble matrikines from an extracellular matrix;

incorporating the plurality of soluble matrikines into a substrate; and

recapitulating one or more of a microstructure, molecular composition, and biomechanical property of a native biological tissue with the substrate.

9. The method of claim 8, wherein incorporating the plurality of soluble matrikines into the substrate includes incorporating the plurality of soluble matrikines into the substrate as a scaffold.

10. The method of any of claims 8-9, wherein incorporating the plurality of soluble matrikines into the substrate includes incorporating the plurality of soluble matrikines into the substrate as a hydrogel.

11. The method of any of claims 8-10, further comprising processing the isolated, soluble matrikines by crosslinking the isolated, soluble matrikines with each other for incorporation into the substrate.

12. The method of any of claims 8-11, further comprising processing the isolated, soluble matrikines by coating a surface of a scaffold for incorporation into the substrate.

13. The method of any of claims 8-12, wherein isolating the plurality of soluble matrikines includes treating a native biological tissue with a CHAPS-based detergent.

14. The method of any of claims 8-13, wherein isolating the plurality of soluble matrikines includes treating a native biological tissue with a Benzonase-based enzyme.

15. The method of any of claims 8-14, wherein the biological tissue model is disease-specific.

16. The method of claim 15, wherein the biological tissue model is a cystic fibrosis biological tissue model.

17. The method of any of claims 8-16, wherein recapitulating one or more of a microstructure, molecular composition, and biomechanical property includes recapitulating one or more of a microstructure, molecular composition, and biomechanical property of a native disease-specific biological tissue.

18. The method of claim 17, wherein recapitulating one or more of a microstructure, molecular composition, and biomechanical property includes recapitulating one or more of a microstructure, molecular composition, and biomechanical property of a native cystic fibrosis biological tissue.

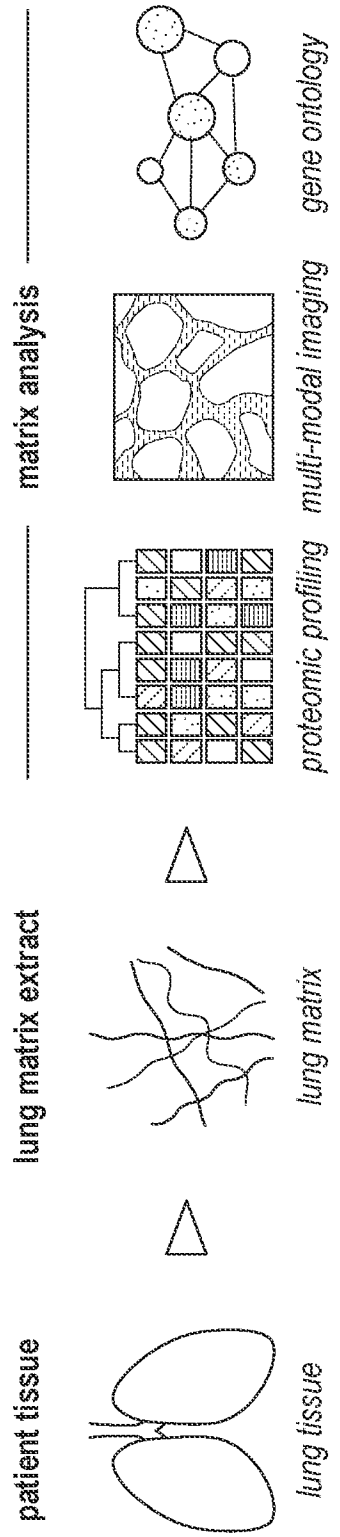
patient tissue
lung matrix extract
matrix analysis
lung tissue
lung matrix
proteomic profiling
multi-modal imaging
gene ontology

FIG. 1A

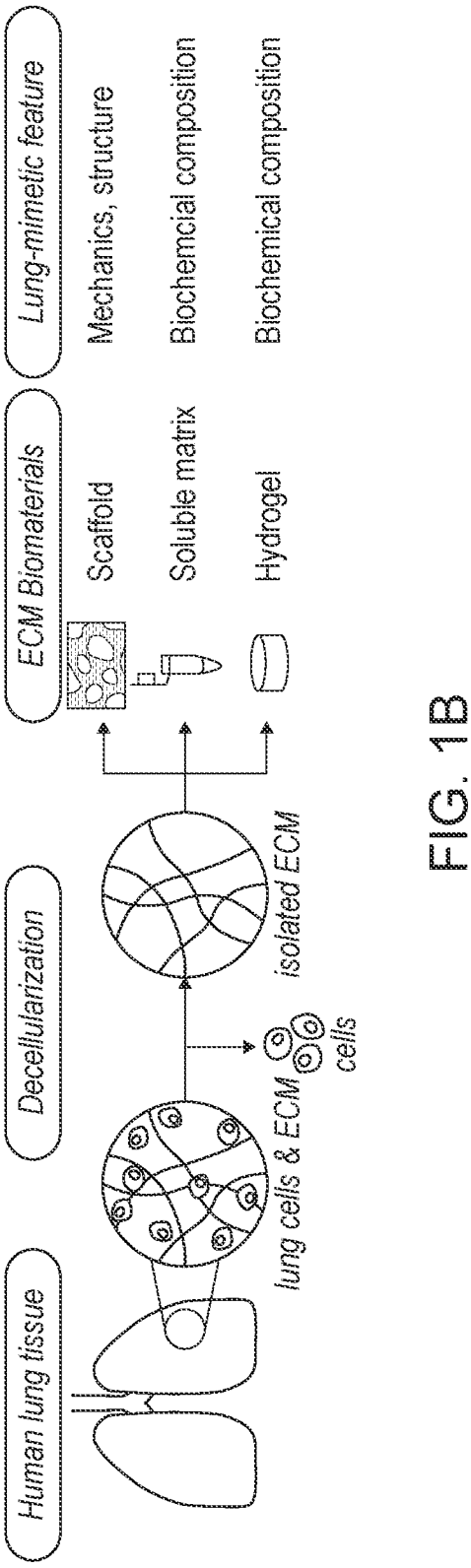
Human lung tissue
Decellularization
lung cells & ECM
cells
isolated ECM
ECM Biomaterials
Scaffold
Soluble matrix
Hydrogel
Lung-mimetic feature
Mechanics, structure
Biochemcial composition
Biochemical composition

FIG. 1B

air-liquid interface

cell type #1

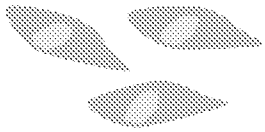

cell type #2

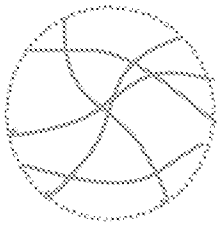

ECM biomaterial

FIG. 2A

mucus properties

TEER test

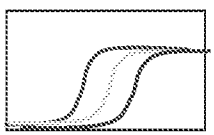

ECM modulation

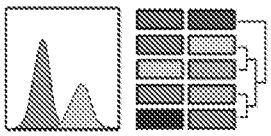

cytokine expression

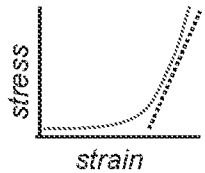

tissue mechanics

FIG. 2B

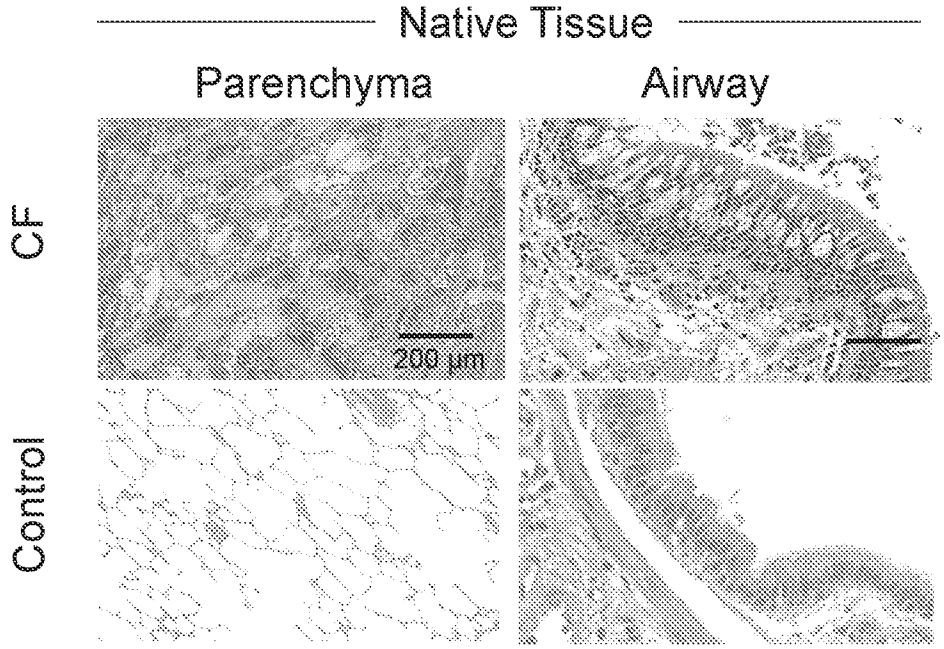
Native Tissue
Parenchyma
Airway
CF
Control
200 μm

FIG. 3A

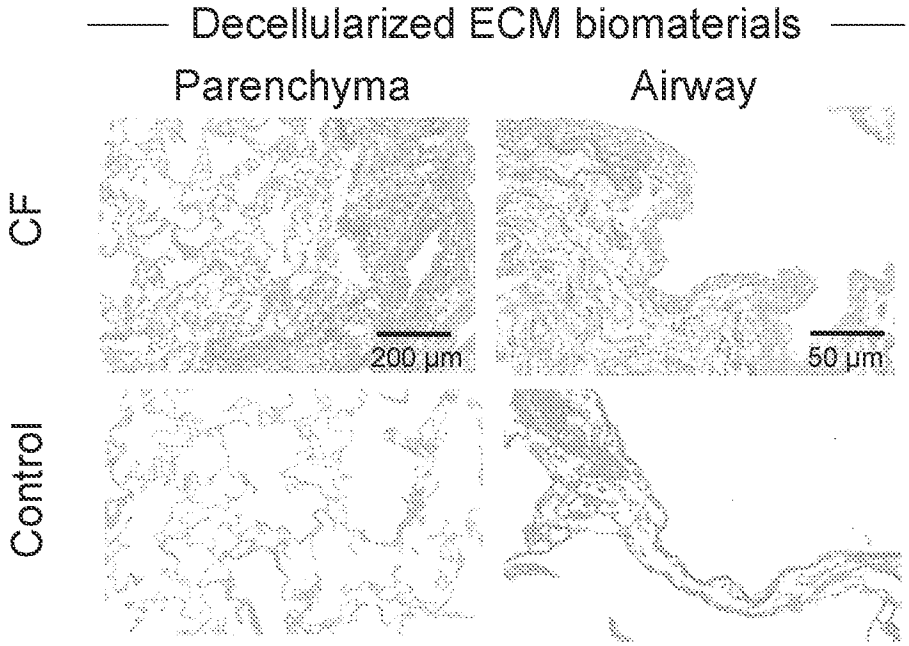
Decellularized ECM biomaterials
Parenchyma
Airway
CF
Control
200 μm
50 μm

FIG. 3B

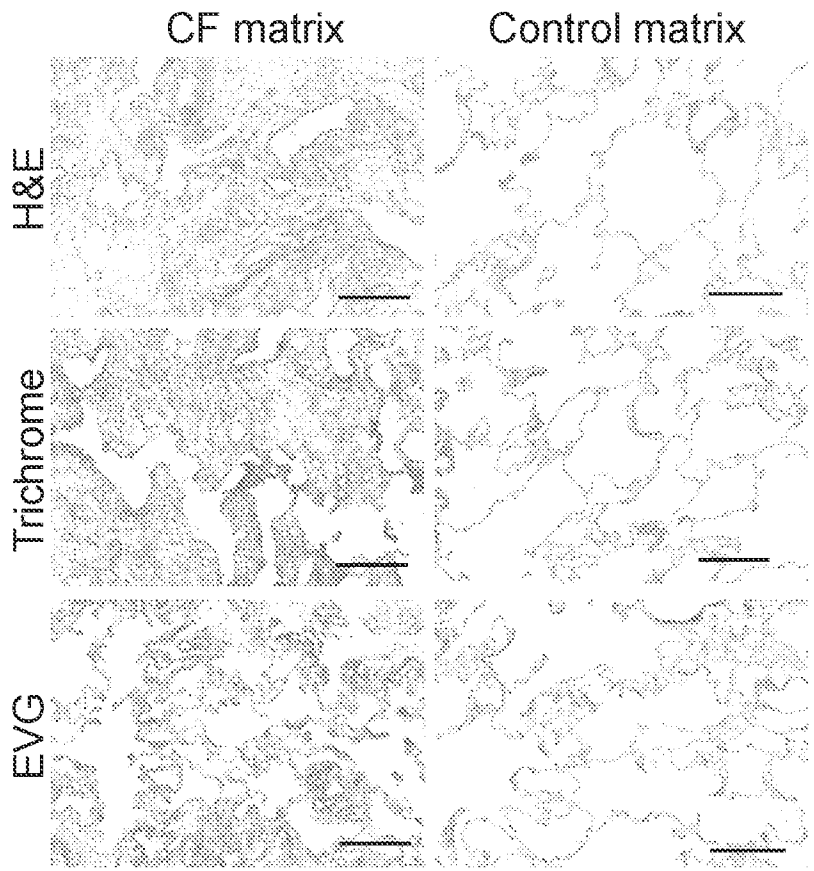

FIG. 4A

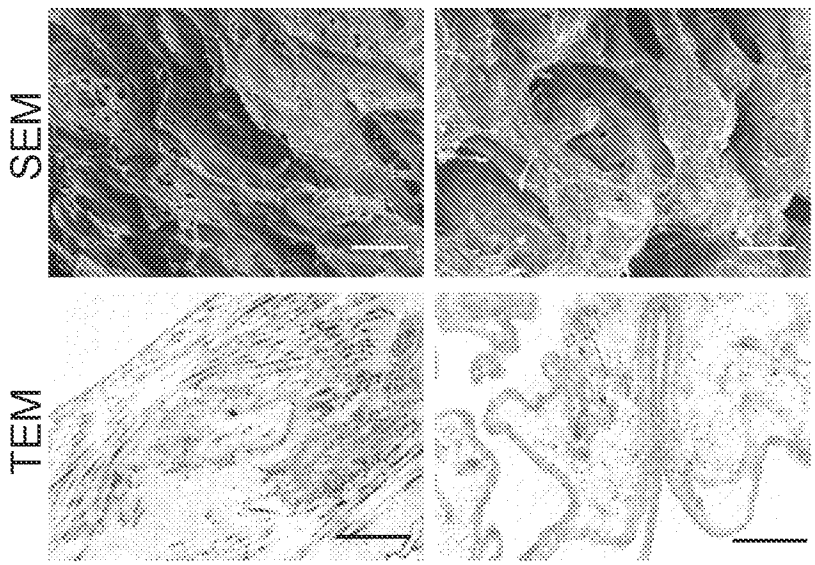

FIG. 4B

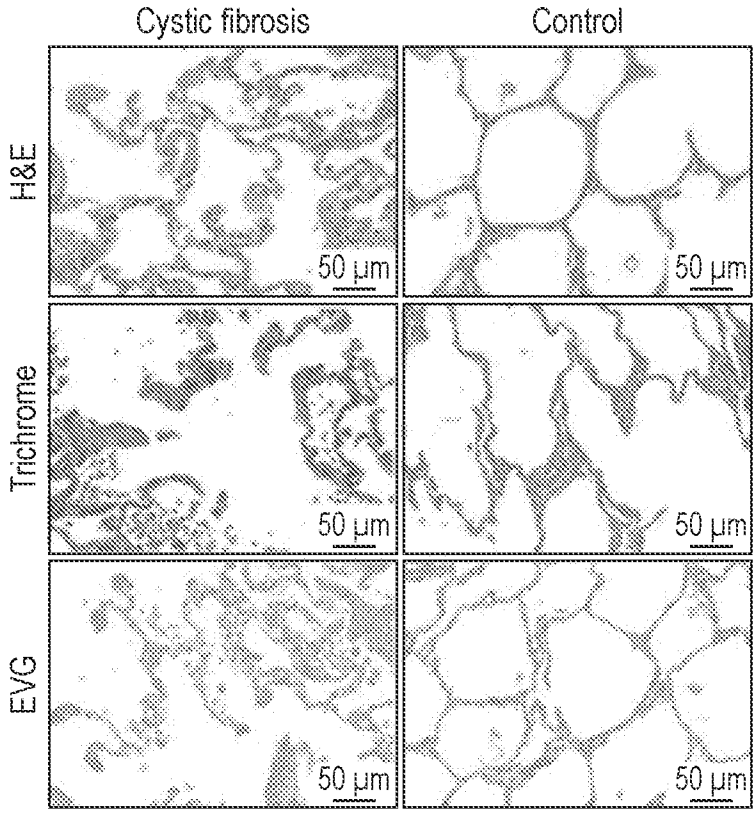
Cystic fibrosis
Control
H&E
Trichrome
EVG
50 µm

FIG. 4C

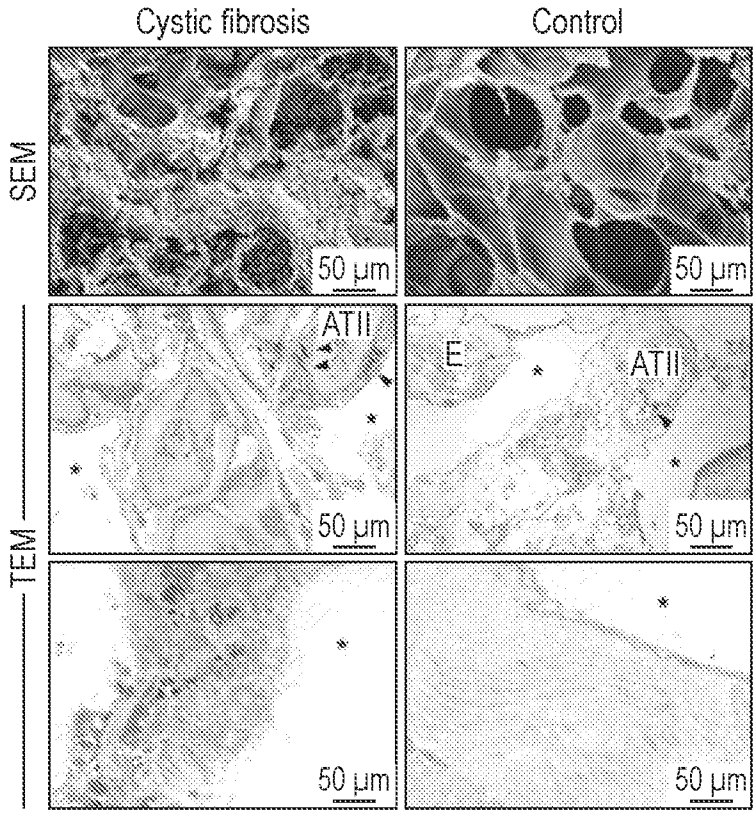
Cystic fibrosis
Control
SEM
TEM
ATII
E
50 µm

FIG. 4D

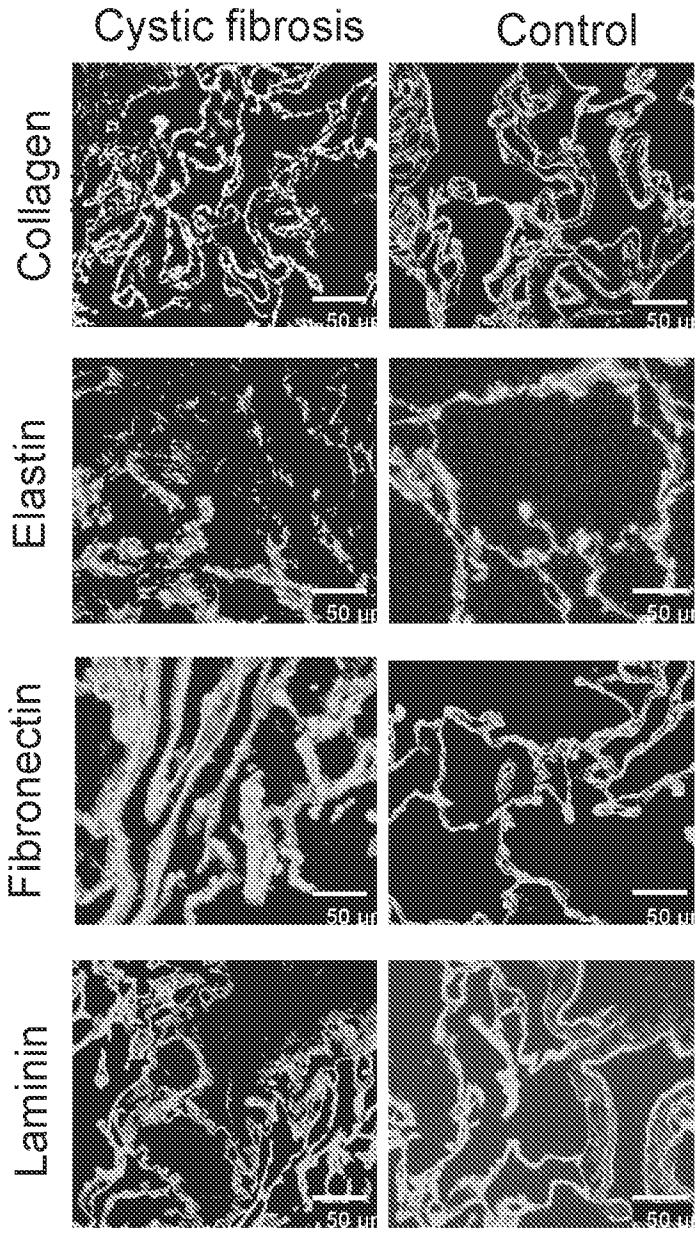
Cystic fibrosis
Control
Collagen
Elastin
Fibronectin
Laminin
50 μm

FIG. 5A

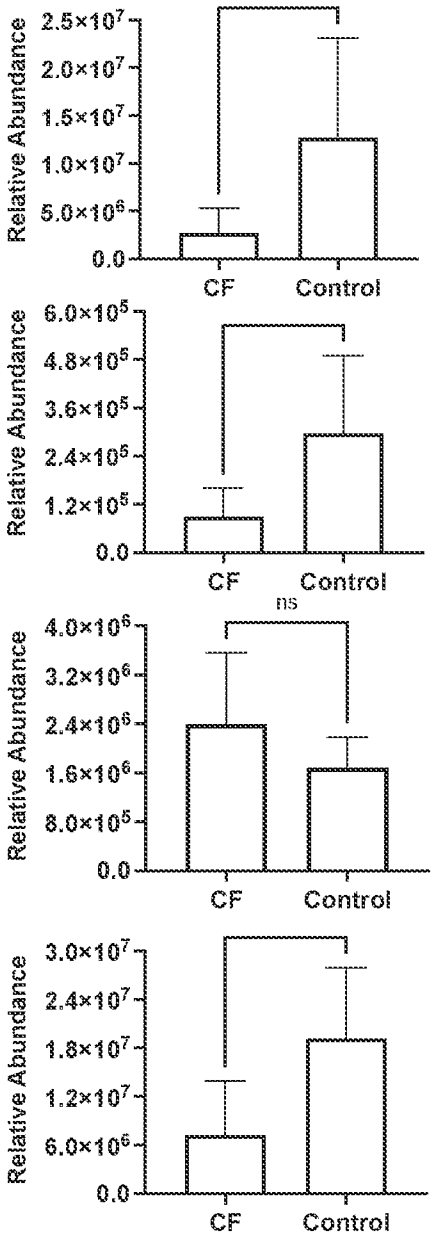
Relative Abundance
2.5×10^7
2.0×10^7
1.5×10^7
1.0×10^7
5.0×10^6
0.0
CF
Control
Relative Abundance
6.0×10^5
4.8×10^5
3.6×10^5
2.4×10^5
1.2×10^5
0.0
CF
Control
ns
Relative Abundance
4.0×10^6
3.2×10^6
2.4×10^6
1.6×10^6
8.0×10^5
0.0
CF
Control
Relative Abundance
3.0×10^7
2.4×10^7
1.8×10^7
1.2×10^7
6.0×10^6
0.0
CF
Control

FIG. 5B

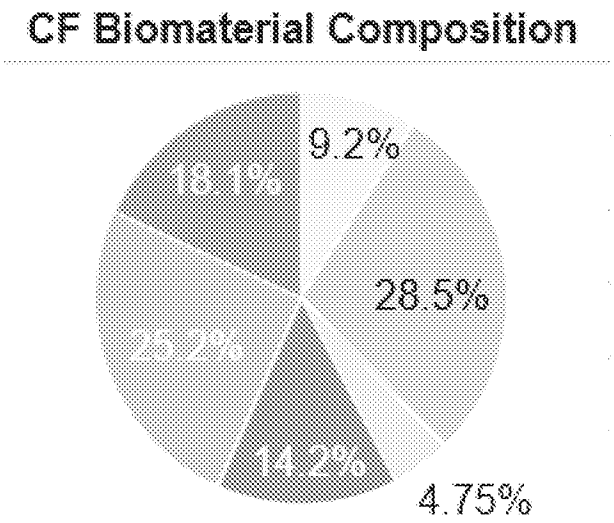

Protein Category	# Proteins
Collagens	31
Glycoproteins	96
Proteoglycans	16
ECM-affiliated	48
ECM-regulators	85
Secreted factors	61

FIG. 6

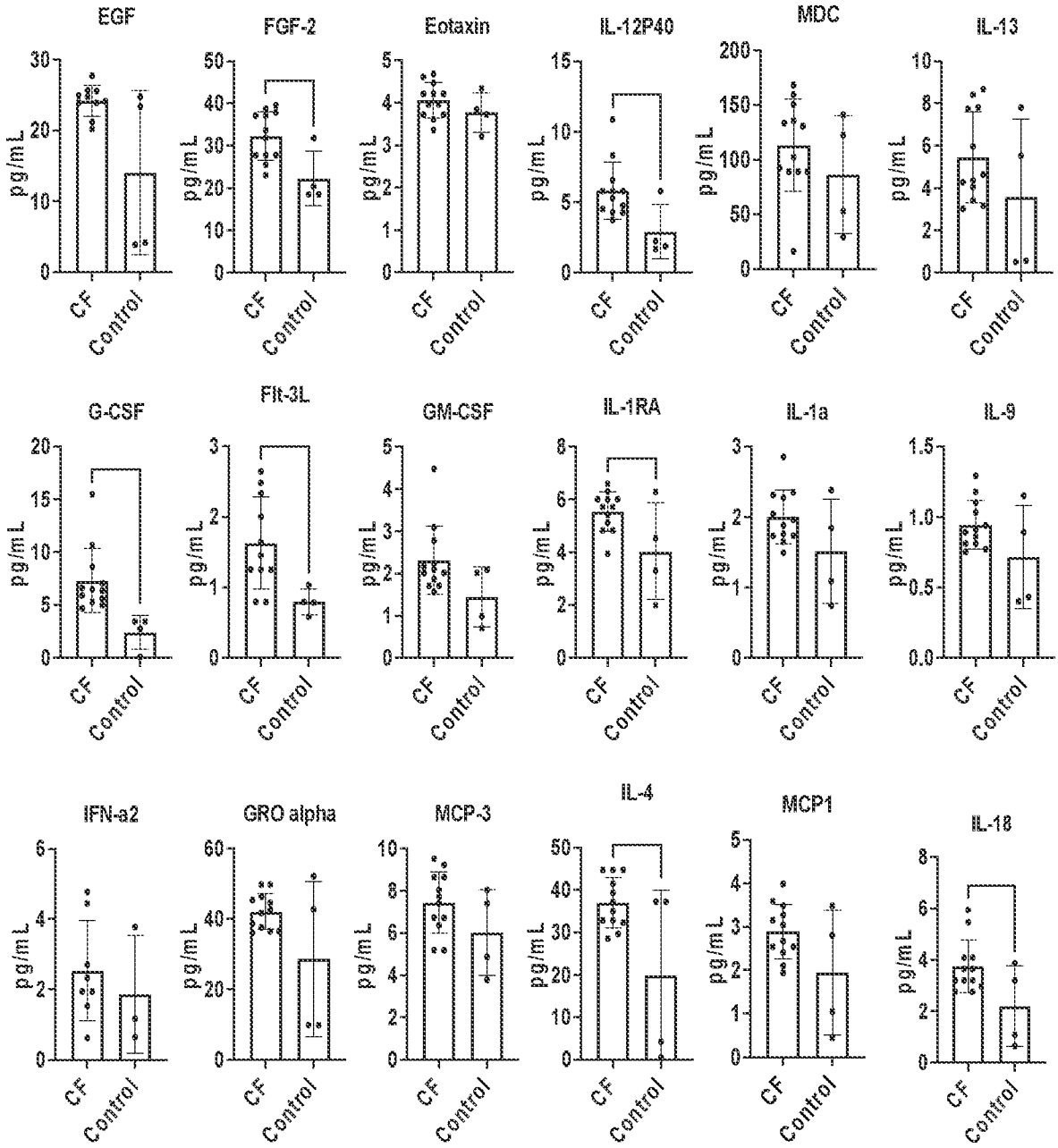
EGF
FGF-2
Eotaxin
IL-12P40
MDC
IL-13
G-CSF
Flt-3L
GM-CSF
IL-1RA
IL-1a
IL-9
IFN-a2
GRO alpha
MCP-3
IL-4
MCP1
IL-18
pg/mL
CF
Control

FIG. 7

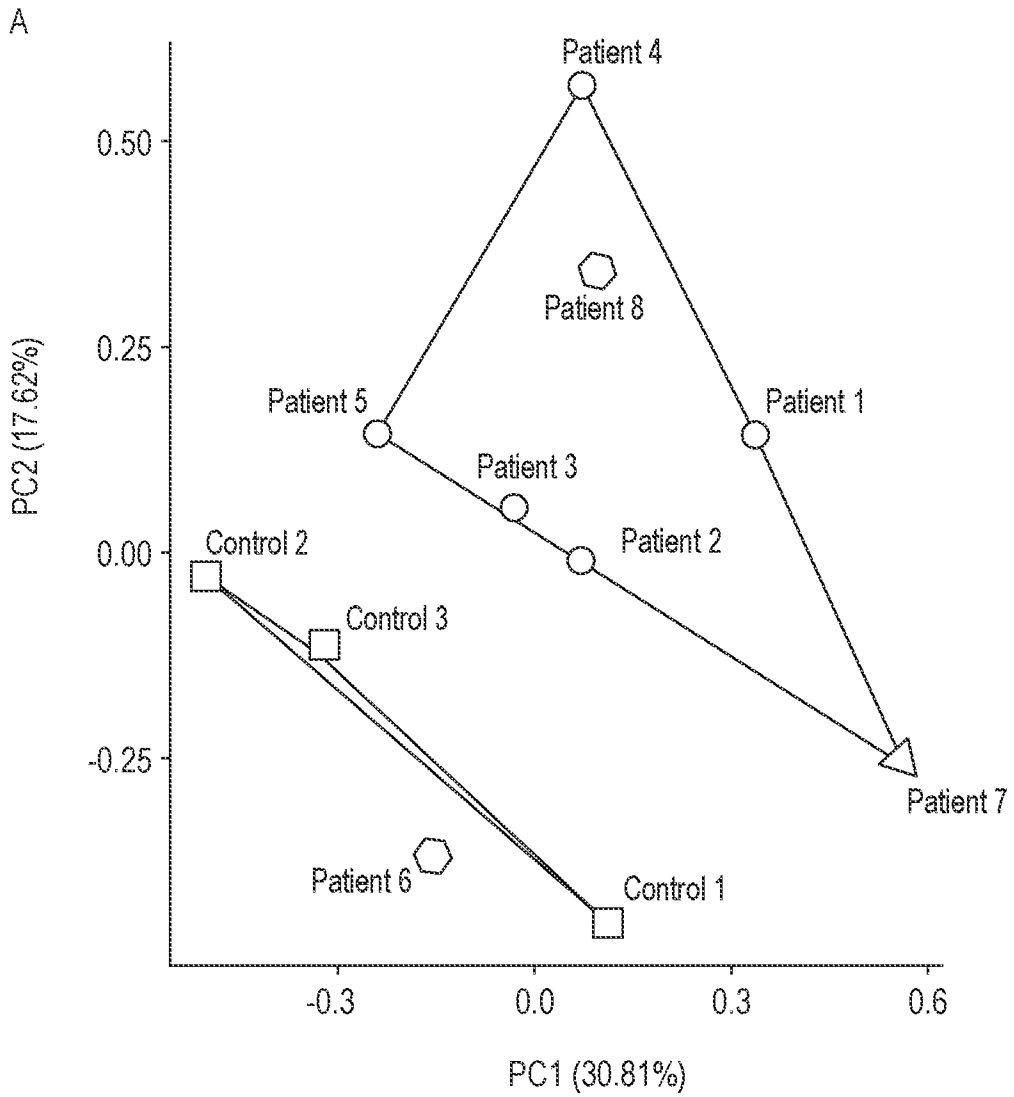
A
Patient 4
0.50
Patient 8
0.25
Patient 5
Patient 1
Patient 3
PC2 (17.62%)
0.00
Control 2
Patient 2
Control 3
-0.25
Patient 7
Patient 6
Control 1
-0.3
0.0
0.3
0.6
PC1 (30.81%)

FIG. 8A

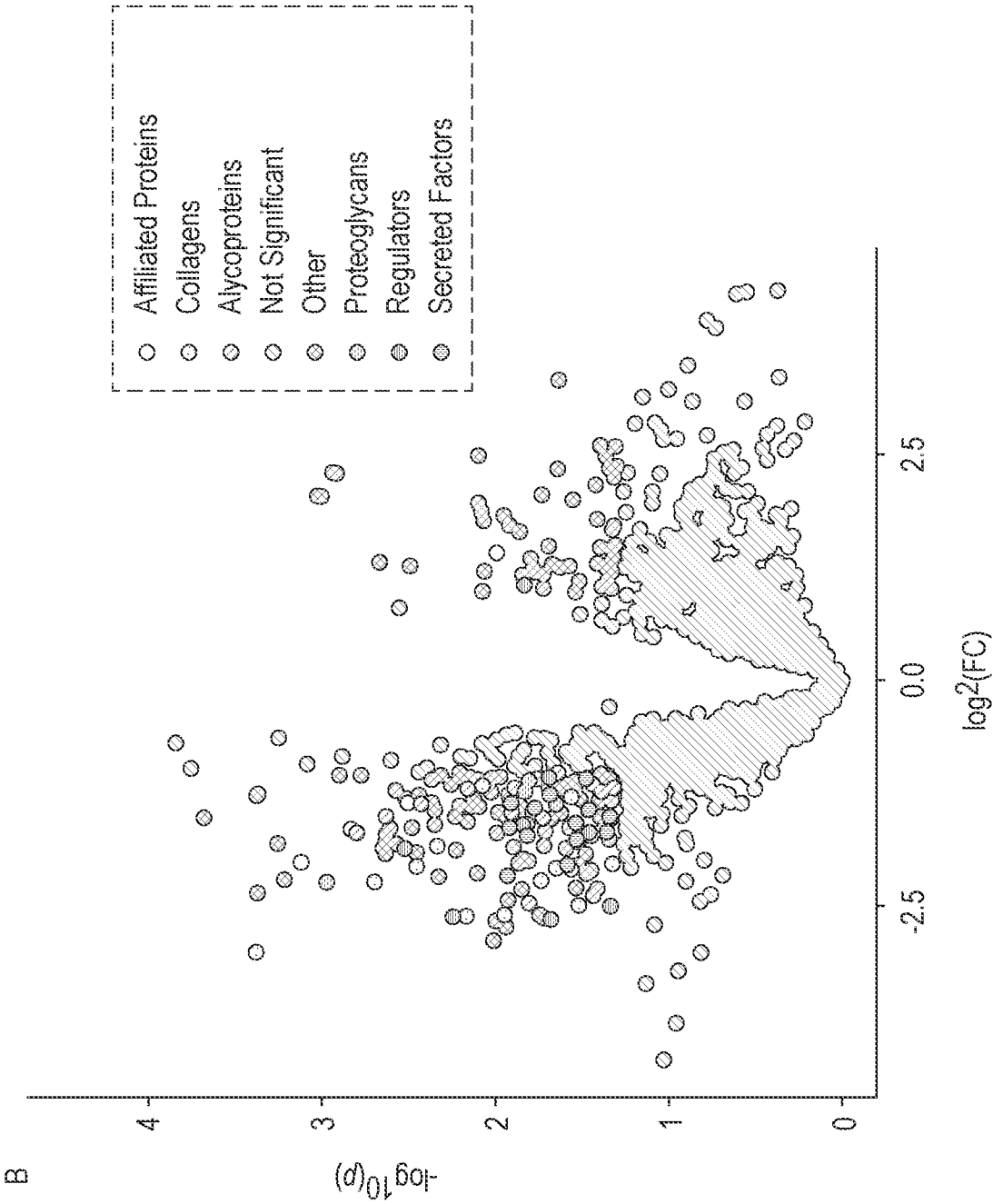
B
Affiliated Proteins
Collagens
Alycoproteins
Not Significant
Other
Proteoglycans
Regulators
Secreted Factors
-log10(p)
0
1
2
3
4
-2.5
0.0
2.5
log2(FC)

FIG. 8B

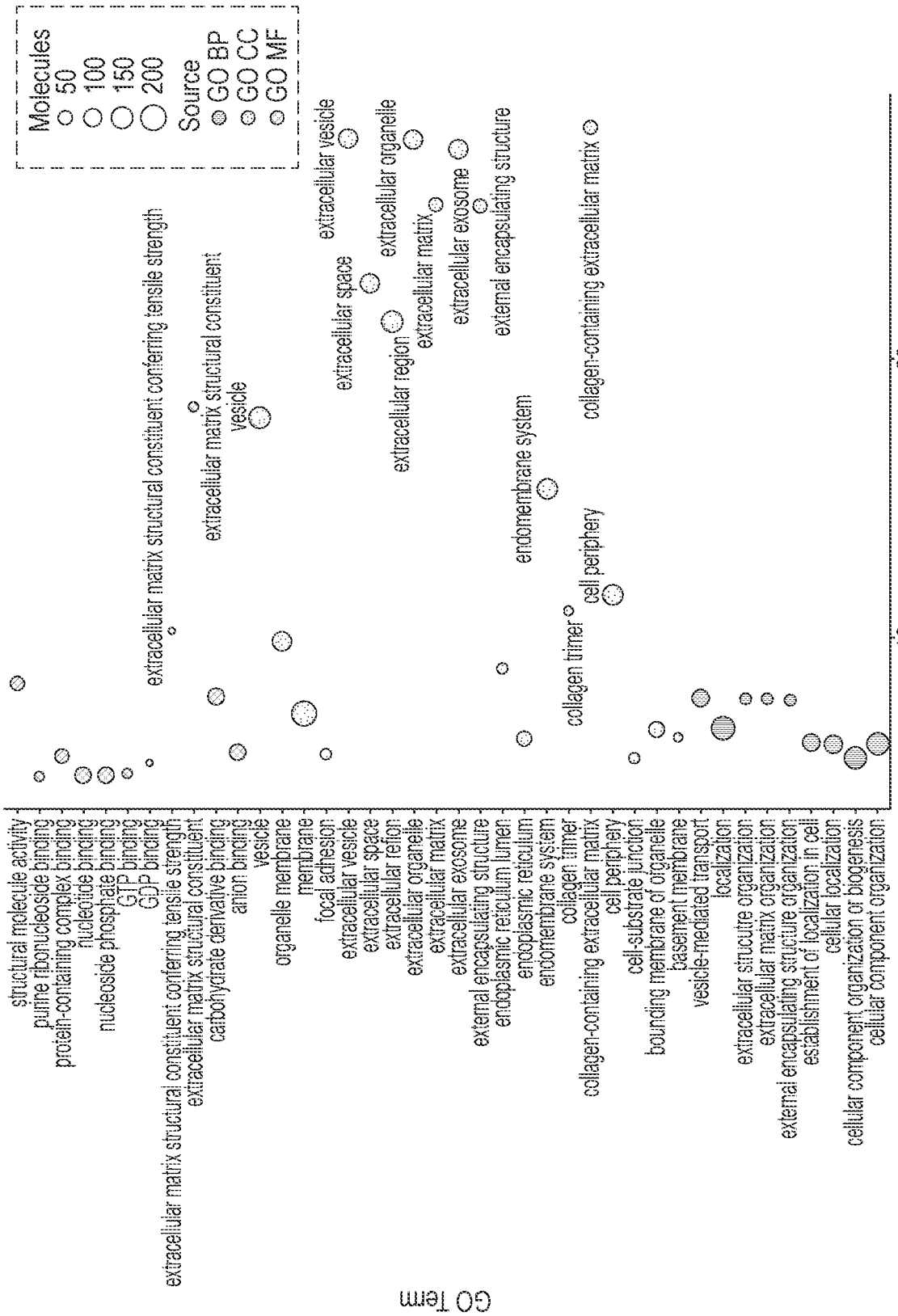
Molecules
50
100
150
200
Source
GO BP
GO CC
GO MF
structural molecule activity
purine ribonucleoside binding
protein-containing complex binding
nucleotide binding
nucleoside phosphate binding
GTP binding
GDP binding
extracellular matrix structural constituent conferring tensile strength
extracellular matrix structural constituent
carbohydrate derivative binding
anion binding
vesicle
organelle membrane
membrane
focal adhesion
extracellular vesicle
extracellular space
extracellular region
extracellular organelle
extracellular matrix
extracellular exosome
external encapsulating structure
endoplasmic reticulum lumen
endoplasmic reticulum
endomembrane system
collagen trimer
collagen-containing extracellular matrix
cell periphery
cell-substrate junction
bounding membrane of organelle
basement membrane
vesicle-mediated transport
localization
extracellular structure organization
extracellular matrix organization
external encapsulating structure organization
establishment of localization in cell
cellular localization
cellular component organization or biogenesis
cellular component organization
extracellular matrix structural constituent conferring tensile strength
extracellular matrix structural constituent
extracellular matrix structural constituent
vesicle
extracellular vesicle
extracellular space
extracellular region
extracellular organelle
extracellular matrix
extracellular exosome
external encapsulating structure
endomembrane system
collagen trimer
cell periphery
collagen-containing extracellular matrix
10
20
-log10(pvalue)
GO Term

FIG. 8C

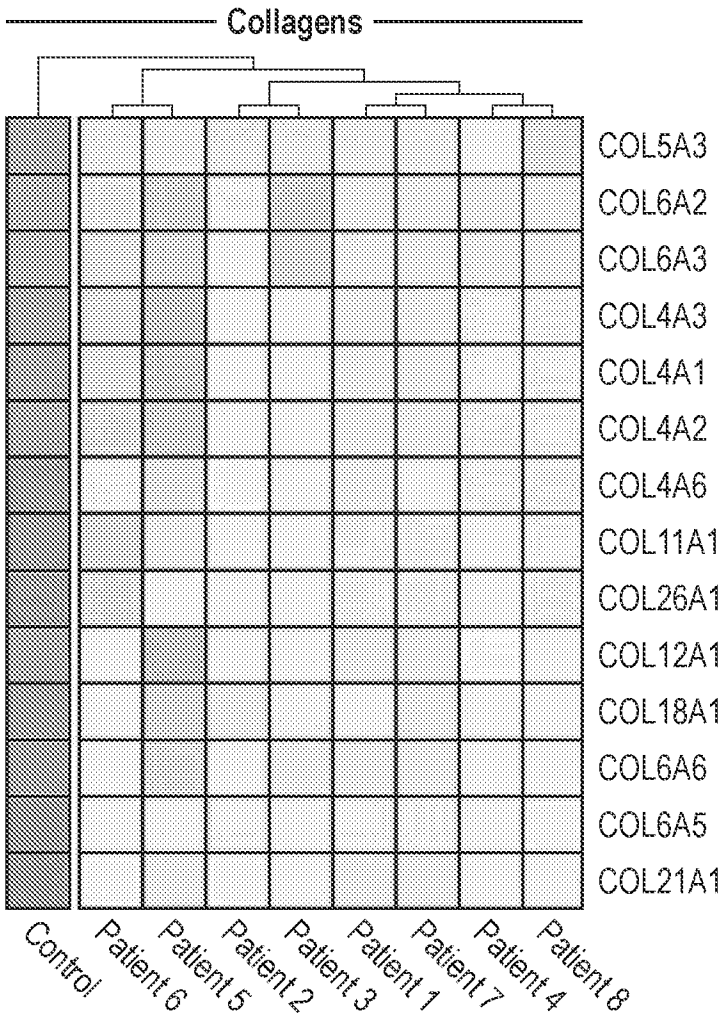
Collagens
COL5A3
COL6A2
COL6A3
COL4A3
COL4A1
COL4A2
COL4A6
COL11A1
COL26A1
COL12A1
COL18A1
COL6A6
COL6A5
COL21A1
Control
Patient 6
Patient 5
Patient 2
Patient 3
Patient 1
Patient 7
Patient 4
Patient 8

FIG. 9A

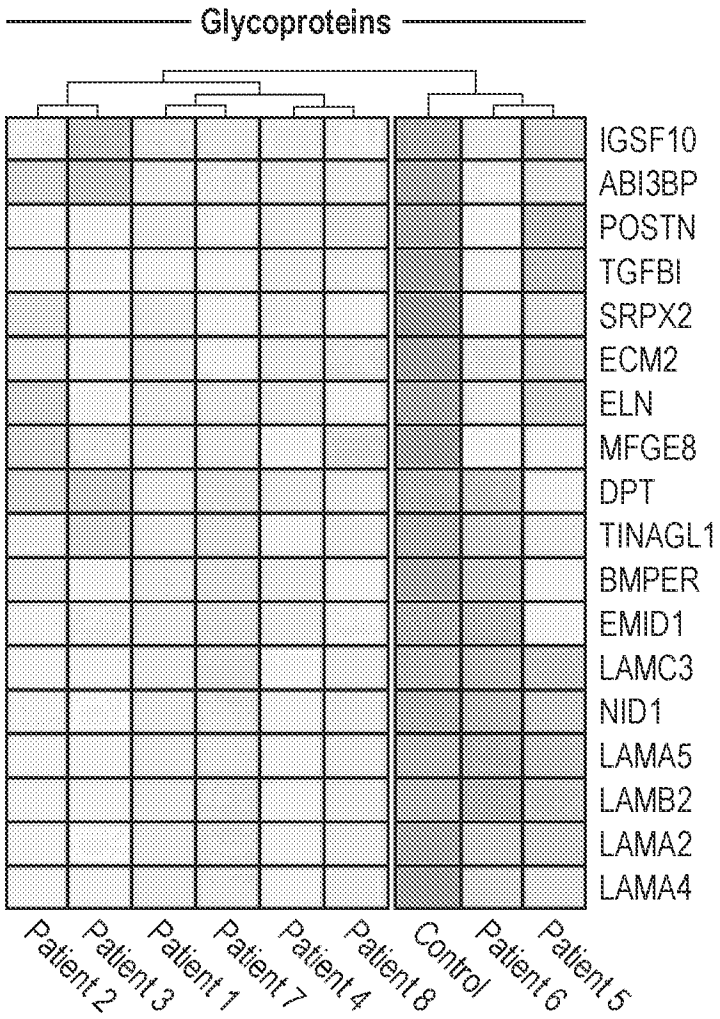
Glycoproteins
IGSF10
ABI3BP
POSTN
TGFBI
SRPX2
ECM2
ELN
MFGE8
DPT
TINAGL1
BMPER
EMID1
LAMC3
NID1
LAMA5
LAMB2
LAMA2
LAMA4
Patient 2
Patient 3
Patient 1
Patient 7
Patient 4
Patient 8
Control
Patient 6
Patient 5

FIG. 9B

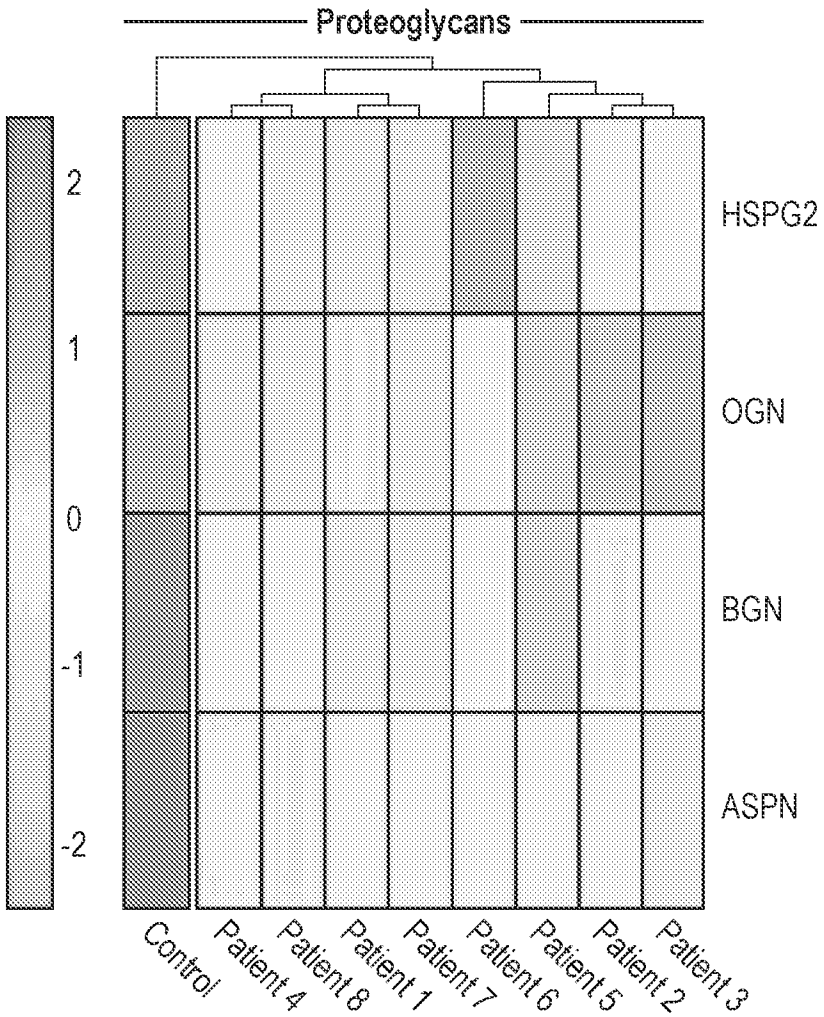
Proteoglycans
2
1
0
-1
-2
HSPG2
OGN
BGN
ASPN
Control
Patient 4
Patient 8
Patient 1
Patient 7
Patient 6
Patient 5
Patient 2
Patient 3

FIG. 9C

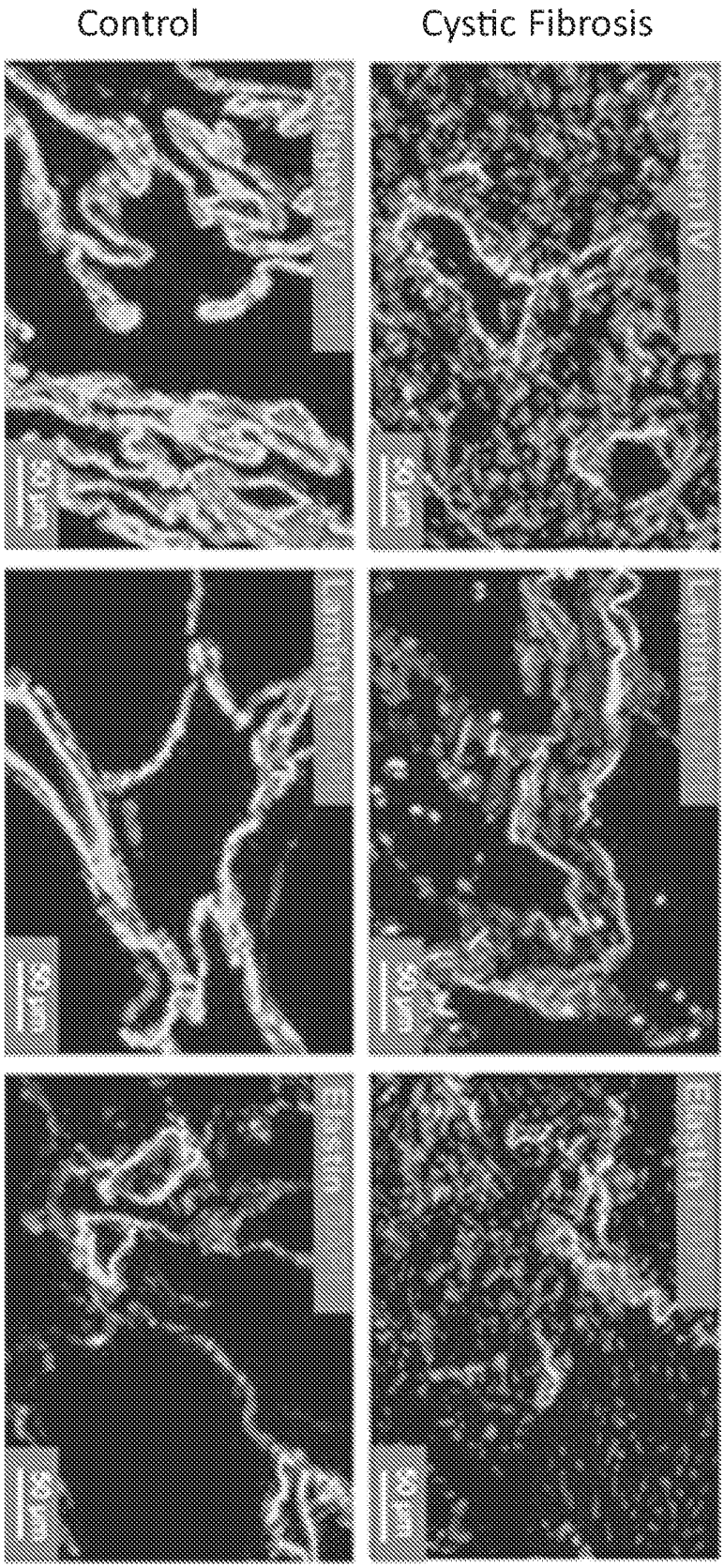

FIG. 9D

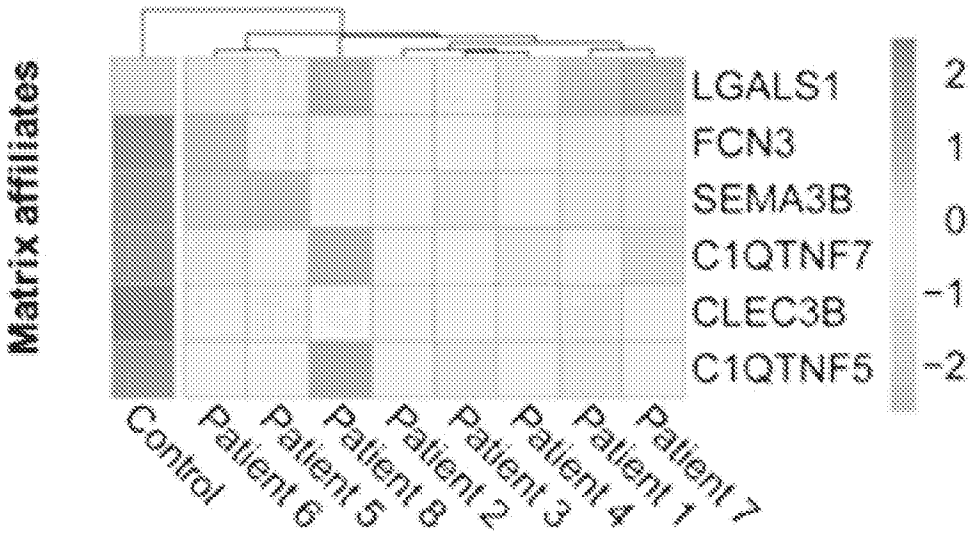

FIG. 10A

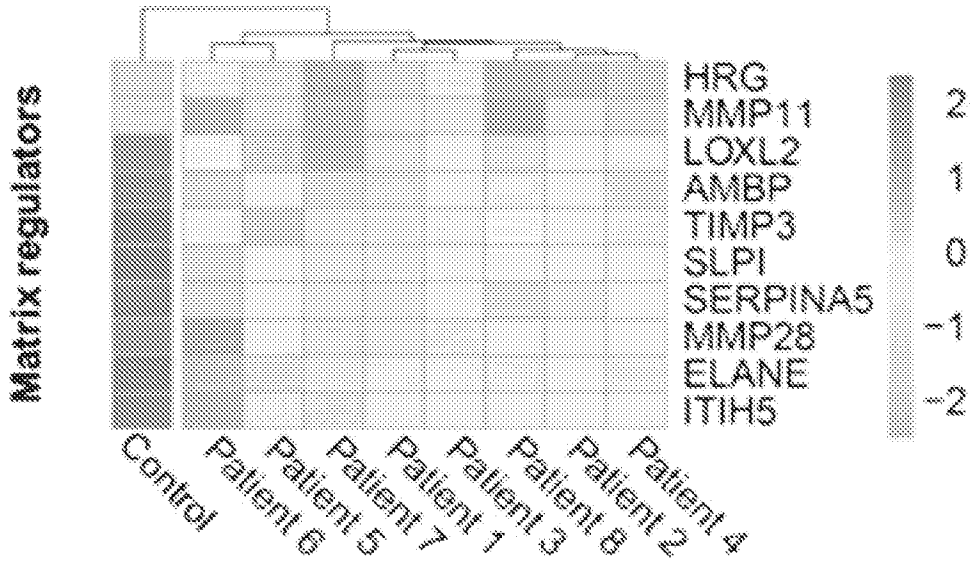

FIG. 10B

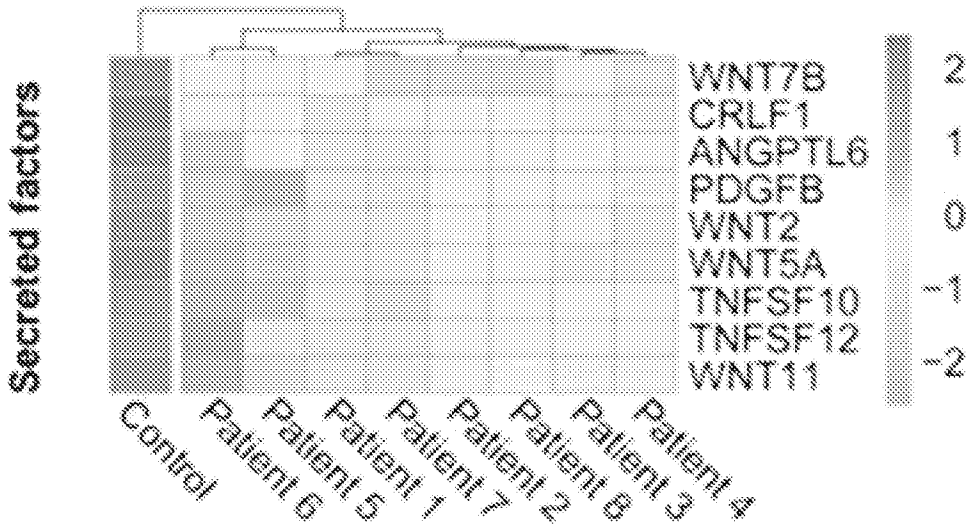
Secreted factors
WNT7B
CRLF1
ANGPTL6
PDGFB
WNT2
WNT5A
TNFSF10
TNFSF12
WNT11
2
1
0
−1
−2
Control
Patient 6
Patient 5
Patient 1
Patient 7
Patient 2
Patient 8
Patient 3
Patient 4

FIG. 10C

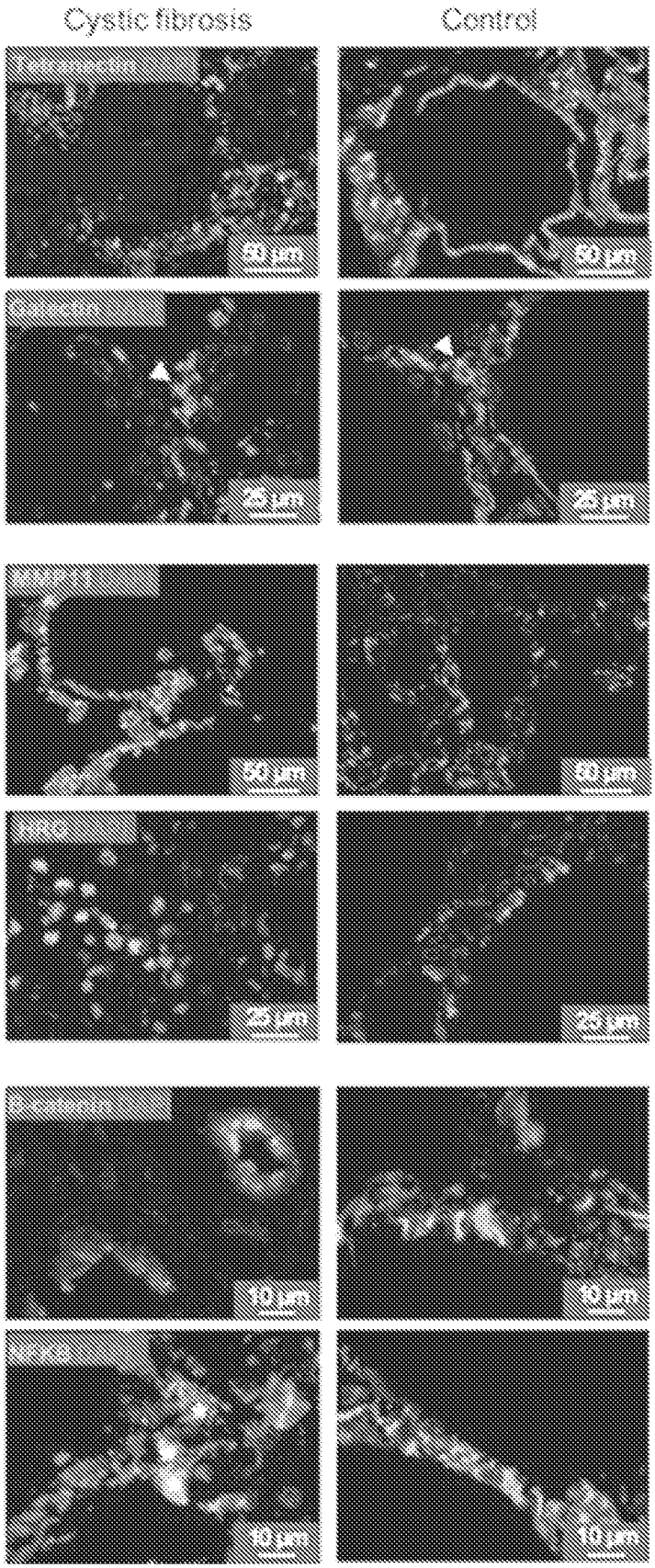
Cystic fibrosis
Control
50 µm
50 µm
25 µm
25 µm
50 µm
50 µm
25 µm
25 µm
10 µm
10 µm
10 µm
10 µm

FIG. 10D

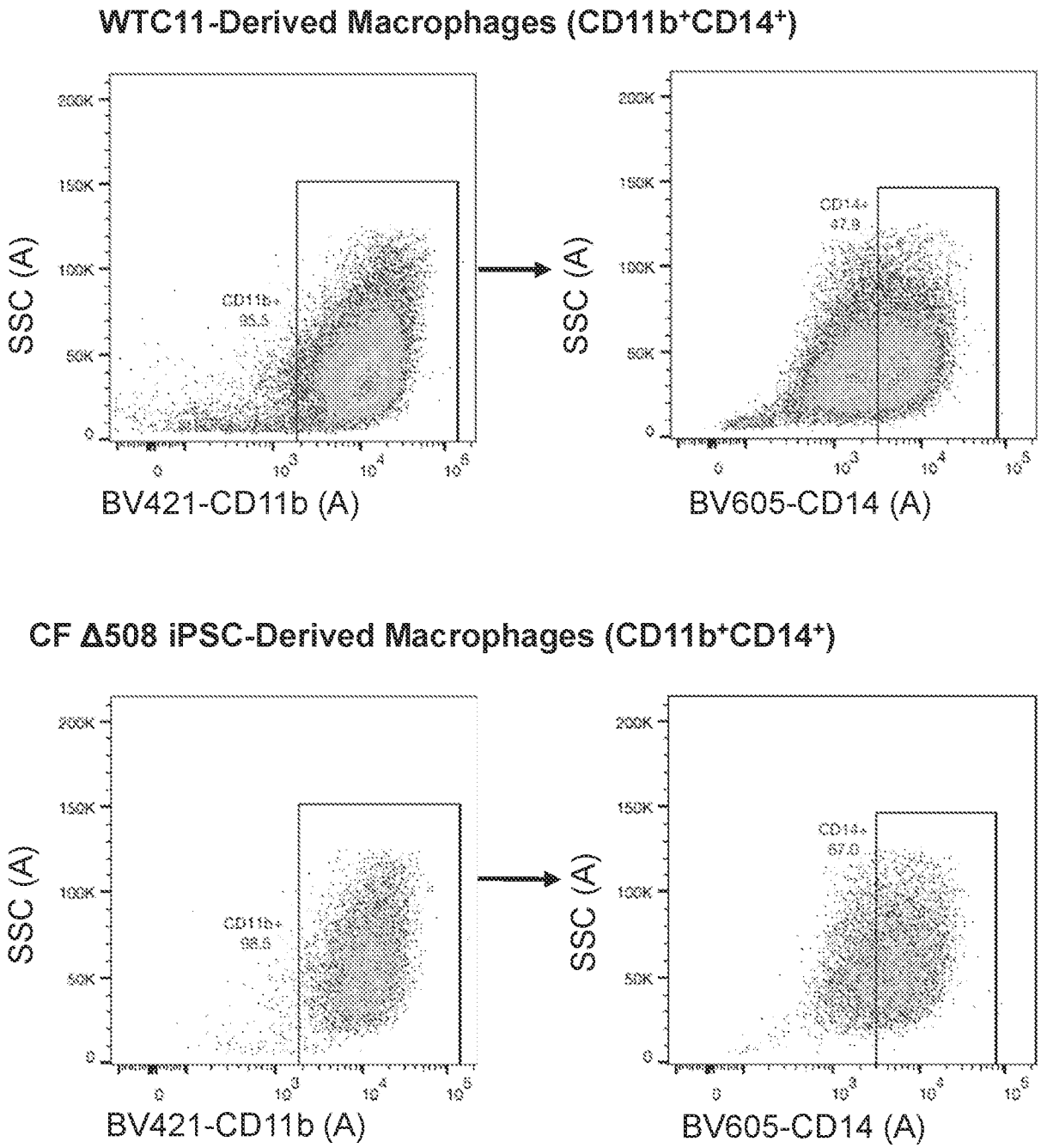
WTC11-Derived Macrophages (CD11b+CD14+)
SSC (A)
BV421-CD11b (A)
CD11b+
85.5
BV605-CD14 (A)
CD14+
87.8
CF Δ508 iPSC-Derived Macrophages (CD11b+CD14+)
SSC (A)
BV421-CD11b (A)
CD11b+
98.6
BV605-CD14 (A)
CD14+
87.0

FIG. 11

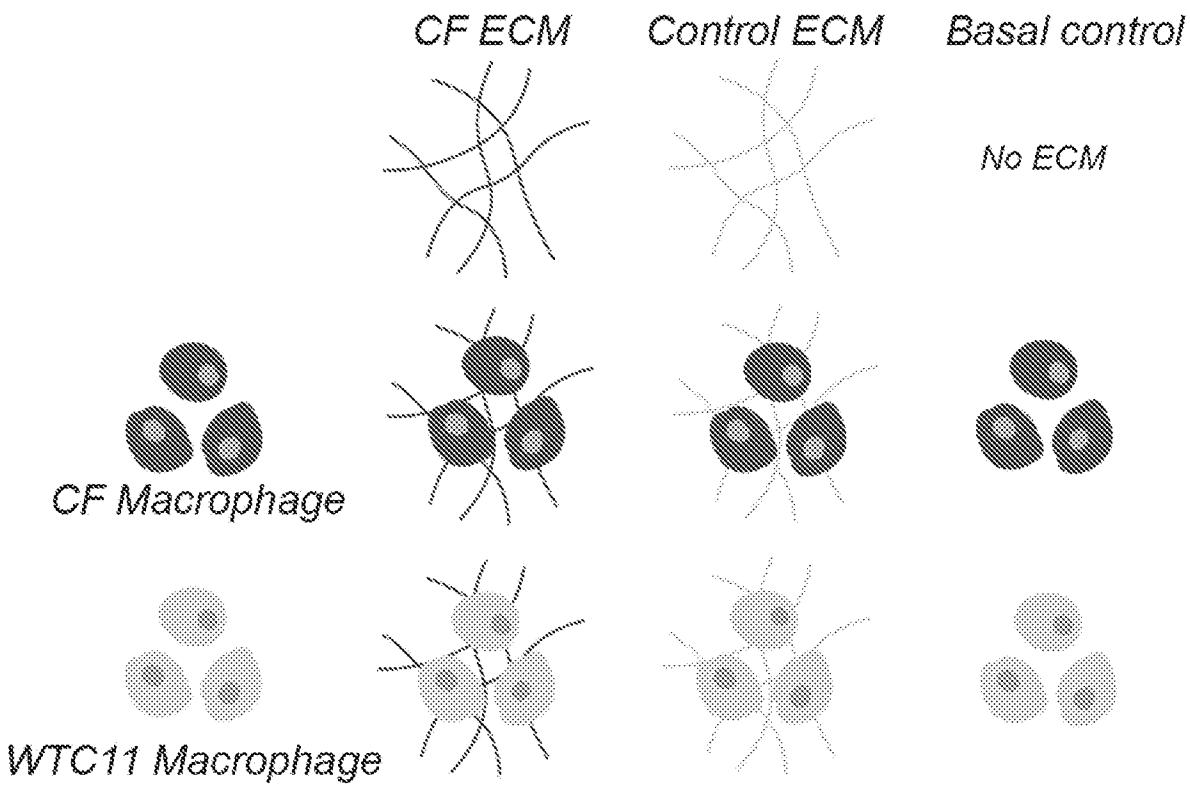
CF ECM
Control ECM
Basal control
No ECM
CF Macrophage
WTC11 Macrophage

FIG. 12

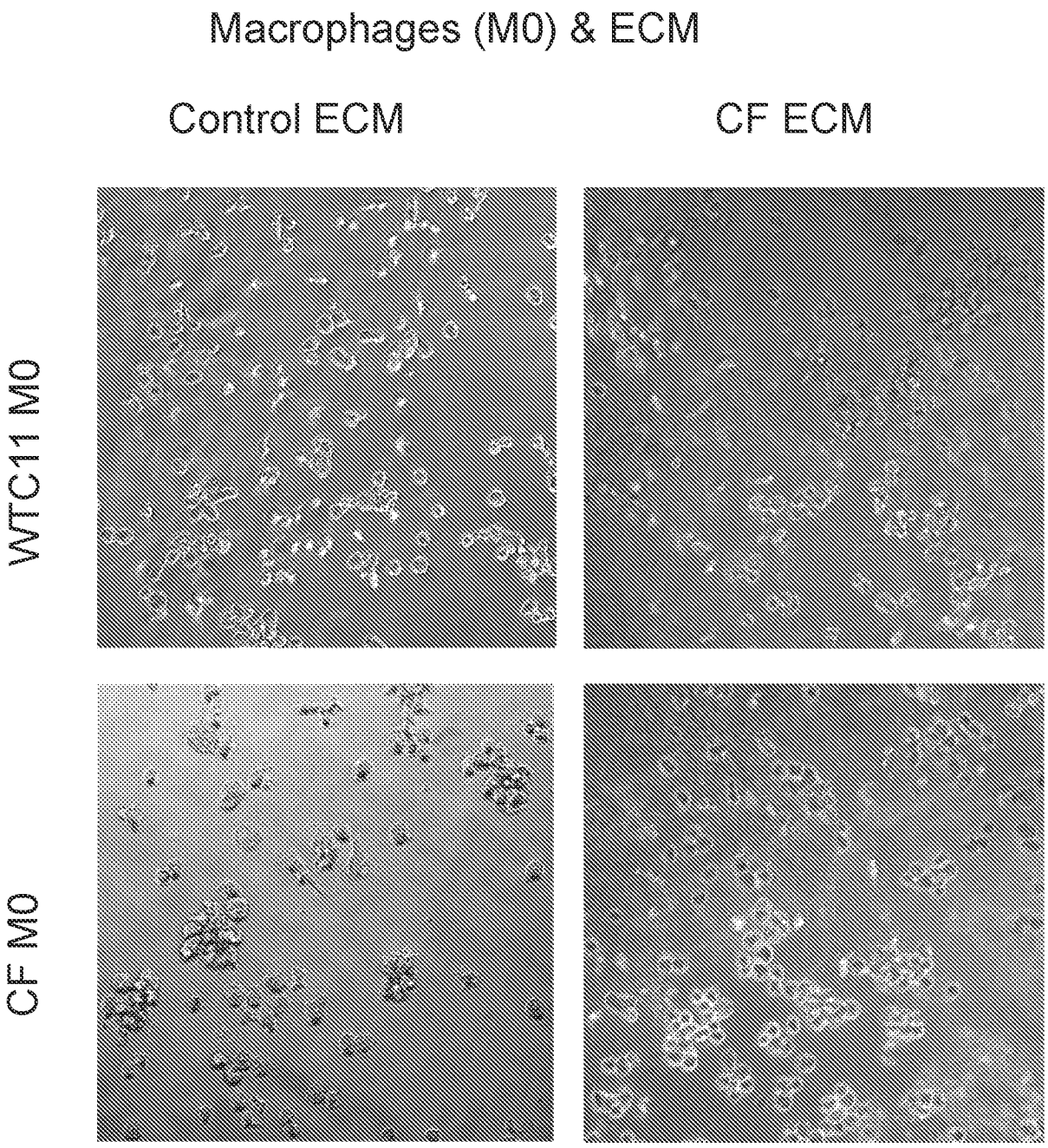

FIG. 13

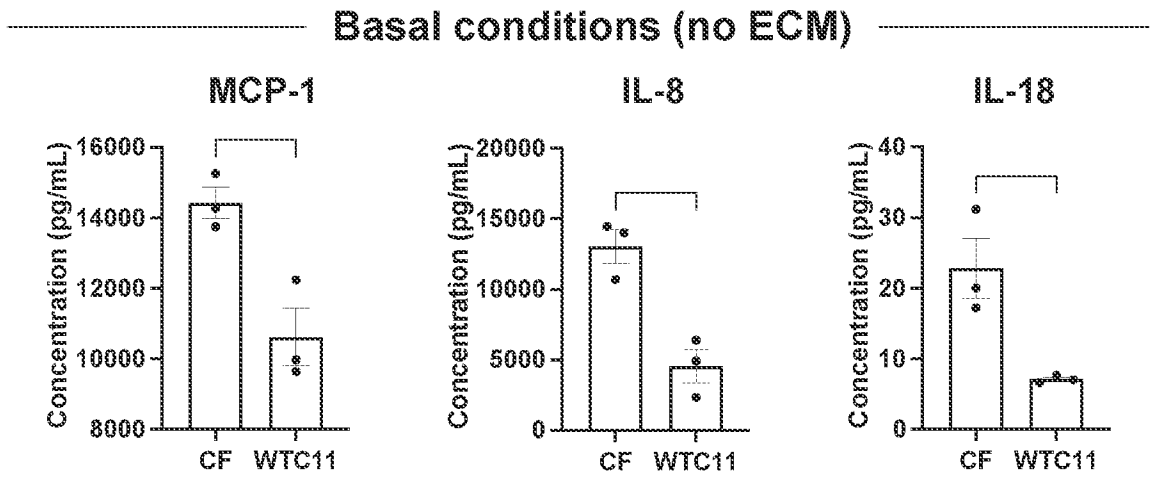

FIG. 14A

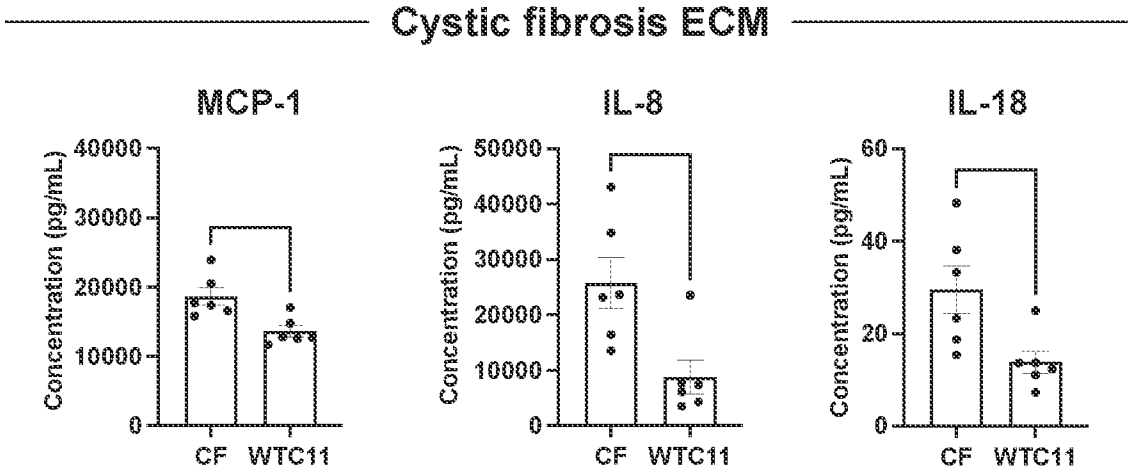

FIG. 14B

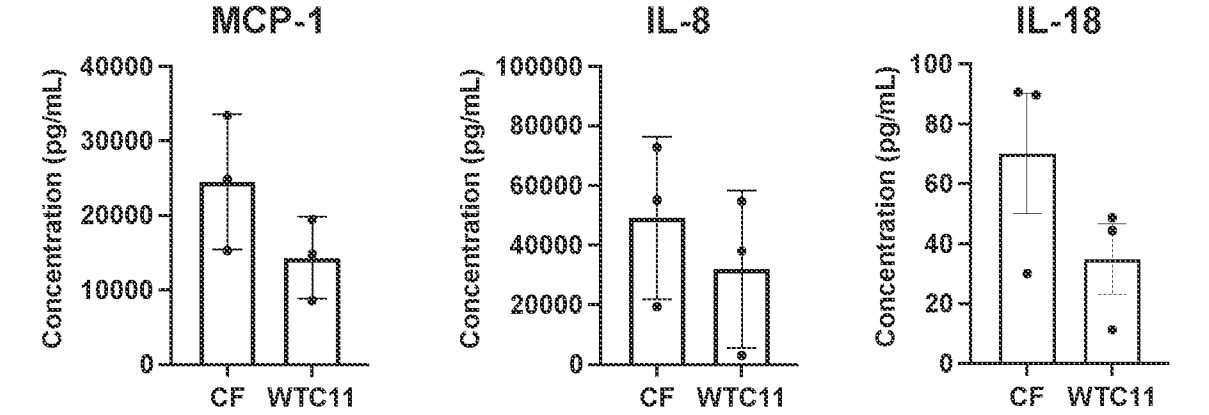

FIG. 14C

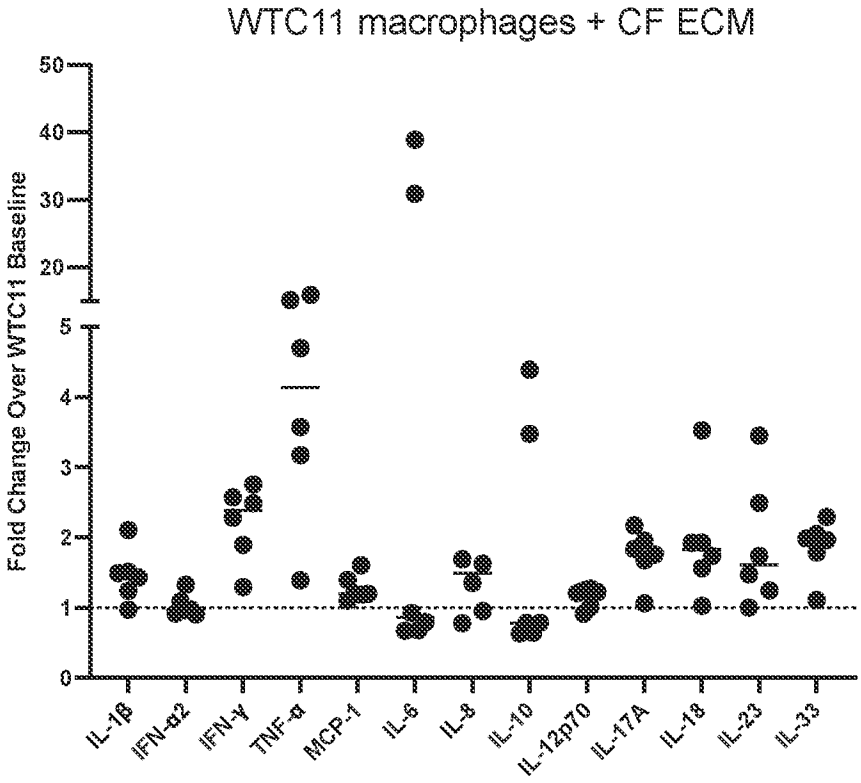

FIG. 15A

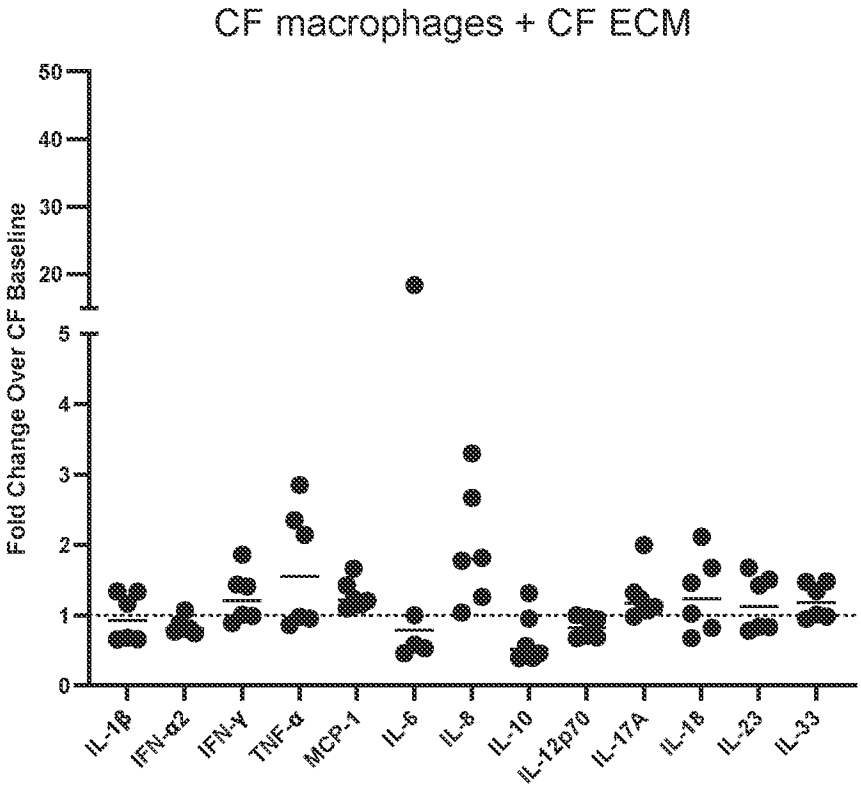

FIG. 15B

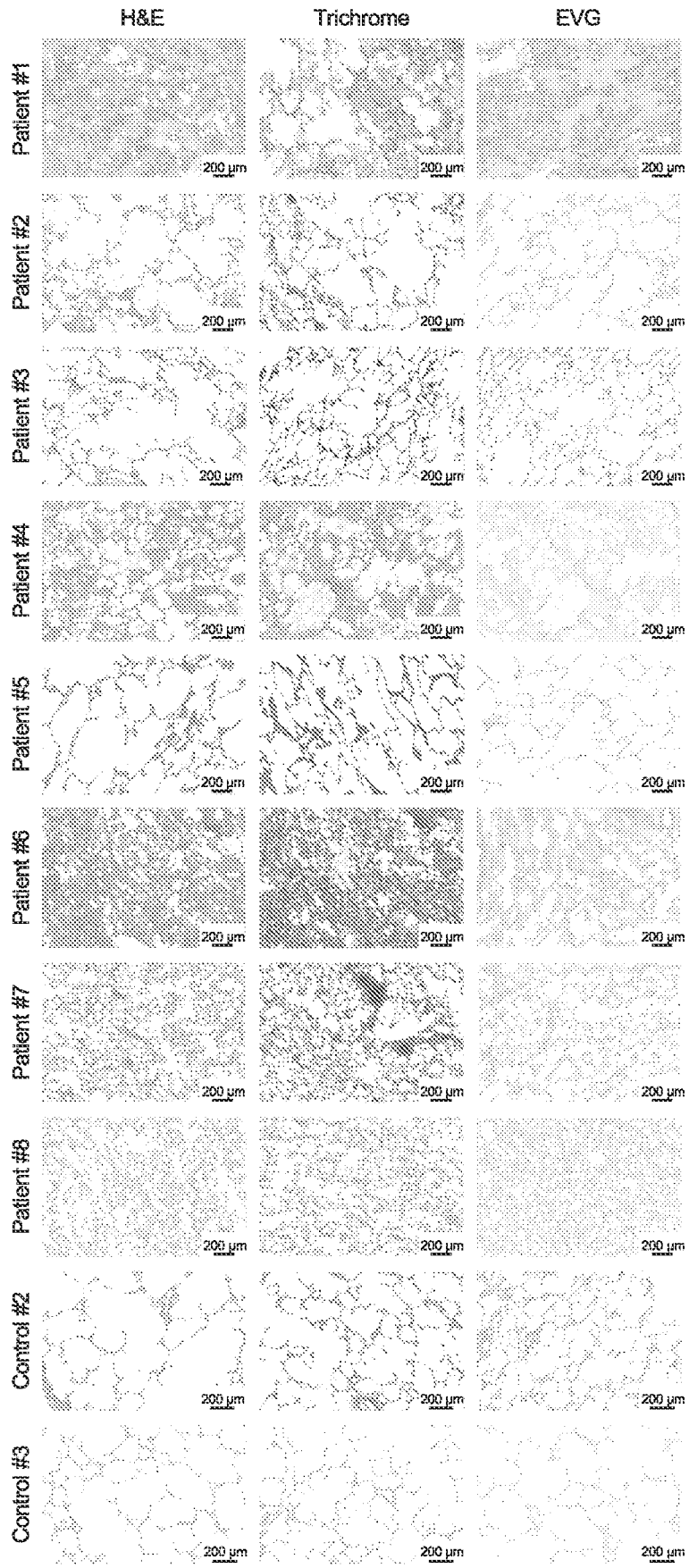
H&E
Trichrome
EVG
Patient #1
Patient #2
Patient #3
Patient #4
Patient #5
Patient #6
Patient #7
Patient #8
Control #2
Control #3
200 µm

FIG. 16

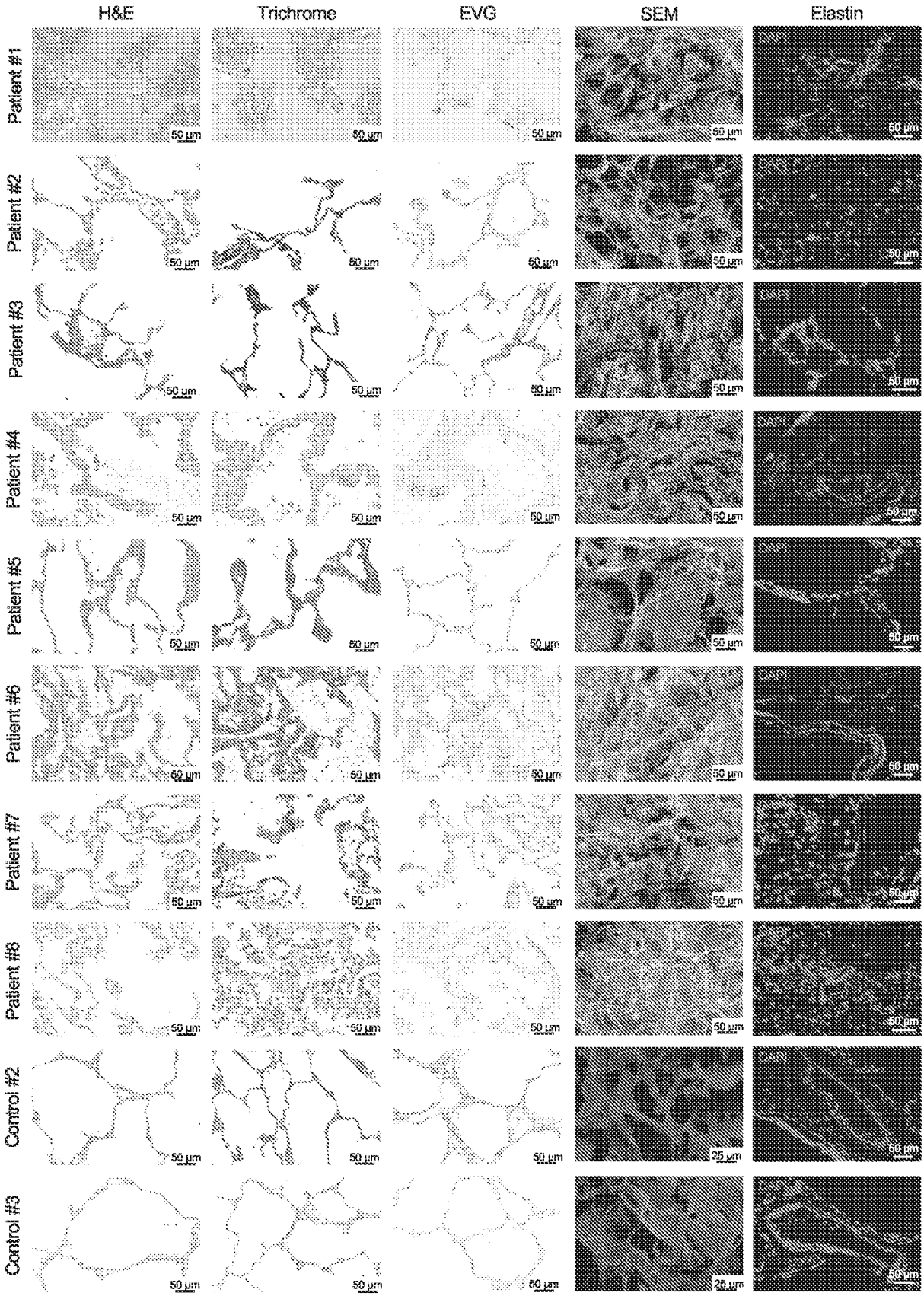
H&E
Trichrome
EVG
SEM
Elastin
Patient #1
Patient #2
Patient #3
Patient #4
Patient #5
Patient #6
Patient #7
Patient #8
Control #2
Control #3
50 µm
25 µm

FIG. 17

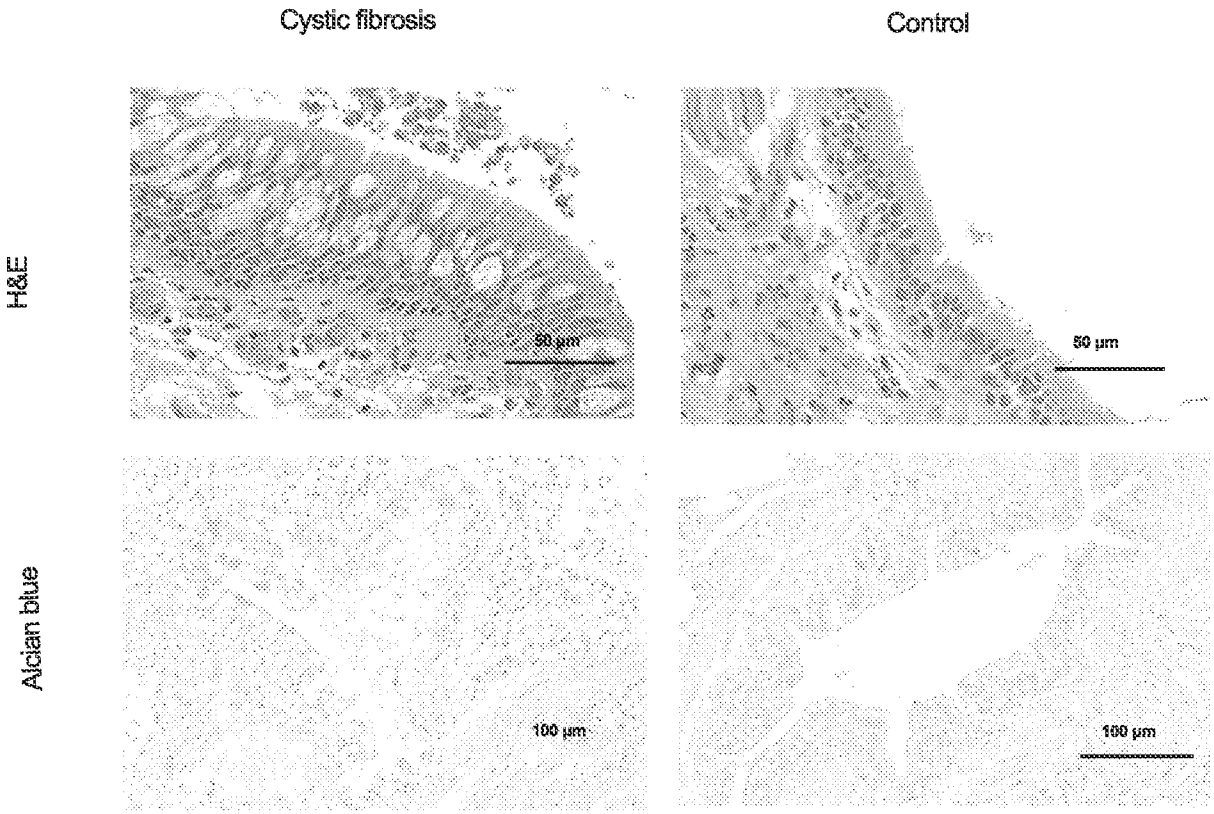
Cystic fibrosis
Control
H&E
Alcian blue
50 µm
50 µm
100 µm
100 µm

FIG. 18

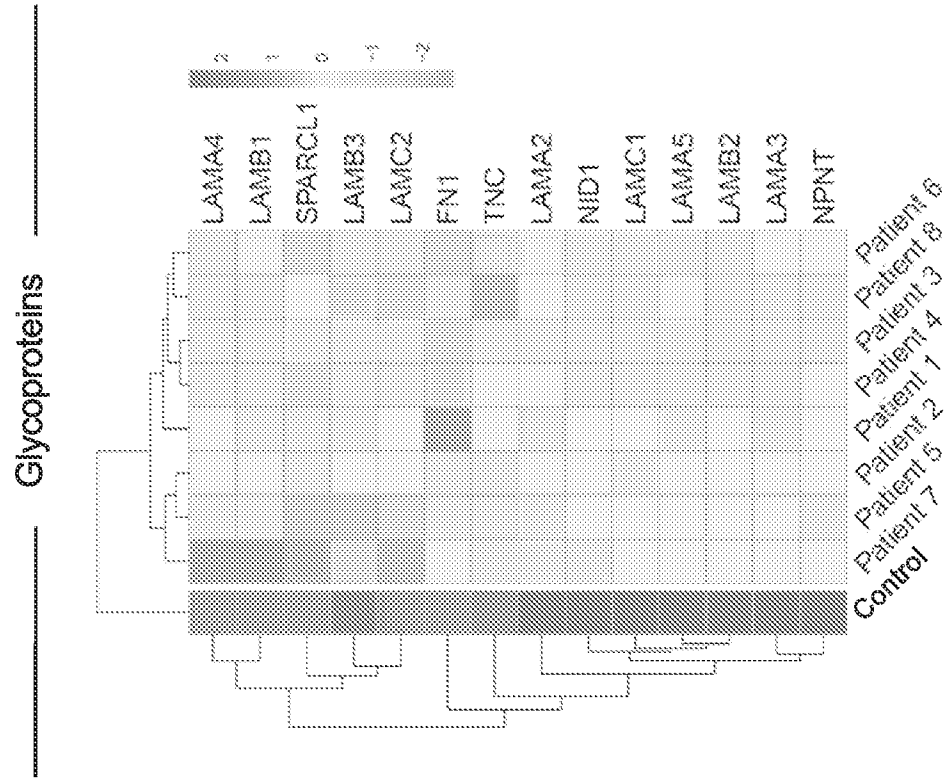

FIG. 19B

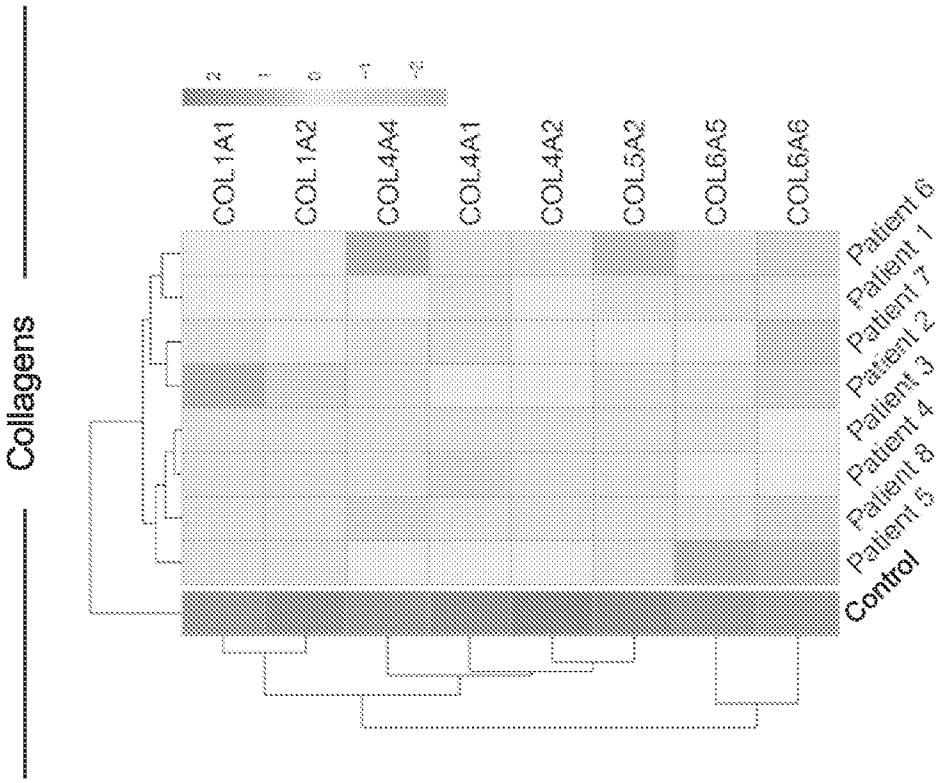

FIG. 19A

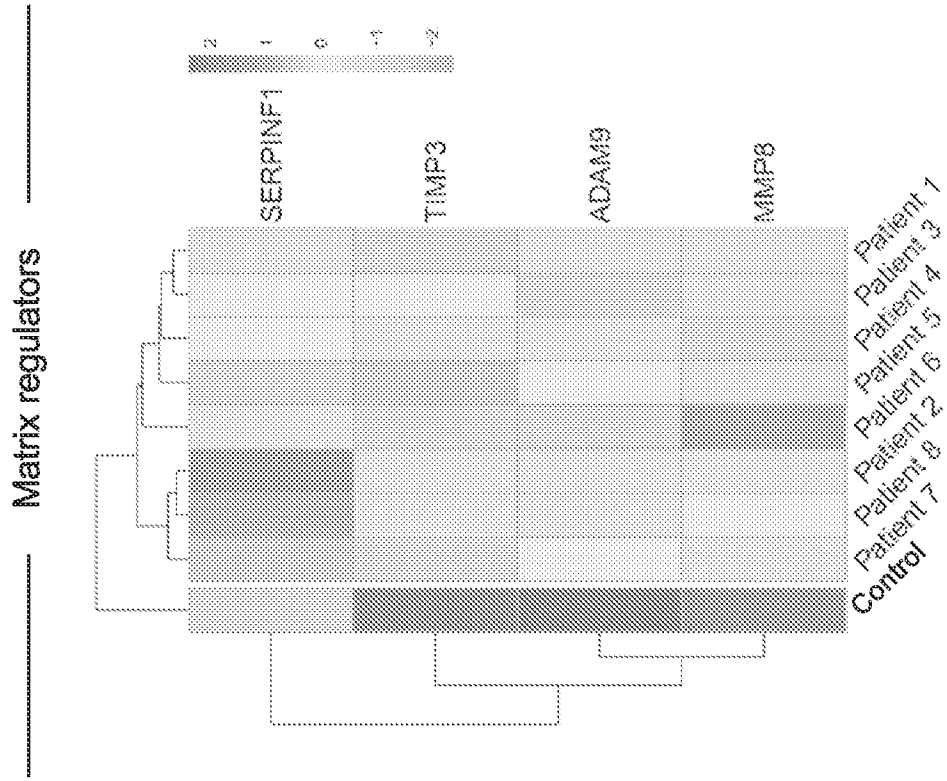

FIG. 19D

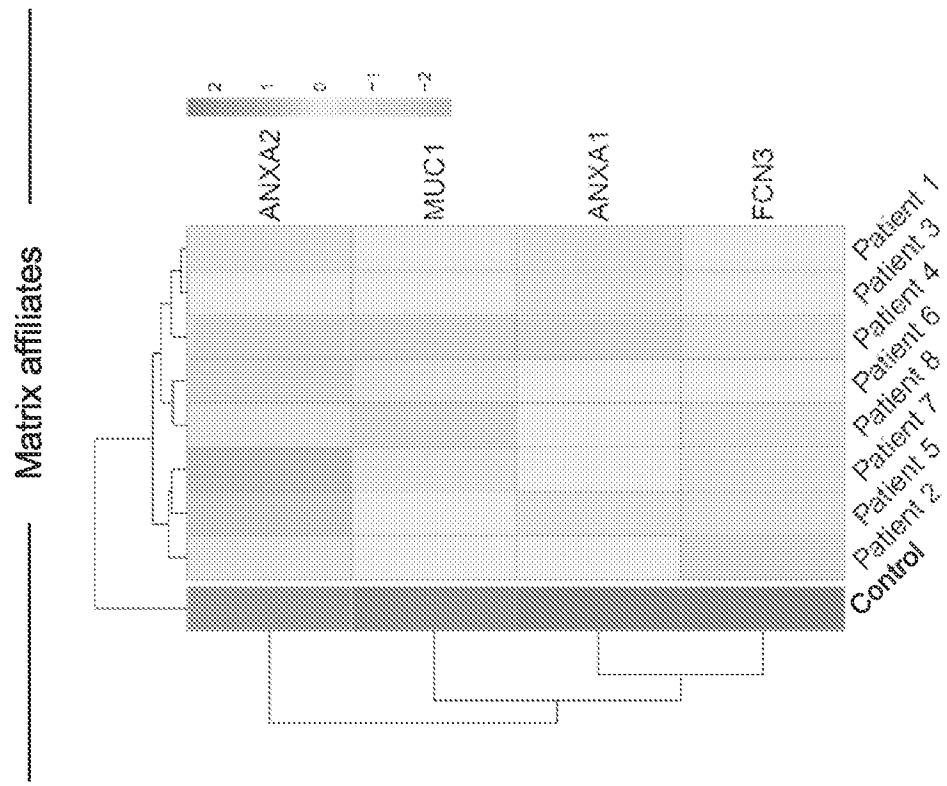

FIG. 19C

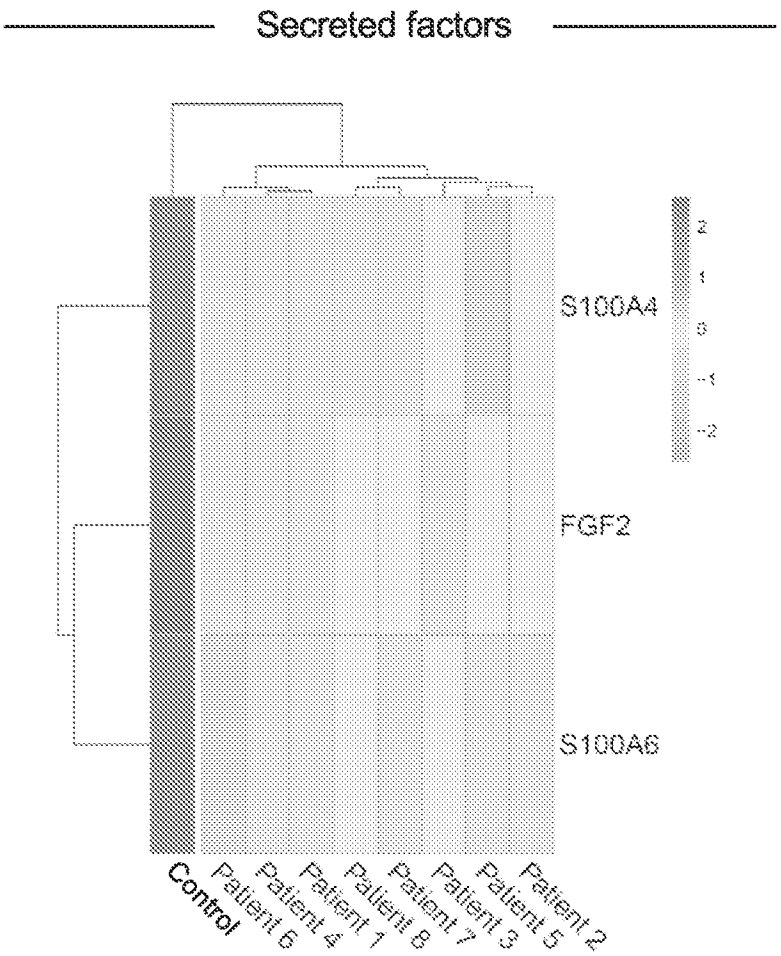
Secreted factors
S100A4
FGF2
S100A6
2
1
0
-1
-2
Control
Patient 6
Patient 4
Patient 1
Patient 8
Patient 7
Patient 3
Patient 5
Patient 2

FIG. 19E

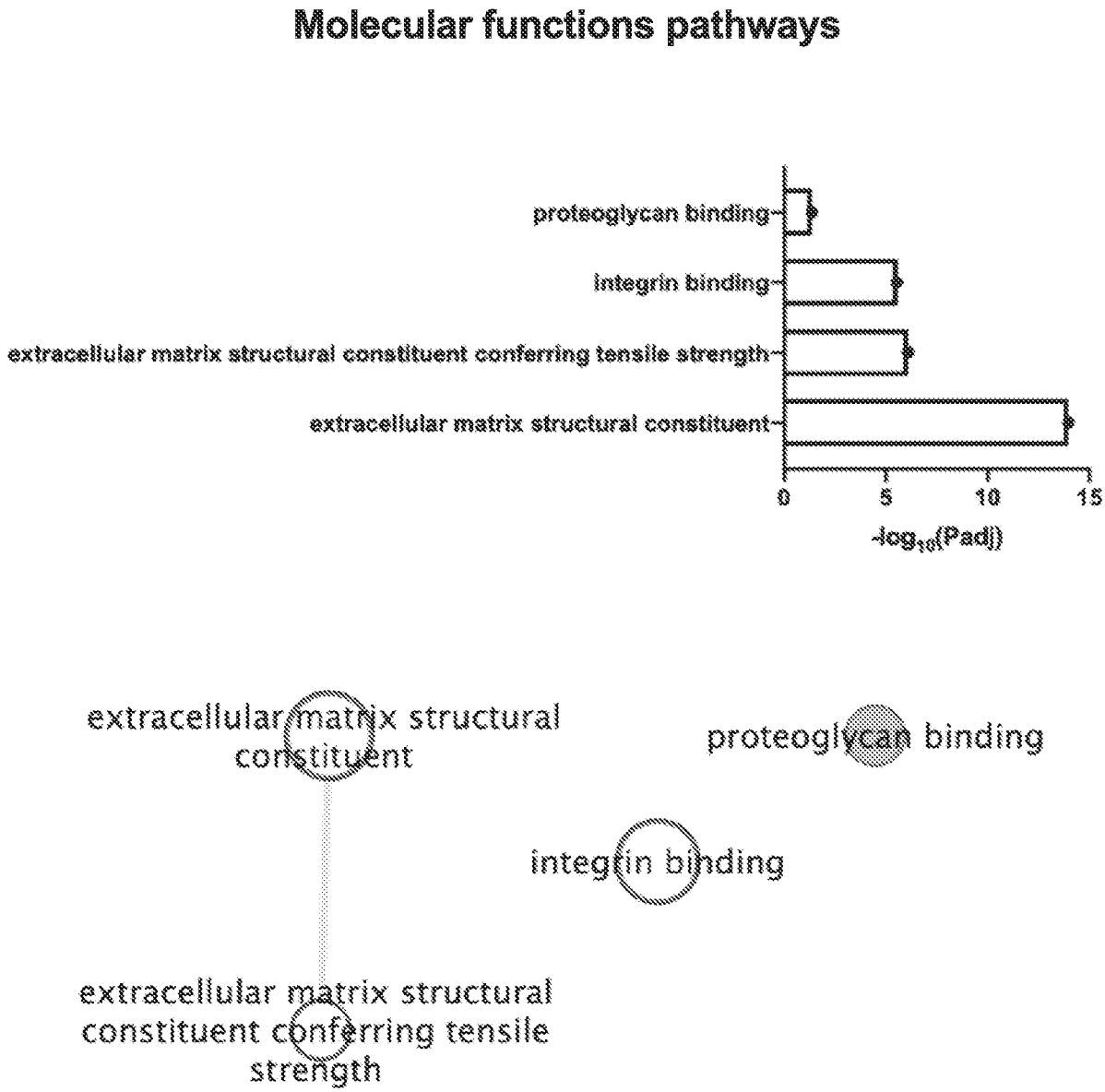
Molecular functions pathways
proteoglycan binding
integrin binding
extracellular matrix structural constituent conferring tensile strength
extracellular matrix structural constituent
0
5
10
15
-log10(Padj)
extracellular matrix structural constituent
proteoglycan binding
integrin binding
extracellular matrix structural constituent conferring tensile strength

FIG. 20

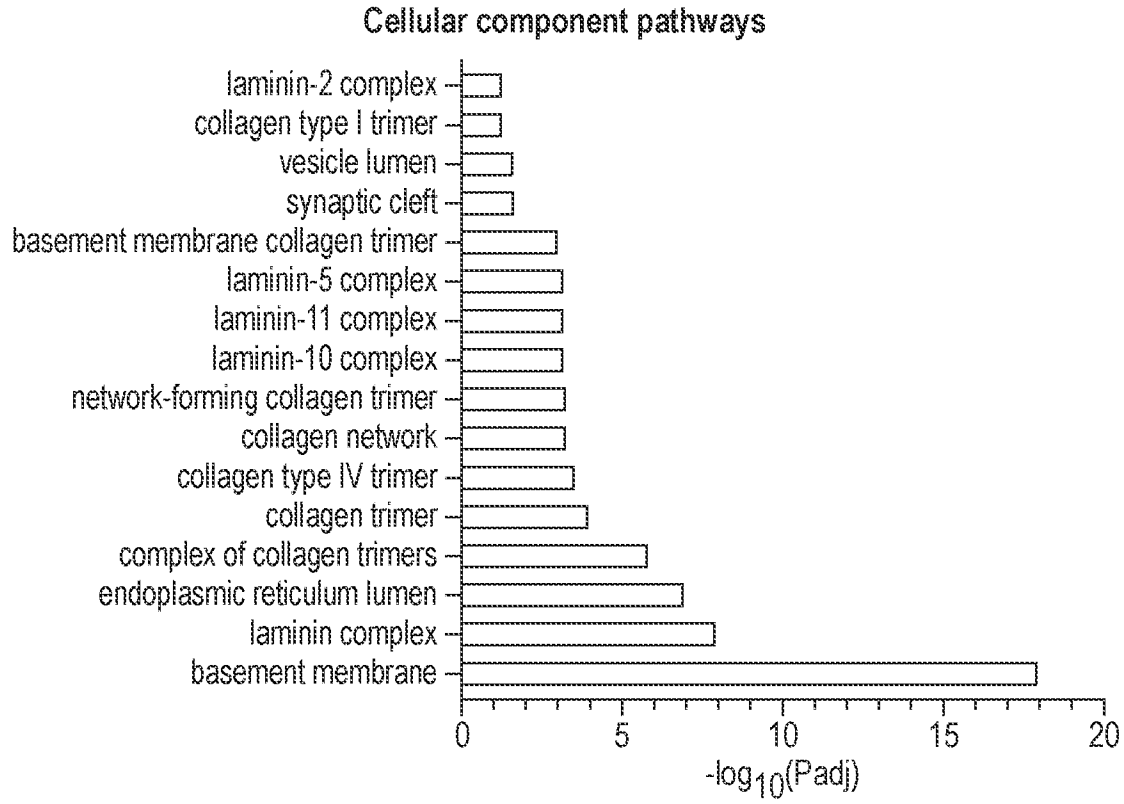

FIG. 21A

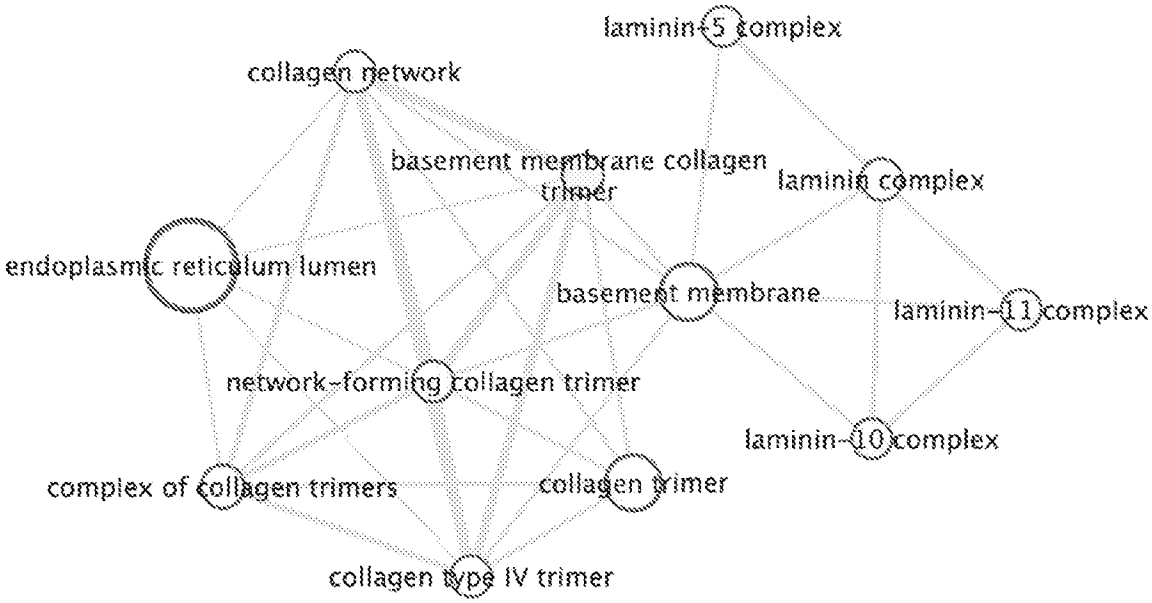

FIG. 21B

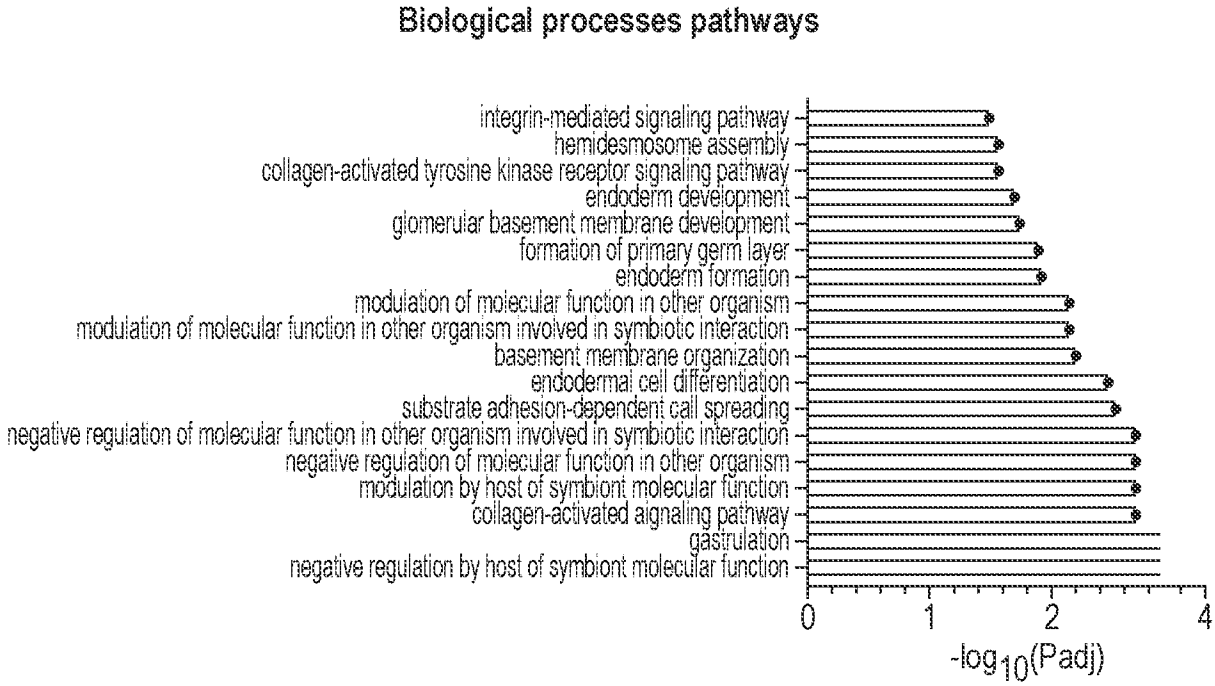

FIG. 22A

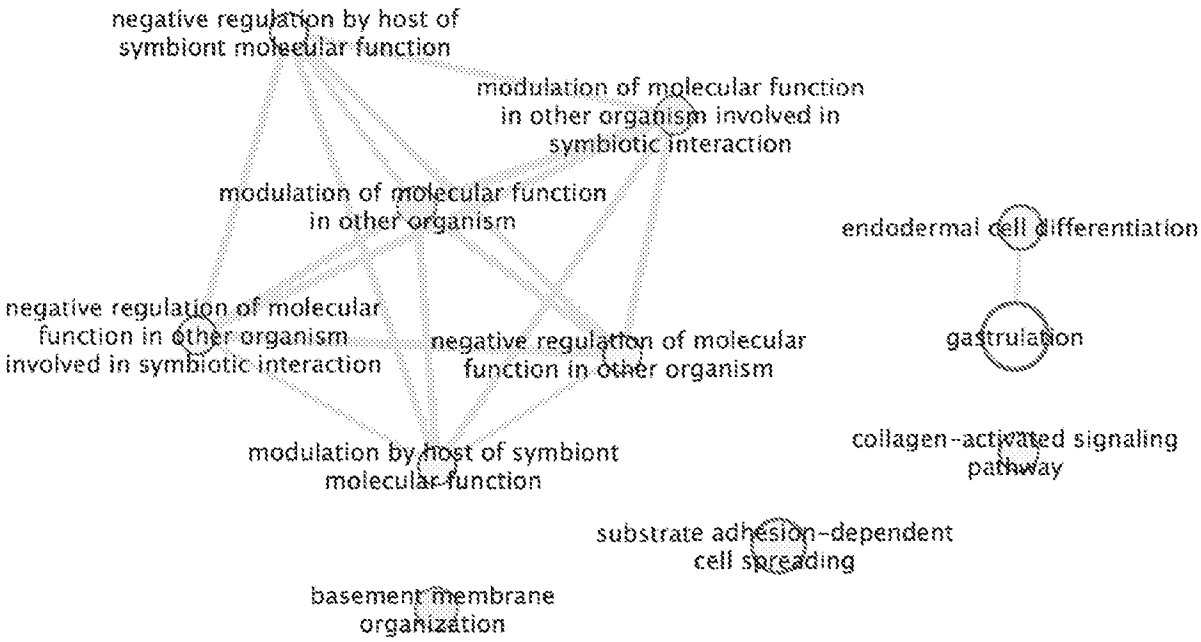

FIG. 22B

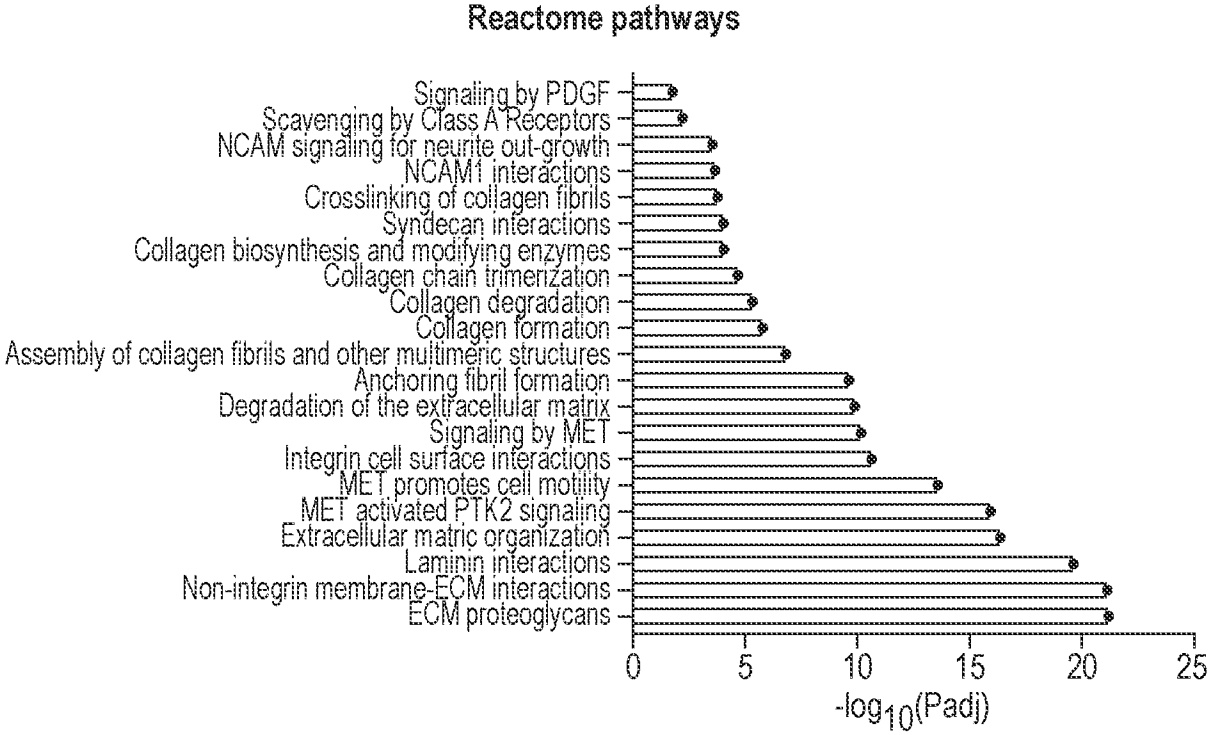

FIG. 23A

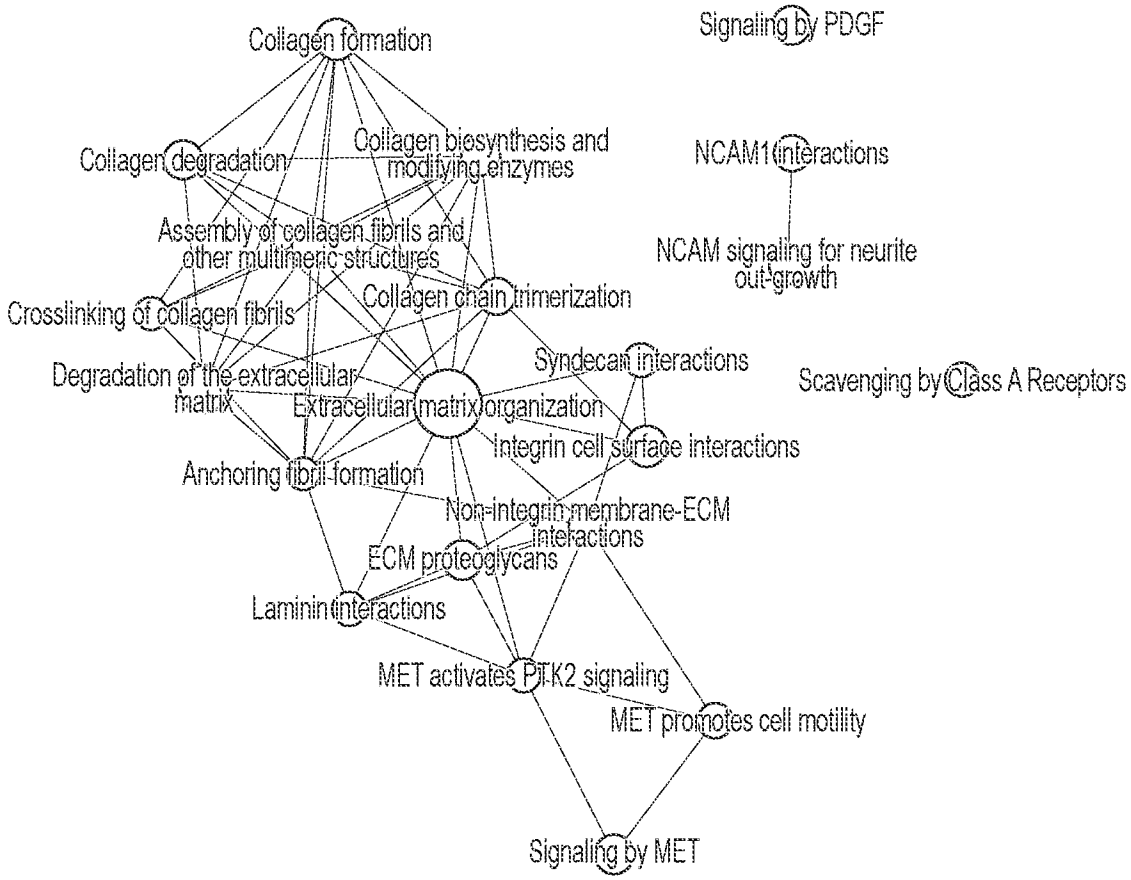

FIG. 23B

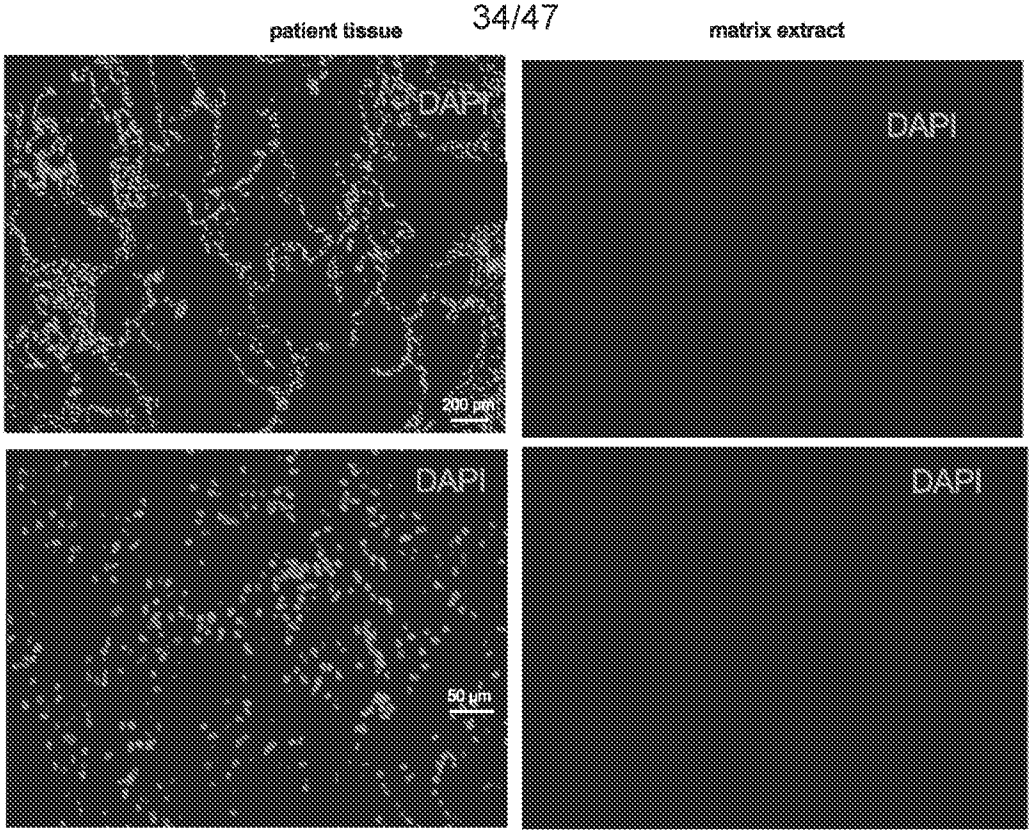

FIG. 24A

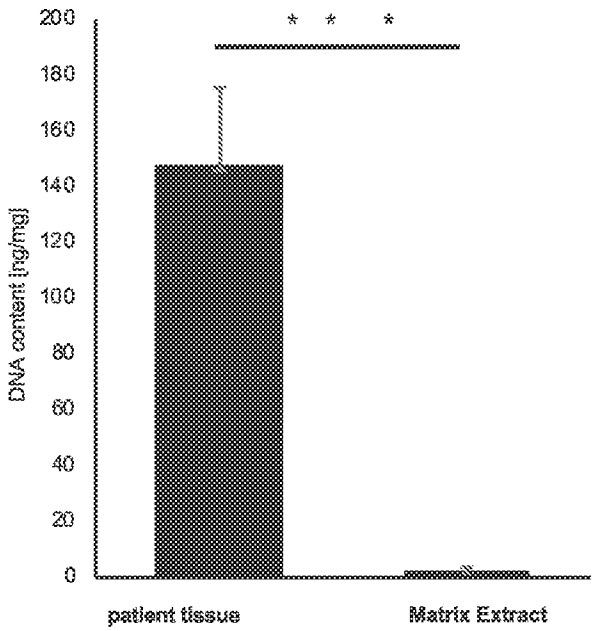

FIG. 24B

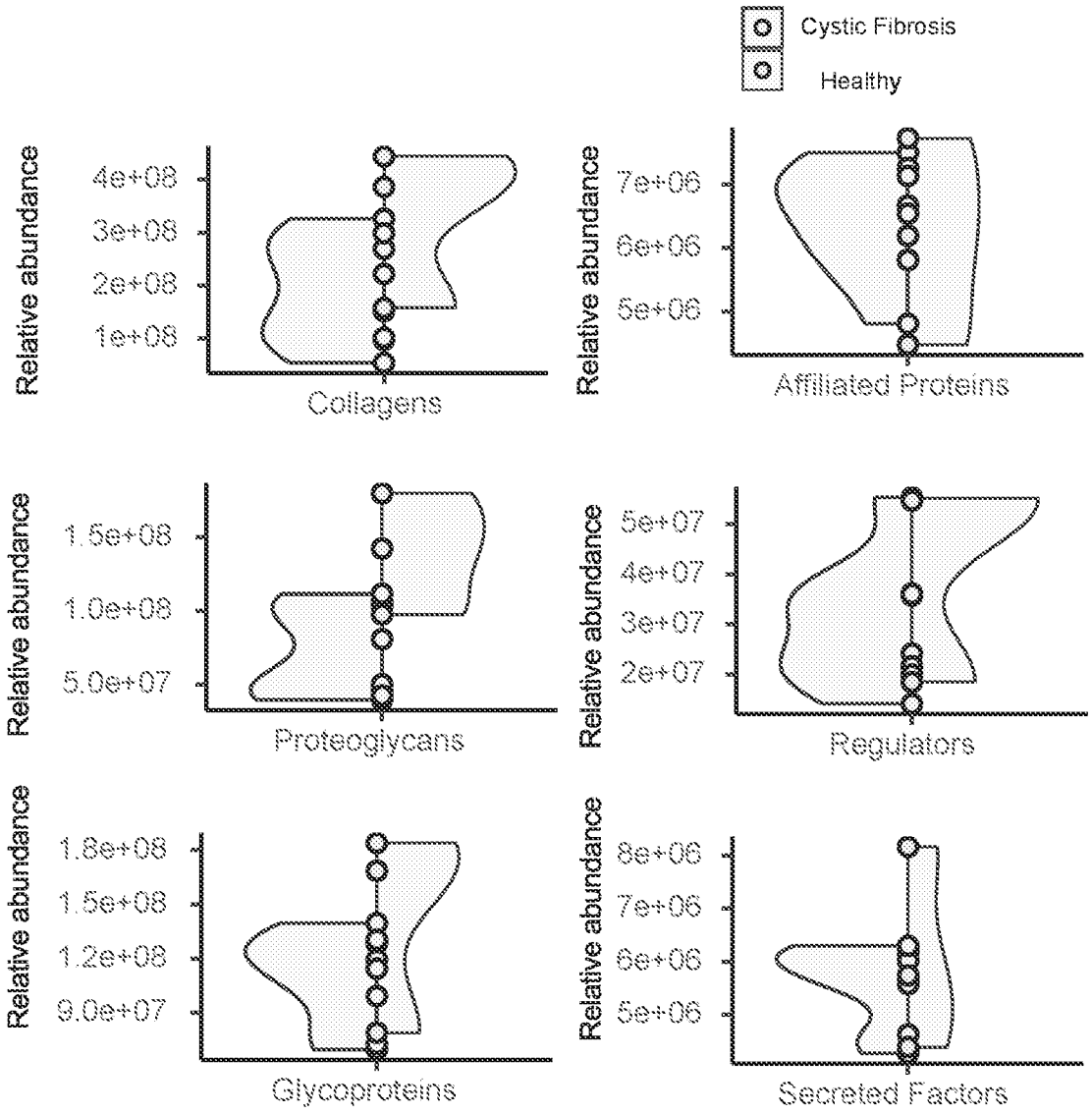
Cystic Fibrosis
Healthy
Relative abundance
4e+08
3e+08
2e+08
1e+08
Collagens
Relative abundance
7e+06
6e+06
5e+06
Affiliated Proteins
Relative abundance
1.5e+08
1.0e+08
5.0e+07
Proteoglycans
Relative abundance
5e+07
4e+07
3e+07
2e+07
Regulators
Relative abundance
1.8e+08
1.5e+08
1.2e+08
9.0e+07
Glycoproteins
Relative abundance
8e+06
7e+06
6e+06
5e+06
Secreted Factors

FIG. 25

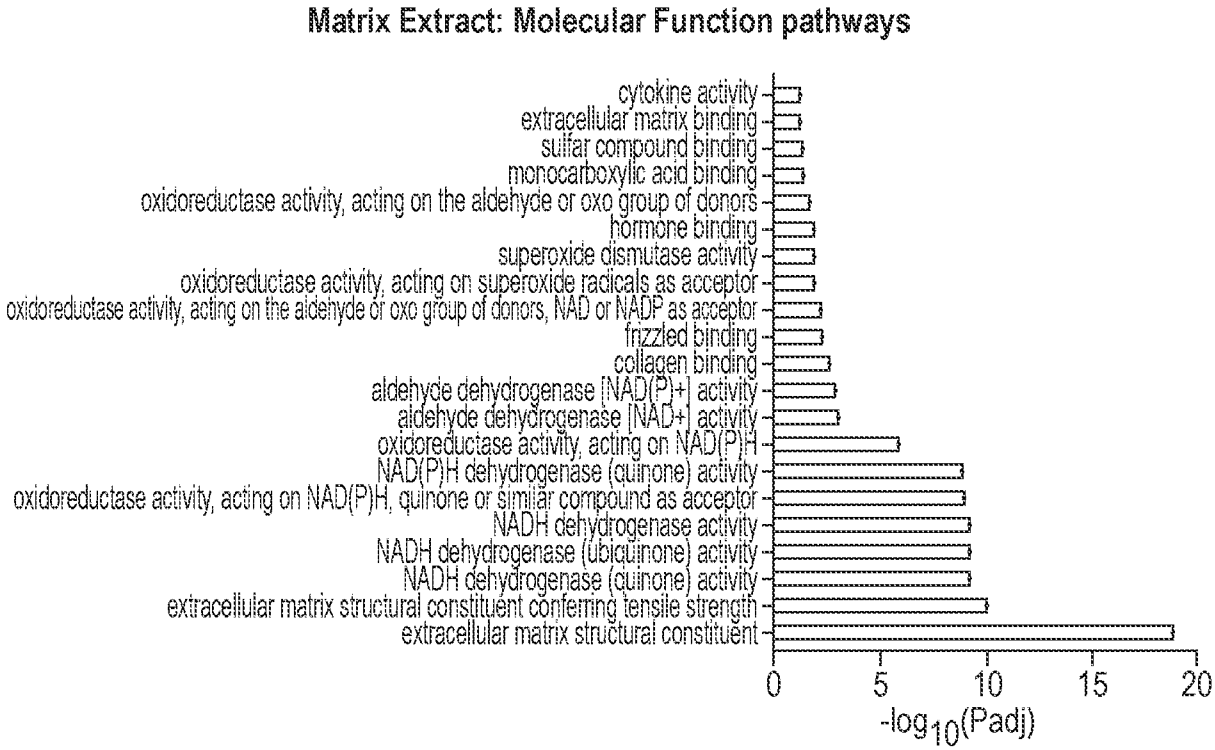

FIG. 26A

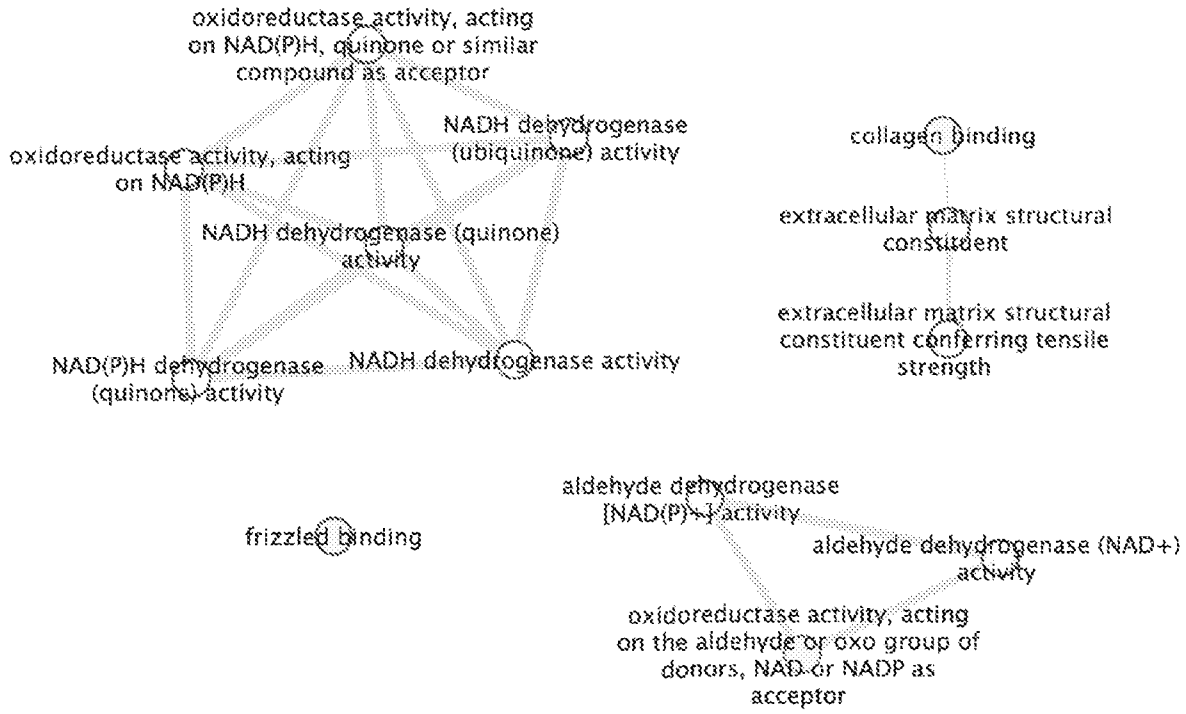

FIG. 26B

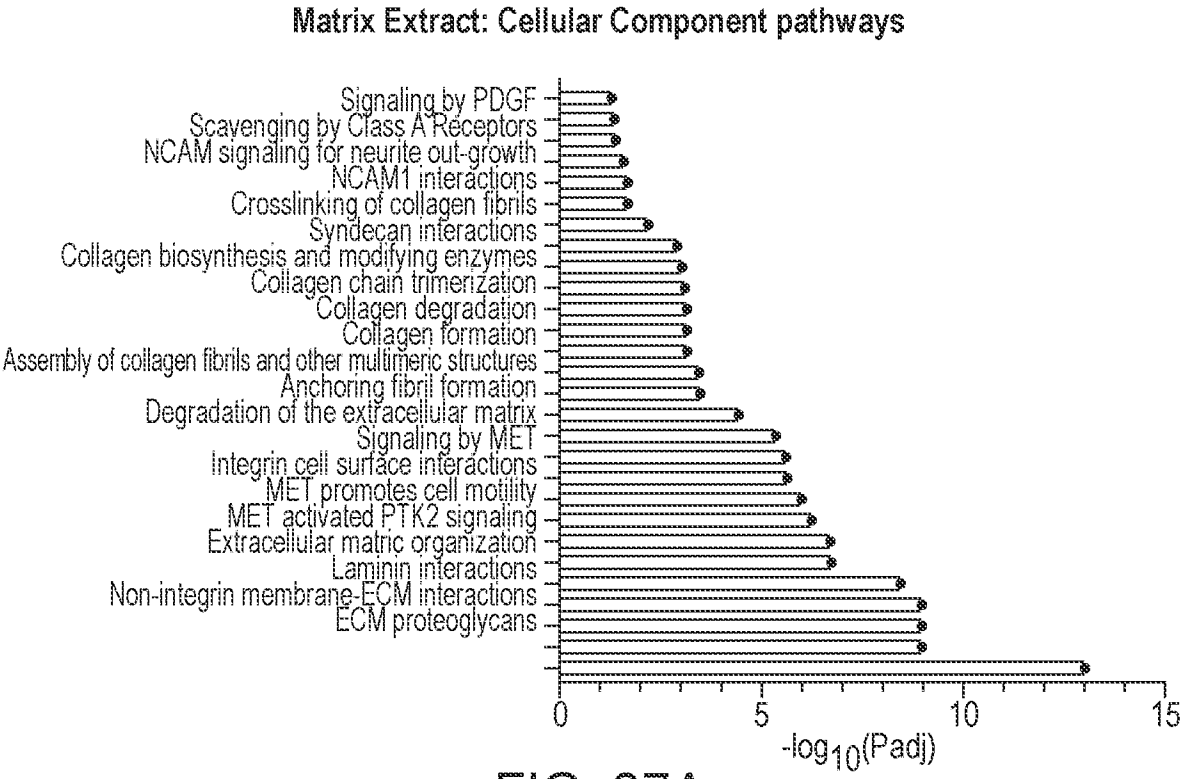

FIG. 27A

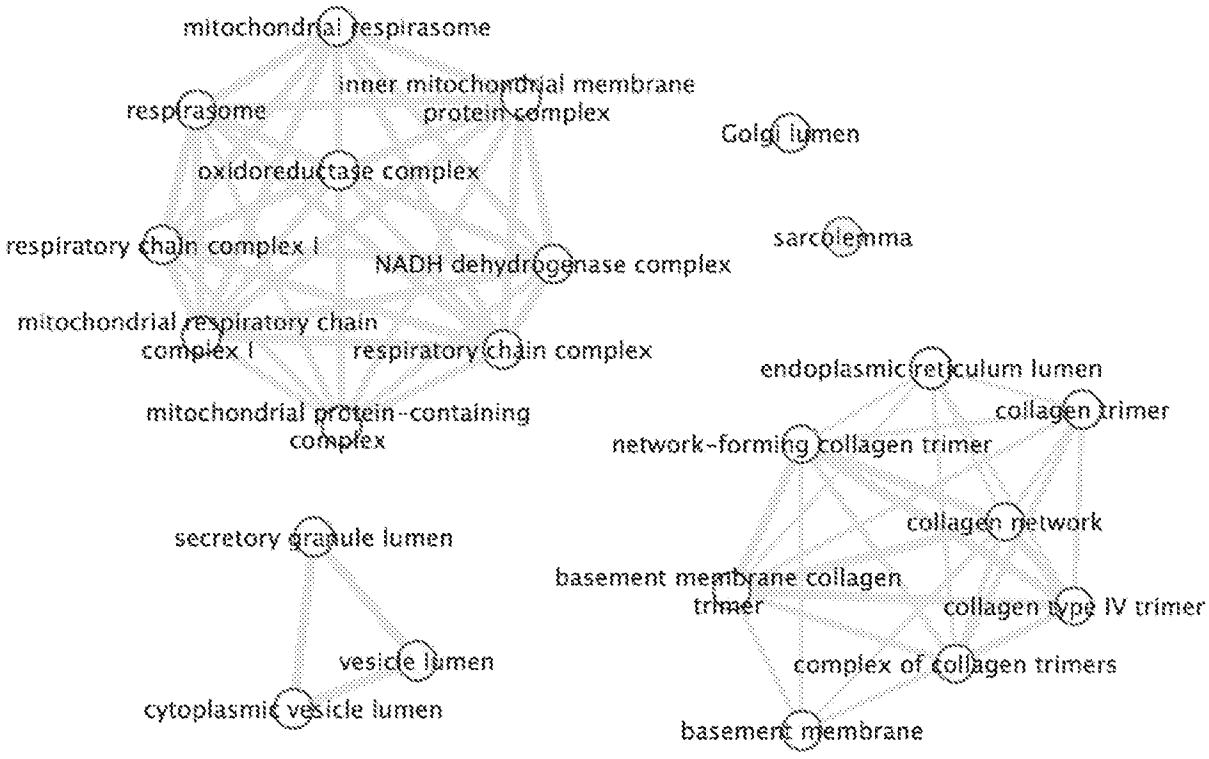

FIG. 27B

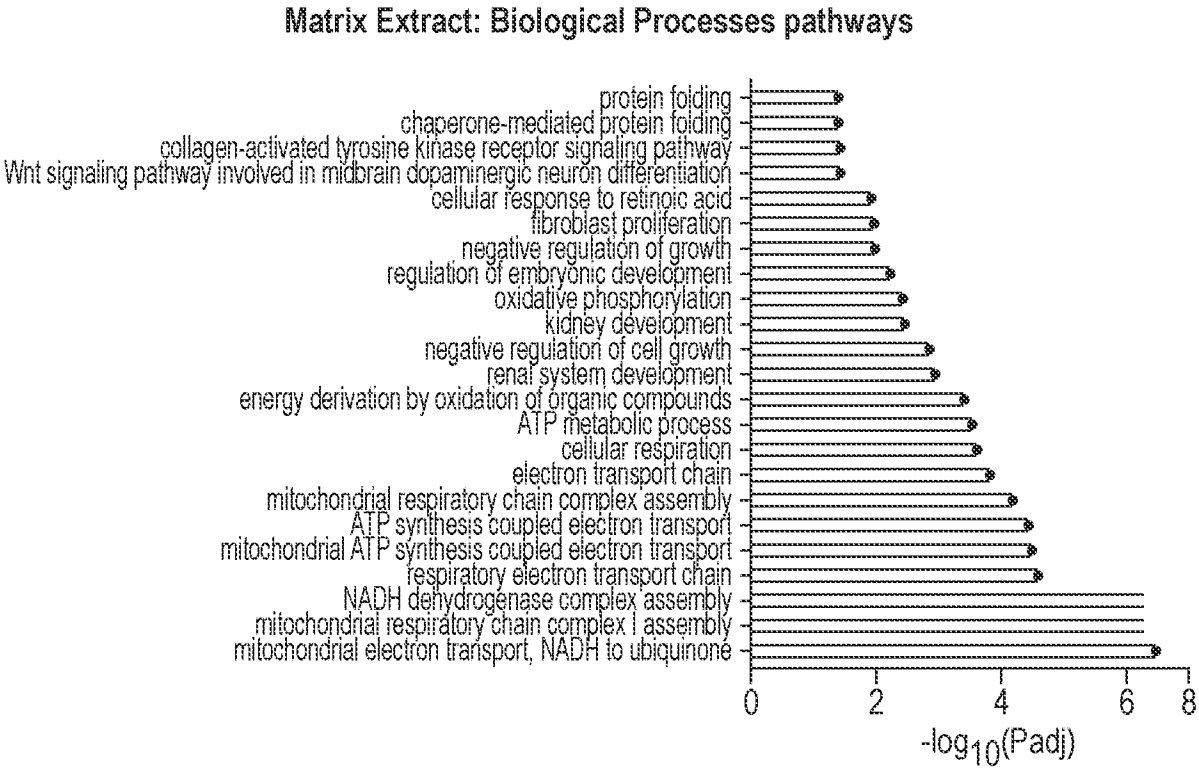

FIG. 28A

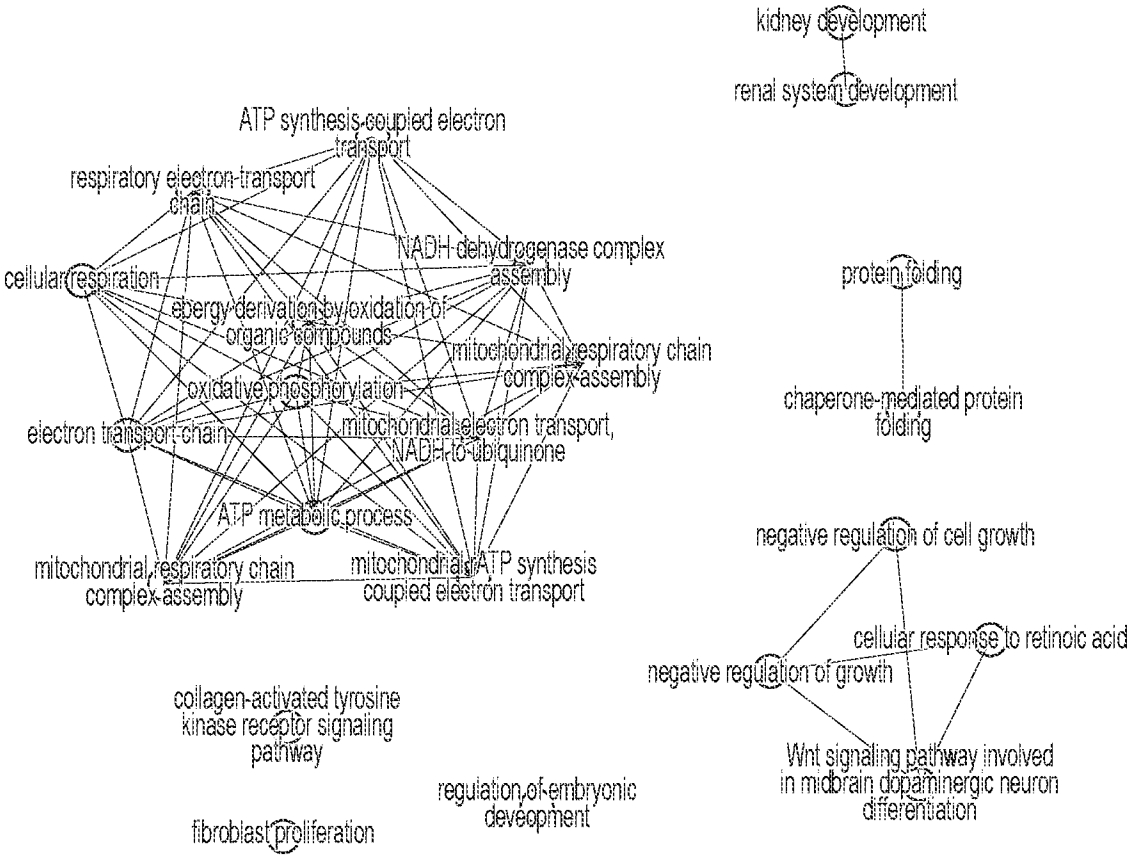

FIG. 28B

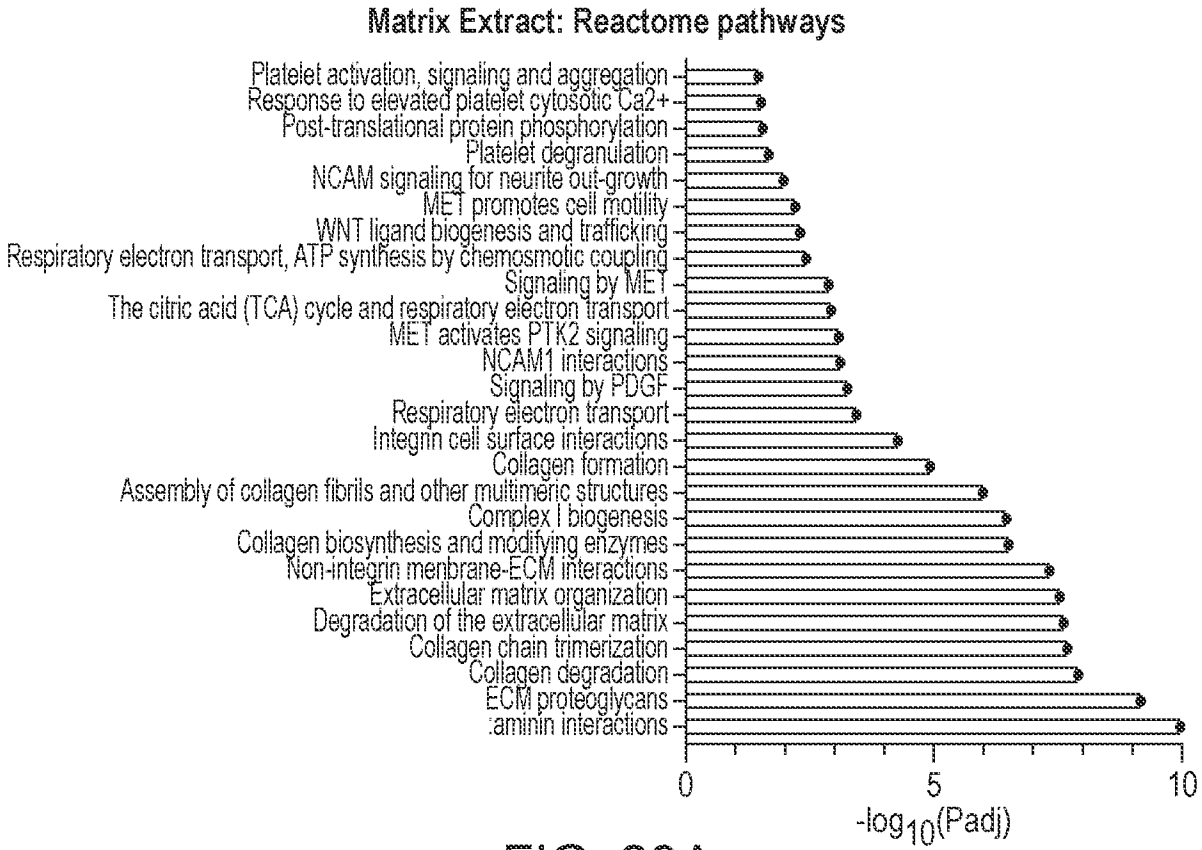

FIG. 29A

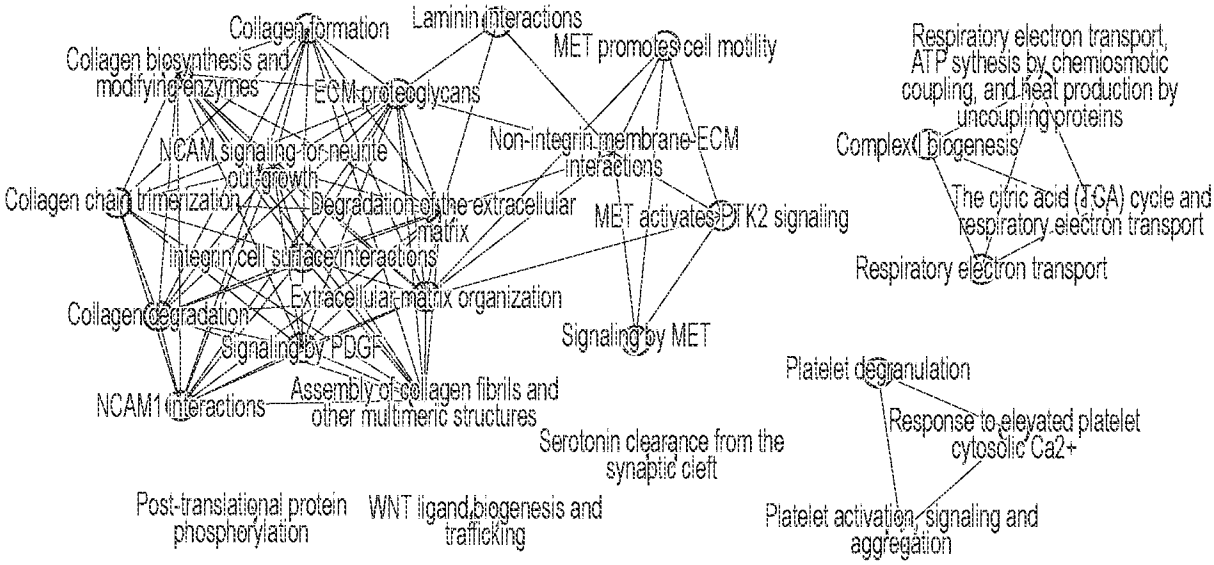

FIG. 29B

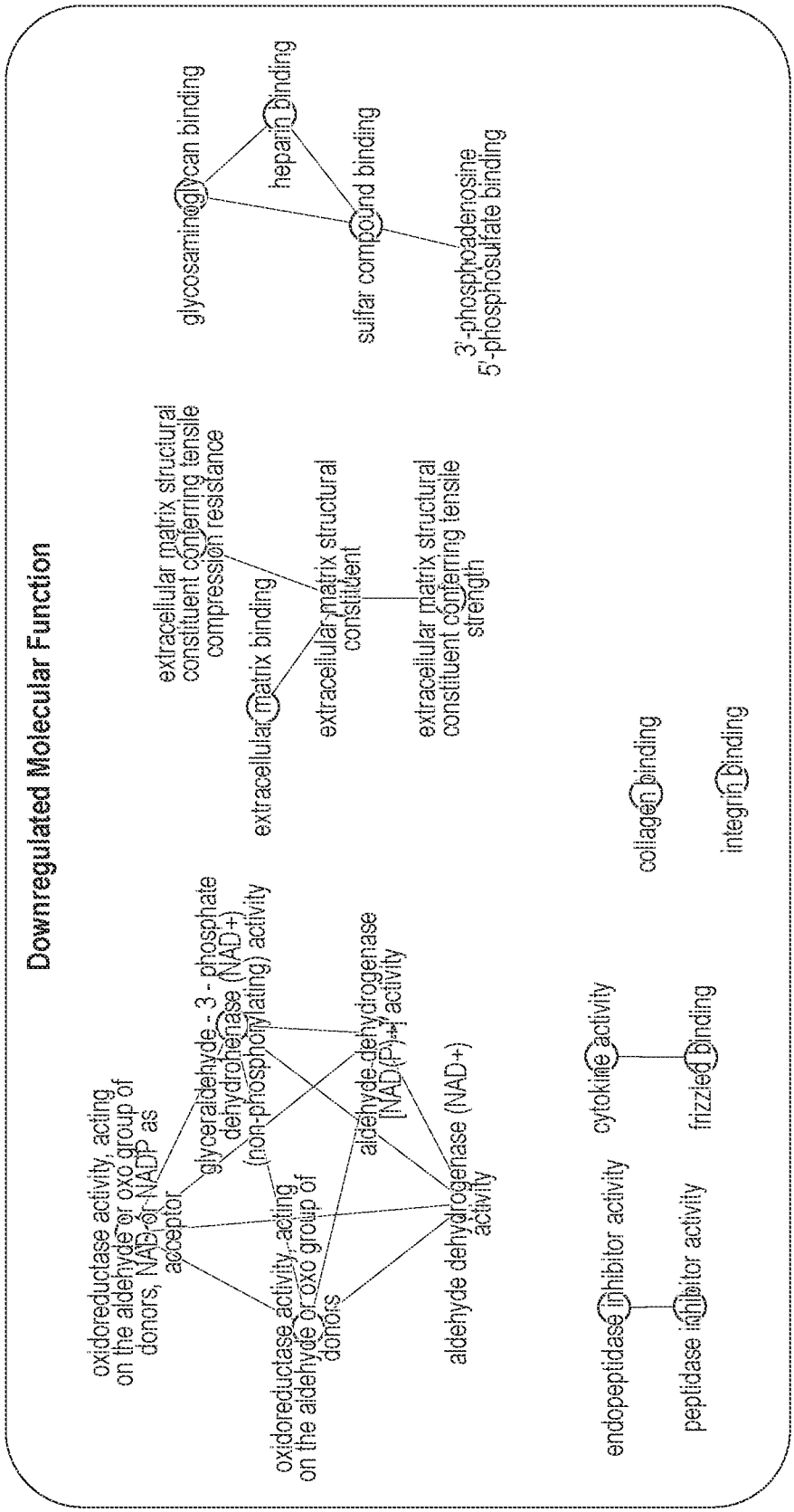
Downregulated Molecular Function
glycosaminoglycan binding
heparin binding
sulfur compound binding
3'-phosphoadenosine 5'-phosphosulfate binding
extracellular matrix structural constituent conferring tensile compression resistance
extracellular matrix binding
extracellular matrix structural constituent
extracellular matrix structural constituent conferring tensile strength
collagen binding
integrin binding
oxidoreductase activity, acting on the aldehyde or oxo group of donors, NAD or NADP as acceptor
glyceraldehyde-3-phosphate dehydrogenase (NAD+) (non-phosphorylating) activity
oxidoreductase activity, acting on the aldehyde or oxo group of donors
aldehyde dehydrogenase [NAD(P)+] activity
aldehyde dehydrogenase (NAD+) activity
cytokine activity
endopeptidase inhibitor activity
frizzled binding
peptidase inhibitor activity

FIG. 30A

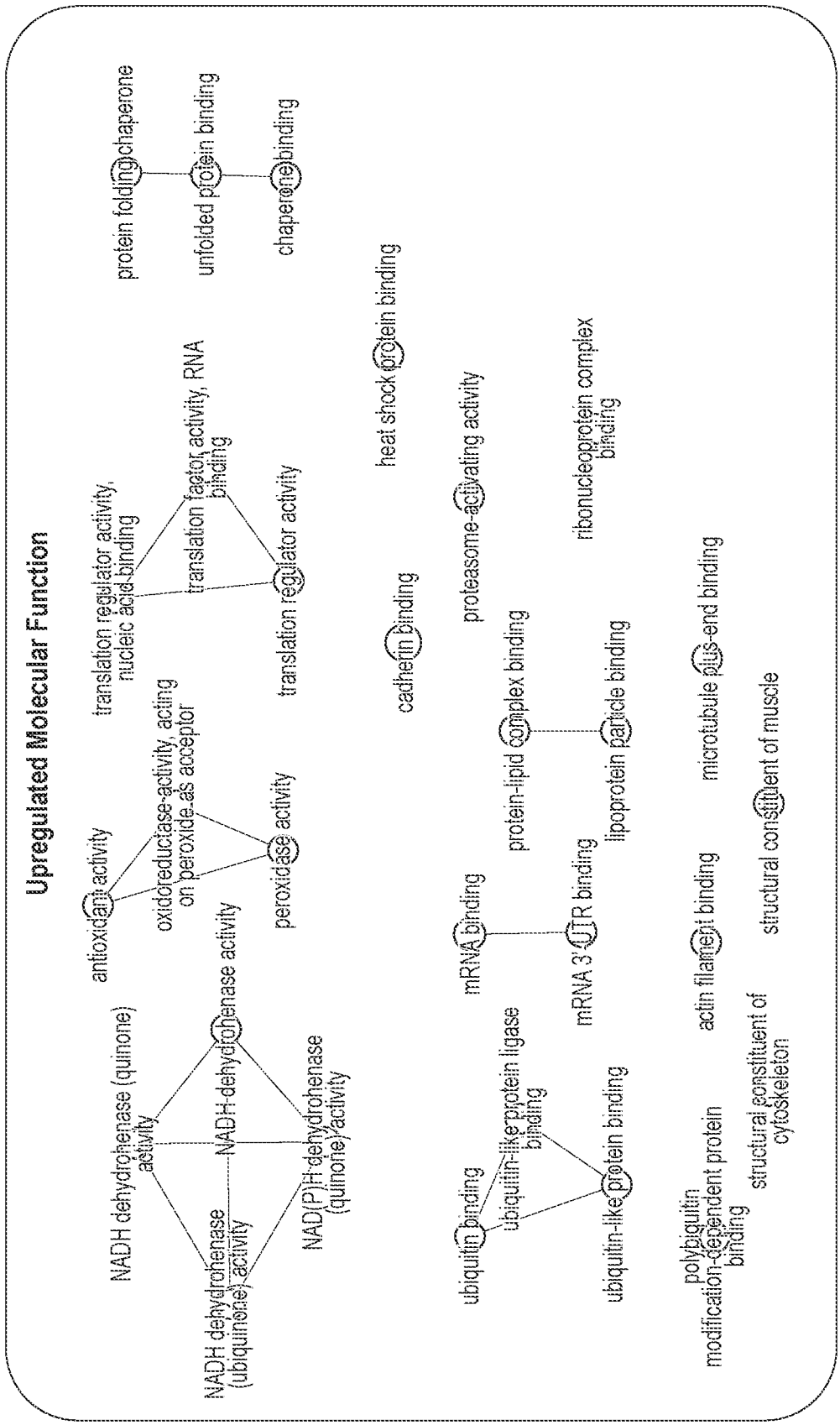
Upregulated Molecular Function
protein folding chaperone
unfolded protein binding
chaperone binding
translation regulator activity, nucleic acid binding
translation factor activity, RNA binding
translation regulator activity
antioxidant activity
oxidoreductase activity, acting on peroxide as acceptor
peroxidase activity
NADH dehydrogenase (quinone) activity
NADH dehydrogenase activity
NADH dehydrogenase (ubiquinone) activity
NAD(P)H dehydrogenase (quinone) activity
heat shock protein binding
cadherin binding
proteasome-activating activity
ribonucleoprotein complex binding
protein-lipid complex binding
mRNA binding
mRNA 3'-UTR binding
lipoprotein particle binding
ubiquitin binding
ubiquitin-like protein ligase binding
ubiquitin-like protein binding
polyubiquitin modification-dependent protein binding
actin filament binding
microtubule plus-end binding
structural constituent of cytoskeleton
structural constituent of muscle

FIG. 30B

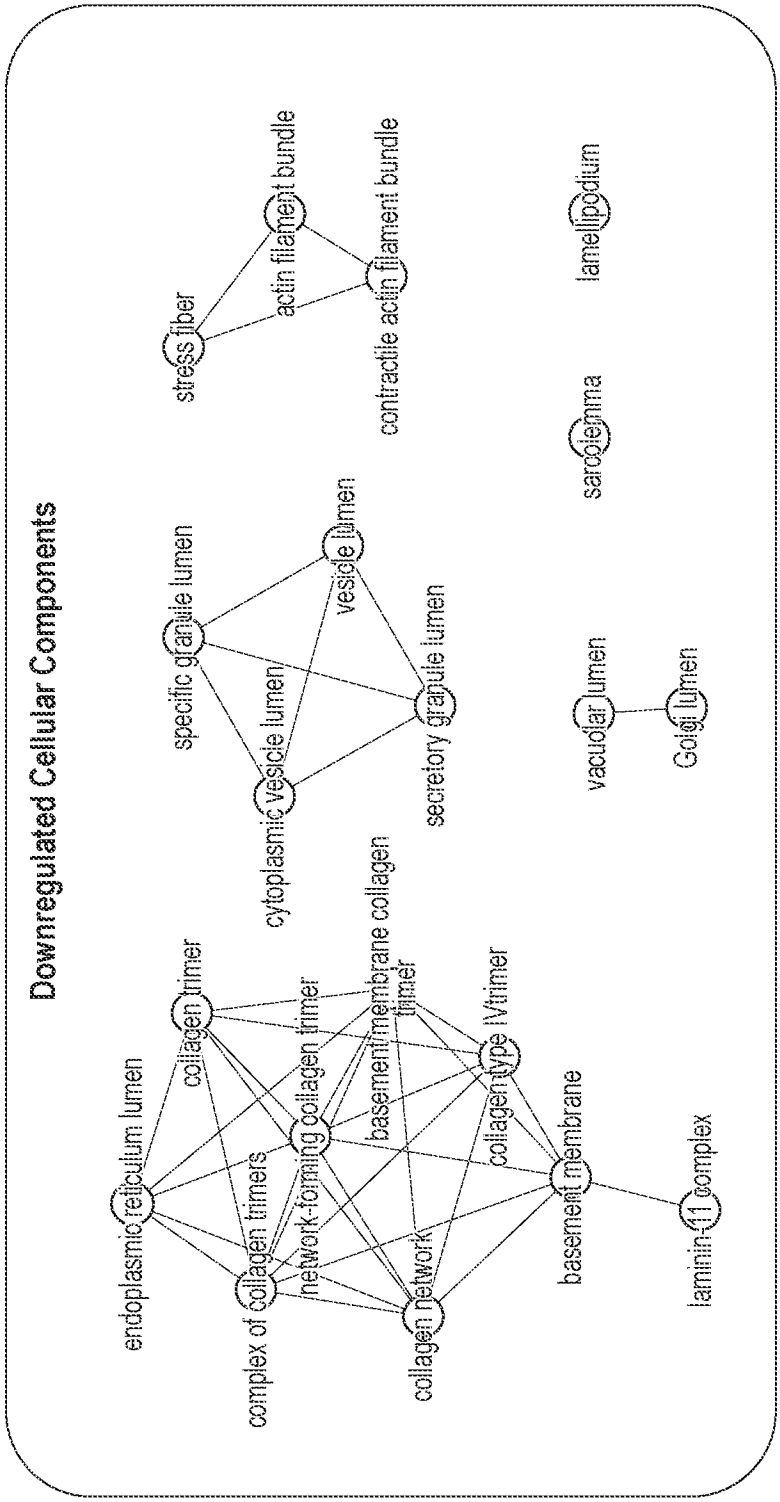
Downregulated Cellular Components
endoplasmic reticulum lumen
collagen trimer
complex of collagen trimers
network-forming collagen trimer
basement membrane collagen trimer
collagen network
collagen type IV trimer
basement membrane
laminin-11 complex
specific granule lumen
vesicle lumen
cytoplasmic vesicle lumen
secretory granule lumen
stress fiber
actin filament bundle
contractile actin filament bundle
sarcolemma
lamellipodium
vacuolar lumen
Golgi lumen

FIG. 30C

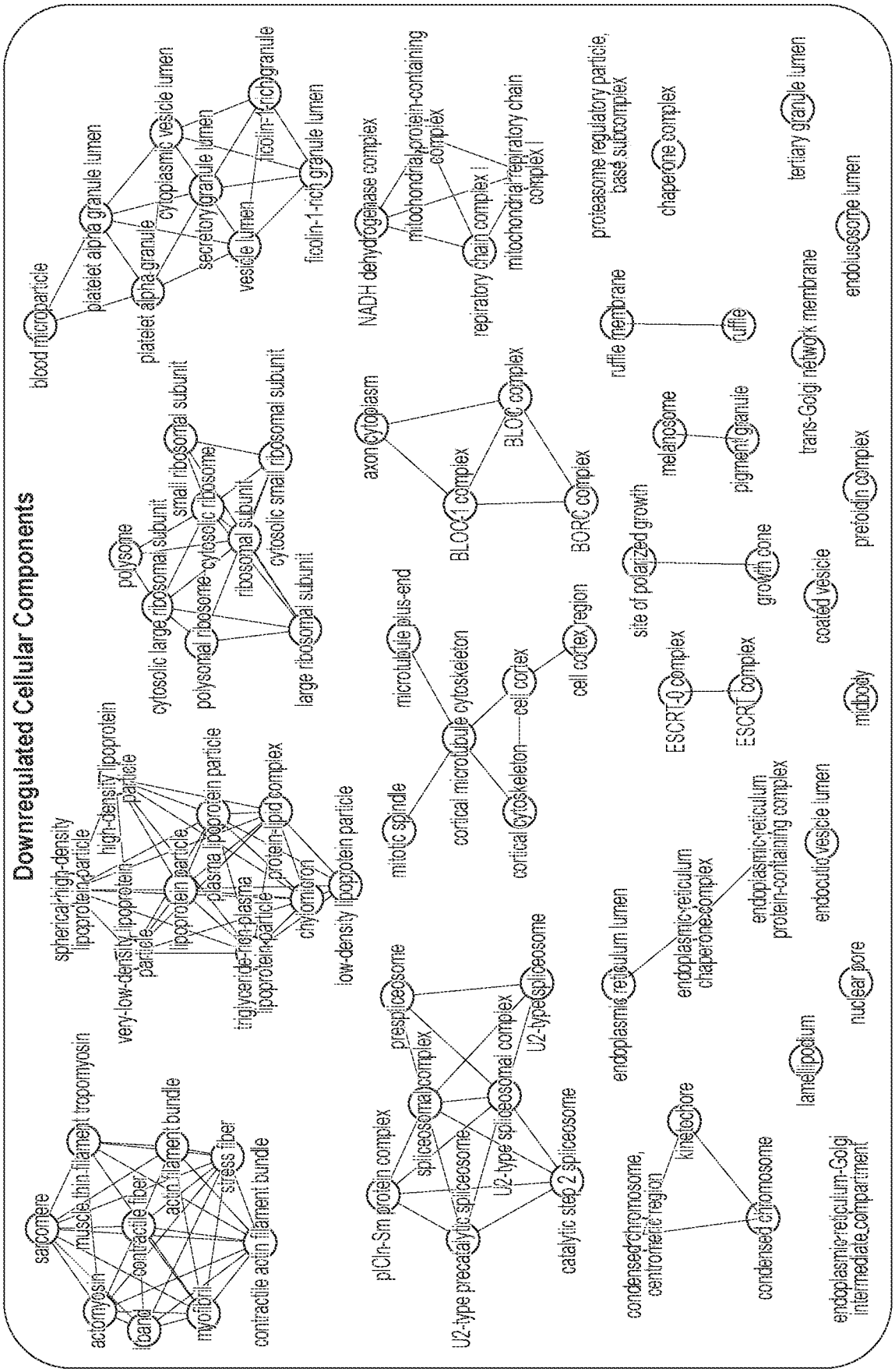
Downregulated Cellular Components
sarcomere
muscle thin filament tropomyosin
actomyosin
contractile fiber
actin filament bundle
I band
myofibril
stress fiber
contractile actin filament bundle
spherical high-density lipoprotein particle
high-density lipoprotein particle
very-low-density lipoprotein particle
lipoprotein particle
plasma lipoprotein particle
triglyceride-rich plasma lipoprotein particle
protein-lipid complex
chylomicron
low-density lipoprotein particle
cytosolic large ribosomal subunit
polysome
polysomal ribosome
cytosolic ribosome
small ribosomal subunit
ribosomal subunit
cytosolic small ribosomal subunit
large ribosomal subunit
blood microparticle
platelet alpha granule lumen
platelet alpha granule
cytoplasmic vesicle lumen
secretory granule lumen
vesicle lumen
ficolin-1-rich granule
ficolin-1-rich granule lumen
axon cytoplasm
BLOC-1 complex
BLOC complex
BORC complex
microtubule plus-end
mitotic spindle
cortical microtubule cytoskeleton
cortical cytoskeleton
cell cortex
cell cortex region
NADH dehydrogenase complex
mitochondrial protein-containing complex
respiratory chain complex I
mitochondrial respiratory chain complex I
site of polarized growth
melanosome
pigment granule
growth cone
ESCRT-0 complex
ESCRT complex
ruffle membrane
ruffle
proteasome regulatory particle, base subcomplex
chaperone complex
tertiary granule lumen
endolysosome lumen
trans-Golgi network membrane
prefoldin complex
coated vesicle
midbody
pICln-Sm protein complex
spliceosomal complex
U2-type precatalytic spliceosome
U2-type spliceosomal complex
U2-type prespliceosome
U2-type spliceosome
catalytic step 2 spliceosome
endoplasmic reticulum lumen
endoplasmic reticulum chaperone complex
endoplasmic reticulum protein-containing complex
endocytic vesicle lumen
condensed chromosome, centromeric region
kinetochore
condensed chromosome
lamellipodium
nuclear pore
endoplasmic reticulum-Golgi intermediate compartment

FIG. 30D

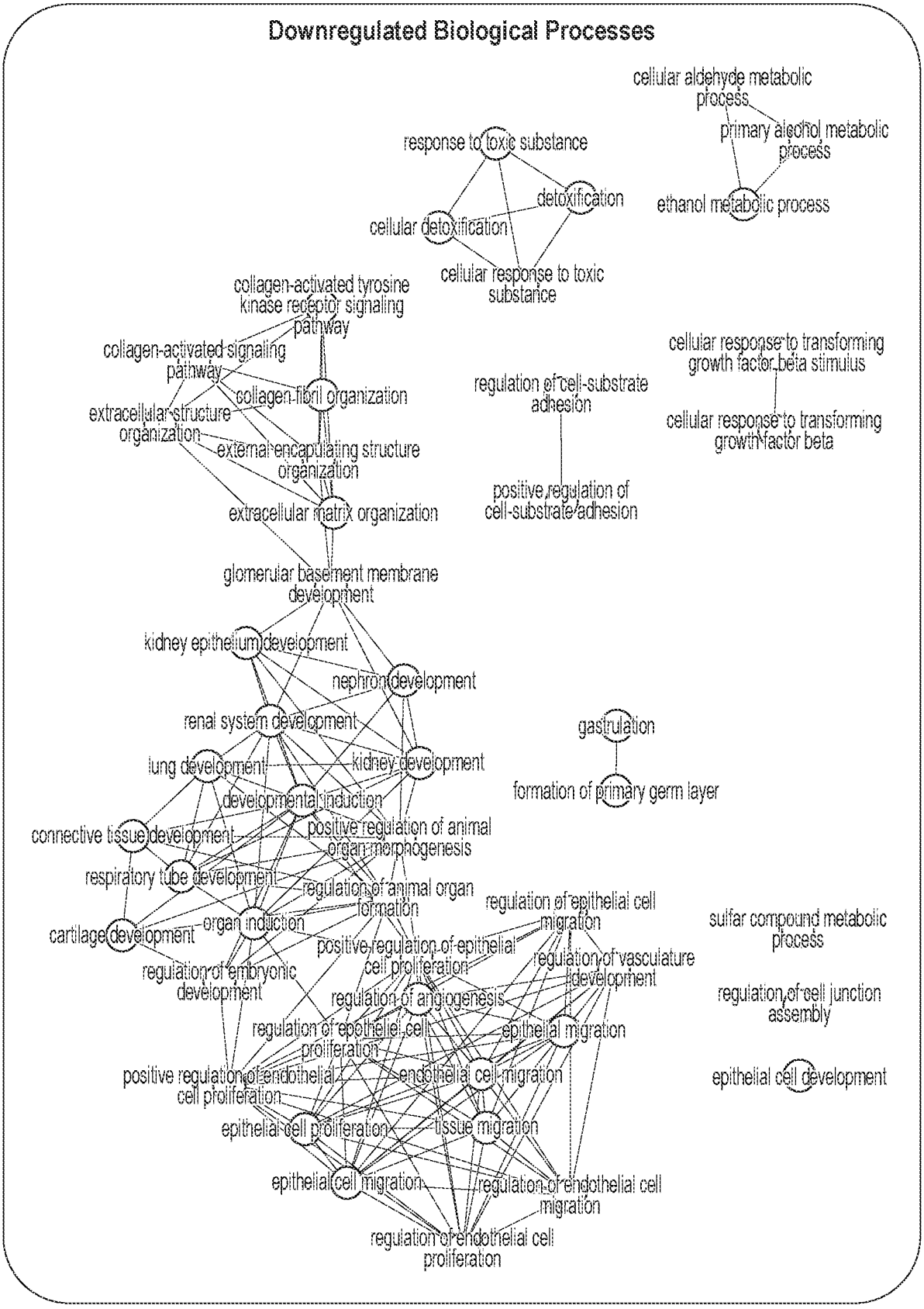
Downregulated Biological Processes
cellular aldehyde metabolic process
primary alcohol metabolic process
response to toxic substance
detoxification
ethanol metabolic process
cellular detoxification
cellular response to toxic substance
collagen-activated tyrosine kinase receptor signaling pathway
collagen-activated signaling pathway
cellular response to transforming growth factor beta stimulus
regulation of cell-substrate adhesion
collagen fibril organization
extracellular structure organization
cellular response to transforming growth factor beta
external encapsulating structure organization
positive regulation of cell-substrate adhesion
extracellular matrix organization
glomerular basement membrane development
kidney epithelium development
nephron development
renal system development
gastrulation
lung development
kidney development
formation of primary germ layer
developmental induction
connective tissue development
positive regulation of animal organ morphogenesis
respiratory tube development
regulation of animal organ formation
regulation of epithelial cell migration
sulfur compound metabolic process
cartilage development
organ induction
positive regulation of epithelial cell proliferation
regulation of vasculature development
regulation of embryonic development
regulation of angiogenesis
regulation of cell junction assembly
regulation of epithelial cell proliferation
epithelial migration
positive regulation of endothelial cell proliferation
endothelial cell migration
epithelial cell development
epithelial cell proliferation
tissue migration
epithelial cell migration
regulation of endothelial cell migration
regulation of endothelial cell proliferation

FIG. 30E

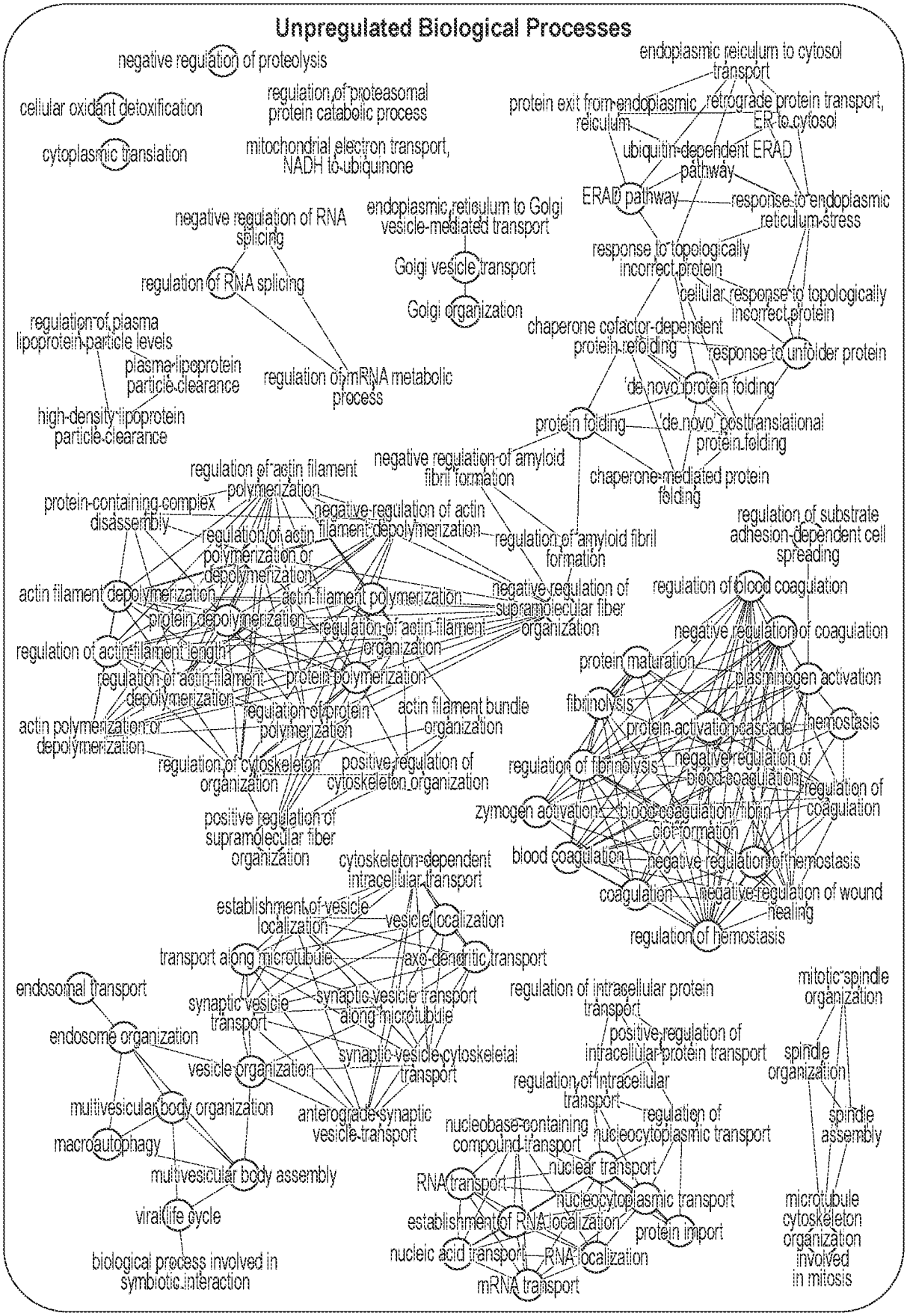
Unpregulated Biological Processes
negative regulation of proteolysis
cellular oxidant detoxification
regulation of proteasomal protein catabolic process
cytoplasmic translation
mitochondrial electron transport, NADH to ubiquinone
endoplasmic reticulum to cytosol transport
protein exit from endoplasmic reticulum
retrograde protein transport, ER to cytosol
ubiquitin-dependent ERAD pathway
ERAD pathway
response to endoplasmic reticulum stress
negative regulation of RNA splicing
endoplasmic reticulum to Golgi vesicle-mediated transport
response to topologically incorrect protein
Golgi vesicle transport
regulation of RNA splicing
cellular response to topologically incorrect protein
Golgi organization
chaperone cofactor-dependent protein refolding
regulation of plasma lipoprotein particle levels
response to unfolded protein
plasma lipoprotein particle clearance
regulation of mRNA metabolic process
de novo protein folding
high-density lipoprotein particle clearance
protein folding
de novo posttranslational protein folding
negative regulation of amyloid fibril formation
chaperone-mediated protein folding
regulation of actin filament polymerization
protein-containing complex disassembly
negative regulation of actin filament depolymerization
regulation of substrate adhesion-dependent cell spreading
regulation of actin filament polymerization or depolymerization
regulation of amyloid fibril formation
actin filament depolymerization
actin filament polymerization
negative regulation of supramolecular fiber organization
regulation of blood coagulation
protein depolymerization
regulation of actin filament organization
negative regulation of coagulation
regulation of actin filament length
protein maturation
regulation of actin filament depolymerization
protein polymerization
plasminogen activation
fibrinolysis
actin polymerization or depolymerization
regulation of protein polymerization
actin filament bundle organization
protein activation cascade
hemostasis
regulation of cytoskeleton organization
positive regulation of cytoskeleton organization
regulation of fibrinolysis
negative regulation of blood coagulation
regulation of coagulation
zymogen activation
blood coagulation, fibrin clot formation
positive regulation of supramolecular fiber organization
cytoskeleton-dependent intracellular transport
blood coagulation
negative regulation of hemostasis
establishment of vesicle localization
vesicle localization
coagulation
negative regulation of wound healing
regulation of hemostasis
transport along microtubule
axo-dendritic transport
endosomal transport
synaptic vesicle transport
synaptic vesicle transport along microtubule
regulation of intracellular protein transport
mitotic spindle organization
endosome organization
positive regulation of intracellular protein transport
spindle organization
vesicle organization
synaptic vesicle cytoskeletal transport
regulation of intracellular transport
multivesicular body organization
anterograde synaptic vesicle transport
nucleobase-containing compound transport
regulation of nucleocytoplasmic transport
spindle assembly
macroautophagy
nuclear transport
multivesicular body assembly
RNA transport
nucleocytoplasmic transport
viral life cycle
establishment of RNA localization
protein import
microtubule cytoskeleton organization involved in mitosis
nucleic acid transport
RNA localization
biological process involved in symbiotic interaction
mRNA transport

FIG. 30F

Protein	Log_2(FC)	p-value
COL6A6	-2.02942	0.003288
COL6A5	-2.98302	0.000404
COL1A1	-0.64671	0.270241
COL2A1	-0.13672	0.805396
COL3A1	0.062921	0.921466
COL4A1	-2.08457	0.025967
COL5A2	-0.01326	0.979445
COL1A2	-0.28249	0.56651
COL4A2	-2.19361	0.017304
COL11A1	-2.56443	0.010598
COL6A1	-0.99763	0.065773
COL6A2	-1.26947	0.025677
COL6A3	-1.43455	0.023275
COL5A1	0.270381	0.642739
COL8A2	-0.26398	0.684465
COL5A3	-1.1202	0.007691
COL8A1	-1.17492	0.143501
COL4A5	-2.68087	0.079496
COL15A1	1.42063	0.34466
COL18A1	-2.07474	0.021118
COL4A4	-1.79879	0.050951
COL4A3	-2.00635	0.045391
COL7A1	-1.48997	0.113682
COL10A1	1.614232	0.189129
COL14A1	-0.05834	0.922269
COL16A1	-0.55244	0.248118
COL4A6	-2.45971	0.029438
COL23A1	0.431456	0.703705
COL26A1	-2.60683	0.006398
COL21A1	-2.20662	0.001876
COL12A1	-1.80042	0.004376

FIG. 31A

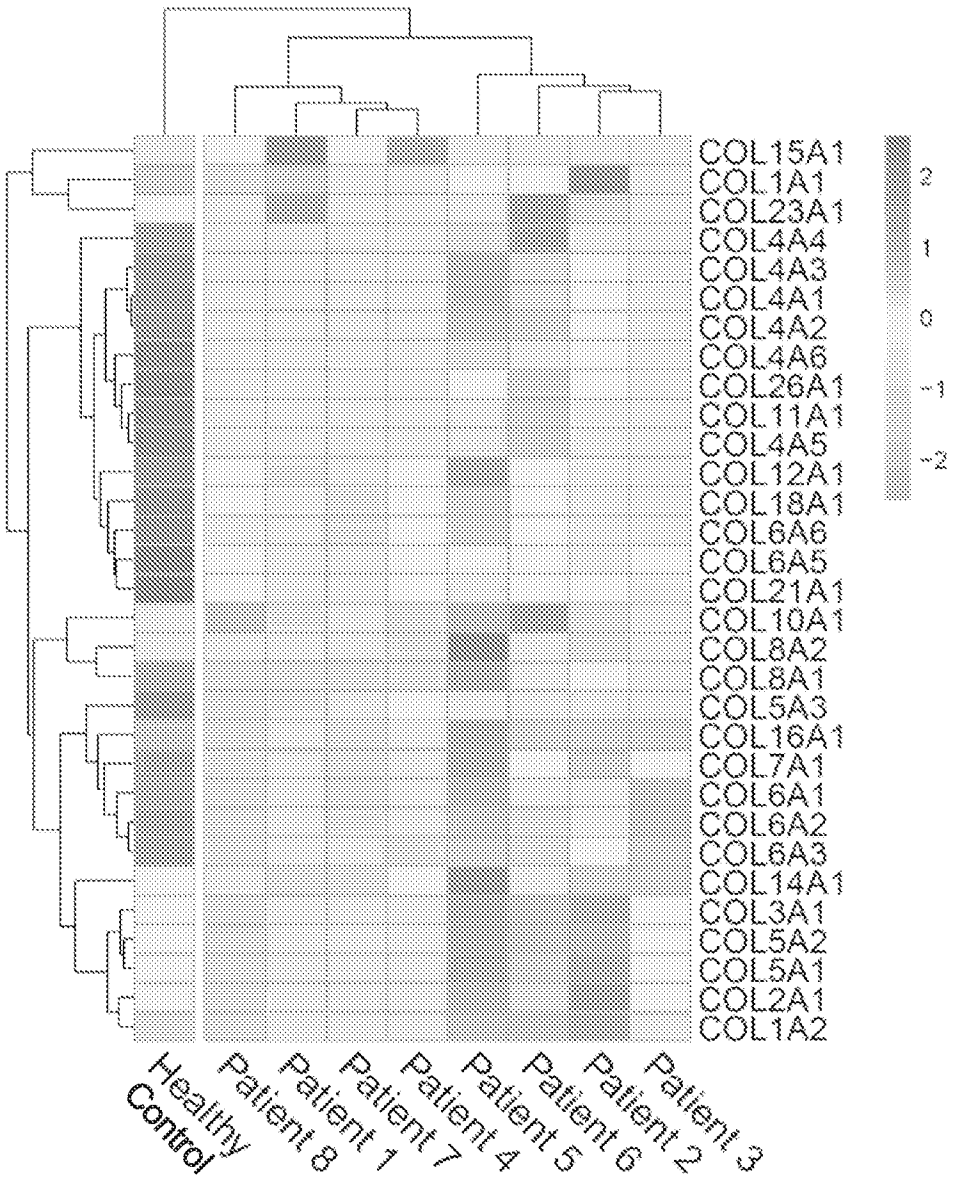
COL15A1
COL1A1
COL23A1
COL4A4
COL4A3
COL4A1
COL4A2
COL4A6
COL26A1
COL11A1
COL4A5
COL12A1
COL18A1
COL6A6
COL6A5
COL21A1
COL10A1
COL8A2
COL8A1
COL5A3
COL16A1
COL7A1
COL6A1
COL6A2
COL6A3
COL14A1
COL3A1
COL5A2
COL5A1
COL2A1
COL1A2
2
1
0
−1
−2
Healthy Control
Patient 8
Patient 1
Patient 7
Patient 4
Patient 5
Patient 6
Patient 2
Patient 3

FIG. 31B